Signals from the Tumor Microenvironment Drive Distinct Epigenetic Features in Terminally Exhausted $CD8^+$ T Cells

by

Brinley Rhodes Ford

Bachelor of Science, McGill University, 2018

Submitted to the Graduate Faculty of the

School of Medicine in partial fulfillment

of the requirements for the degree of

Doctor of Philosophy

University of Pittsburgh

2023

UNIVERSITY OF PITTSBURGH

SCHOOL OF MEDICINE

This dissertation was presented

by

Brinley Rhodes Ford

It was defended on

July 7, 2023

and approved by

Greg Delgoffe, PhD, Associate Professor, Department of Immunology

Larry Kane, PhD, Professor, Department of Immunology

Mandy McGeachy, PhD, Associate Professor, Department of Microbiology and Immunology, Cornell University

Harinder Singh, PhD, Professor, Department of Immunology

Thesis Advisor/Dissertation Director: Amanda Poholek, PhD, Assistant Professor, Department of Pediatrics

Signals from the Tumor Microenvironment Drive Distinct Epigenetic Features in Terminally Exhausted CD8$^+$ T Cells

Brinley Rhodes Ford, PhD

University of Pittsburgh, 2023

Immunotherapy has had major clinical successes, but response rates remain low due in part to increased dysfunctional exhausted CD8$^+$ T cells in the tumor, characterized by decreased cytokine expression and increased expression of co-inhibitory receptors, such as PD-1 and Tim-3. CD8$^+$ T cell differentiation in the tumor is a progressive process, whereby progenitor (PD1$^{lo/mid}$) cells with some functional capacity differentiate further to terminally exhausted cells (PD1^{hi}Tim-3$^+$), which have limited-to-no function. To understand the mechanisms promoting this progression, we used CUT&RUN, a low-input ChIP-seq alternative, to profile four histone modifications in progenitor and terminally exhausted CD8$^+$ T cells in a murine model of melanoma. Unexpectedly, we identified two chromatin features unique to terminally exhausted cells, both of which have limited transcriptional potential at genes associated with stemness and function. First, we found a set of genes characterized by terminal exhaustion-specific active histone modifications without corresponding increases in gene expression. These chromatin regions are enriched for AP-1 transcription factor motifs, despite low expression of most AP-1 family members in terminally exhausted cells. Inducing expression of AP-1 factors using a 4-1BB agonist restored expression of these "anticorrelated" genes, which include genes involved in T cell activation and inflammation. Second, we found a substantial increase in the number of genes with bivalent promoters, defined by the presence of both activating (H3K4me3) and repressive (H3K27me3) marks, as well as

decreased gene expression. Bivalent promoters in terminally exhausted T cells were hypermethylated in response to tumor hypoxia, and decreasing tumor hypoxia was sufficient to recover expression of these genes. Furthermore, overexpressing *Kdm6b,* an oxygen-insensitive histone demethylase for H3K27 was sufficient to recover tumor-infiltrating T cell function without reversing the differentiation state of terminal exhaustion. However, hypoxia alone was not sufficient to lower *Kdm6b* expression and drive increased bivalency *in vitro*. This study has described a unique decoupling of gene transcription from active histone modifications, clarifying how exhaustion is promoted and maintained in the tumor through epigenetic alterations. Modulating the activity of chromatin modifiers, such as *Kdm6b,* can increase the effector function of terminally exhausted cells, suggesting new avenues for immunotherapeutic approaches that specifically target terminally exhausted T cells, rather than their progenitors.

Table of Contents

List of Figures

Preface

The completion of this dissertation would not have been possible without financial support from a variety of funding sources. I am extremely thankful for the time I spent on the Cancer Immunotherapy Training Grant (5T32CA082084-20), which provided an amazing opportunity in which to grow as a scientist and thinker. I also am grateful for the Ruth L. Kirschstein Predoctoral Fellowship (F31) I was awarded (F31CA268670). The work studying the role of hypoxia in regulating bivalent genes could not have been done without support from an NIH R01 from the National Cancer Institute (1R01CA277473-01).

I would also like to thank the University of Pittsburgh Health Sciences Sequencing Core, especially Will MacDonald and Rania Elbakri, for their help in making sure all sequencing experiments went as smoothly as possible. I would also like to thank the Rangos Research Center Flow Cytometry Core for their help with the cell sorting required for all of the sequencing experiments. Thank you also to the University of Pittsburgh Division of Laboratory Animal Resources staff for their assistance in maintaining the mice for all of these experiments.

I cannot overstate how lucky I feel to have spent the last five years training in Dr. Amanda Poholek's lab. I am extraordinarily grateful first-and-foremost for how supportive she has been through the many ups and downs of the last five years, both in the lab and outside of it. In the lab (or on my computer, as it were), she has been so encouraging and motivating, getting me excited about the research questions, even during the most stagnant parts of this project. There will not be a time when I am working on a bioinformatic analysis, where I will not have a sticky note above my computer that outlines the specific biological question of interest, and I will, of course, remember "don't let perfect be the enemy of good enough."

I am also incredibly thankful for the entire Poholek lab, but especially Natalie Rittenhouse, who taught me all of the basics of performing bioinformatic analyses on the computing cluster and in R. Also, thank you to Angela Hettinga and Kun He, who taught me all the wet lab skills I needed in these five years. Thank you to Aaron Yang, who has always been a great sounding board, as well as a welcome distraction when I needed it (and sometimes when I didn't). Also thank you to the Hand lab for all of your support, feedback, and reagents.

Thank you also to the incredible group of collaborators that contributed to this work, without which this ambitious story would not exist. Thank you to Greg Delgoffe, who was a great co-leader of the project and pushed us to think about the project in different ways every time we presented new results. Thank you again to Natalie Rittenhouse, who did all of the CUT&RUN in the initial CD8+ TIL dataset and much of the initial analysis of the anticorrelated genes. Thank you to Nicole Scharping, who did all the mouse tumors and cell sorts required for the many rounds of sequencing necessary to build that dataset. Thank you to Paolo Vignali, who provided key pieces of evidence supporting the bivalent genes story, without which the story would not be complete. Thank you also to Ronal Peralta and Dinos Lontos for their contributions.

I am very grateful for the current and former members of my thesis committee, who helped me to map my way through this sometimes overwhelming PhD journey, always posing interesting questions and sparking interesting discussions to drive the project forward. Thank you, Greg Delgoffe, Larry Kane, Mandy McGeachy, Harinder Singh, and Louise D'Cruz.

There is no way I could have made it through the last five years without the support of all the amazing friends from PMI and outside of it. Thank you to Andrew Frisch, Haley Cartwright, and Ben Murter, who were friends from the first day of orientation. Your support even when you had to hear the same complaints over-and-over again. I know you will be lifelong friends. Andrew

and Haley, thank you for being the best adopted mom and dad, a young 22-year old could ask for. I would also like to thank Ansen Burr, who has been the best climbing/adventure partner, neighbor, coffee bud, and friend I could ask for. I don't think I would have made it through grad school without all the time climbing in the gym and all of the amazing outdoor adventures, especially the hike through the suburban parking lot.

Finally, thank you to my family for all your support throughout the last five years. Thank you to my dad, Mills Ford, who is always there when I need advice about anything or just someone to talk to. Thank you to my sister, who has been there for everything. Even when she is adventuring on the other side of the world, as long as she has cell service, she will be there for me if I need her. Thank you for taking me on adventures when I had time off and getting my mind off of work when I needed it. Thank you especially to my mom, Elise Ford, who passed away in January 2020. You were my biggest cheerleader, believing I could do anything I set my mind to and reading everything that I published, even when I was 17th author. No one celebrated me passing my comprehensive exam as much as you did, and I really wish you could be here to see me defend my dissertation and become a doctor.

1.0 Introduction

1.1 Tumor Immunology and Cancer Immunotherapy

The success of immunotherapy has been a major turning point in the treatment of cancer, marking the culmination of over a century of work. Early work connecting the immune system to cancer included observations that neoplastic tissues had leukocyte-driven inflammation (1). Later, William Bradley Coley conducted the first immunotherapy trials in patients, using bacterial toxins (Coley's toxins) in an attempt to trigger the immune system to fight the growing tumor, with mixed results (2). The idea of bacterial stimulation changing the immune response to cancer was further explored using the live attenuated Bacillus Calmette Guerin (BCG) vaccine. Use of this vaccine was associated with an antitumor immune response and reduced tumor growth in mouse and human studies. This finding has been leveraged to treat bladder cancer, where the BCG vaccine is given after surgery to prevent return of the cancer (3, 4). As the understanding of the immune system progressed, cancer immunotherapy became much more targeted. After the identification and cloning of IL-2, a critical cytokine involved in T cell survival and proliferation, trials using IL-2 to improve the antitumor response by supporting T cell function were moderately successful, with improved responses in some, but not most, patients (5). Despite these early successes in immunotherapy, cancer treatment primarily used strategies to drive general inflammatory and T cell responses until the introduction of immune checkpoint inhibitors (ICI).

Progress in understanding mechanisms of the immune system in general and in response to tumors were integral for the development of ICI and other successful immunotherapies. Studies in tumor immunology have been largely focused on understanding immunosurveillance, the process

by which the immune system senses and kills transformed cells to prevent further growth of cancers, and immunoediting, the broader study of how the immune system shapes the tumor as it grows. The idea of immunosurveillance was introduced by Paul Ehrlich in 1909, when he proposed that transformed cells were constantly arising but were controlled by the immune system (6). The renaissance of immunosurveillance was primarily driven by F. Macfarlane Burnet and Lewis Thomas, who showed that transformed cells present newly arising antigen ("neoantigens") that are recognized by thymic-derived cells (7, 8). Studies of immunoediting have described three phases of this process (the three Es): elimination, equilibrium, and escape (9). Elimination describes the process outlined above by which the immune system can identify transformed cells and remove them. In the equilibrium phase, the tumor cells have proliferated considerably, forming a distinct and complex tumor microenvironment, but the immune response is still intact, with functional cytotoxic T cells and IFNγ production. The final phase, escape, occurs when the tumor grows, despite the presence of immune cells; indeed, in this phase, the tumor microenvironment has become immunosuppressive and the cytotoxic T cells have become dysfunctional. Tumors in human patients are generally diagnosed after this escape phase, which is why the study of the tumor microenvironment and immune contexture have been at the forefront of attempts to understand how to best use the immune system to target tumors.

The important role of $CD8^+$ T cells in the antitumor response has long been appreciated, as shown above in studies exploring their role in immunosurveillance and immunoediting. Further, increased $CD8^+$ T cell infiltration is associated with prolonged patient survival, compared to patients with poorly infiltrated tumors (10-12). However, despite their presence in the tumor, infiltrating $CD8^+$ T cells are not optimally functional. For this reason, reinvigorating $CD8^+$ T cells to improve their antitumor function is a primary goal for cancer immunotherapy. As mentioned

above, treatment with soluble IL-2 had some benefit, but it was ICI therapy that had the first remarkable successes. Immune checkpoint molecules are inhibitory surface proteins, such as programmed cell death protein 1 (PD1), cytotoxic T lymphocyte antigen 4 (CTLA4), lymphocyte activation gene 3 (LAG3), and T cell immunoglobulin and mucin domain-containing protein 3 (Tim-3), which are moderately expressed on T cells after activation and very highly expressed in contexts of chronic antigen stimulation, such as the tumor (13). ICI therapy utilizes antibodies that block the interaction of these inhibitory receptors with their ligands, thereby preventing the transmission of signals that prevent T cell function. In patients who respond to either anti-CTLA4, anti-PD1, or combination therapy, there is a durable survival benefit, in part due to the formation of immune memory (14-16).

The other notably successful branch of cancer immunotherapy has been adoptive cell therapy (ACT), in which T cells are extracted from patients and *in vitro* approaches are used to manipulate the cells before transferring them back into the patient (17). Early studies simply removed the $CD8^+$ tumor infiltrating lymphocytes (TIL) expanded them *in vitro*, and transferred them back with a high dose of IL-2, with the goal of inducing an improved antitumor response (18). Unfortunately, while there were improved responses to this therapy, they were often short lived. A variety of methods were developed to improve the efficacy of ACT, mostly focusing on the antigen specificity of the transferred T cells. However, a major barrier to ACT was the restriction of the T cell receptor (TCR) to antigens presented by major histocompatibility complex (MHC) molecules. Chimeric antigen receptor (CAR) T cells provided a major breakthrough in this regard. In this approach, T cells are engineered to express a CAR, which contains an antibody-derived antigen recognition domain, a transmembrane domain, and intracellular signaling domains, which provide T cell activation and co-stimulatory downstream signals (19). CAR T cell therapy has had

impressive success in hematologic malignancies, leading to a long-term survival benefit (20-23). In fact, a recently published study reported that the first patients' CAR T cells can still be found ten years after treatment (24). However, this success has not been seen in solid tumors. While some barriers to successful ICI and ACT response have been identified, such as lack of T cell infiltration into the tumor and the nutrient-deficient tumor microenvironment, the mechanisms by which cells become dysfunctional in the tumor are incompletely understood.

1.2 $CD8^+$ T Cell Differentiation and Exhaustion

$CD8^+$ T cells are crucial players in the adaptive immune response, generating cytotoxic effector responses to combat intracellular infections while also having the power to mediate antitumor responses. Differentiation of $CD8^+$ T cells upon activation by antigen is regulated by a variety of signals, including co-stimulation, cytokines, and nutrient availability, leading to a heterogeneous pool of highly cytotoxic effector cells followed by formation of memory T cells that provide a faster, more specialized secondary response upon restimulation (25). The multifaceted functions and dynamic nature of $CD8^+$ T cells underline their potential as therapeutic targets. Thus, extensive research has been performed to understand each step of the $CD8^+$ T cell response.

1.2.1 $CD8^+$ T Cell Activation

The activation of $CD8^+$ T cells is tightly regulated to maintain immune tolerance. $CD8^+$ T cells are activated when the TCR encounters its cognate antigen presented by MHC-I molecules.

In this interaction, $CD8^+$ T cells receive two necessary signals: TCR stimulation and co-stimulation through CD28 (26). Antigen recognition triggers a cascade of signaling events, leading to the activation and proliferation of $CD8^+$ T cells. For $CD8^+$ T cells, the TCR interaction with MHC I happens in two different contexts, priming and killing.

First, $CD8^+$ T cells interact with MHC I expressed on dendritic cells (DCs) during priming in the secondary lymphoid tissue (Fig. 1, left). DCs constantly survey the tissue until they encounter foreign material, after which they become activated and traffic to the lymph node. While TCR and CD28 stimulation from the DC is generally sufficient for the primary $CD8^+$ T cell response to infections such as *Listeria monocytogenes* and lymphocytic choriomeningitis virus (LCMV), $CD4^+$ T cell help during priming is necessary for optimal memory formation and secondary responses (27-29). After priming, $CD8^+$ T cells undergo clonal expansion and effector differentiation, during which they acquire the ability to produce the cytokine IFNγ and the cytotoxic molecules perforin and granzyme B (30).

After priming, $CD8^+$ T cells use chemokines and other signals to migrate to the inflamed tissue, where they will encounter antigen presented by MHC I on infected cells (31). Here, they unleash their cytotoxic potential, releasing perforin and granzyme B to induce apoptosis of the infected cell (Fig. 1, right top). After the antigen is cleared, the population of $CD8^+$ T cells contracts, with a pool of these cells differentiating into memory T cells, which allows these cells to respond more rapidly and with improved effector function upon secondary challenge, thus conferring long-term protection to that pathogen (25). However, these differentiation decisions are much more complicated, and we still do not have a complete understanding of the factors that define which T cells become terminal effector cells or memory cells, nor all of the signals involved.

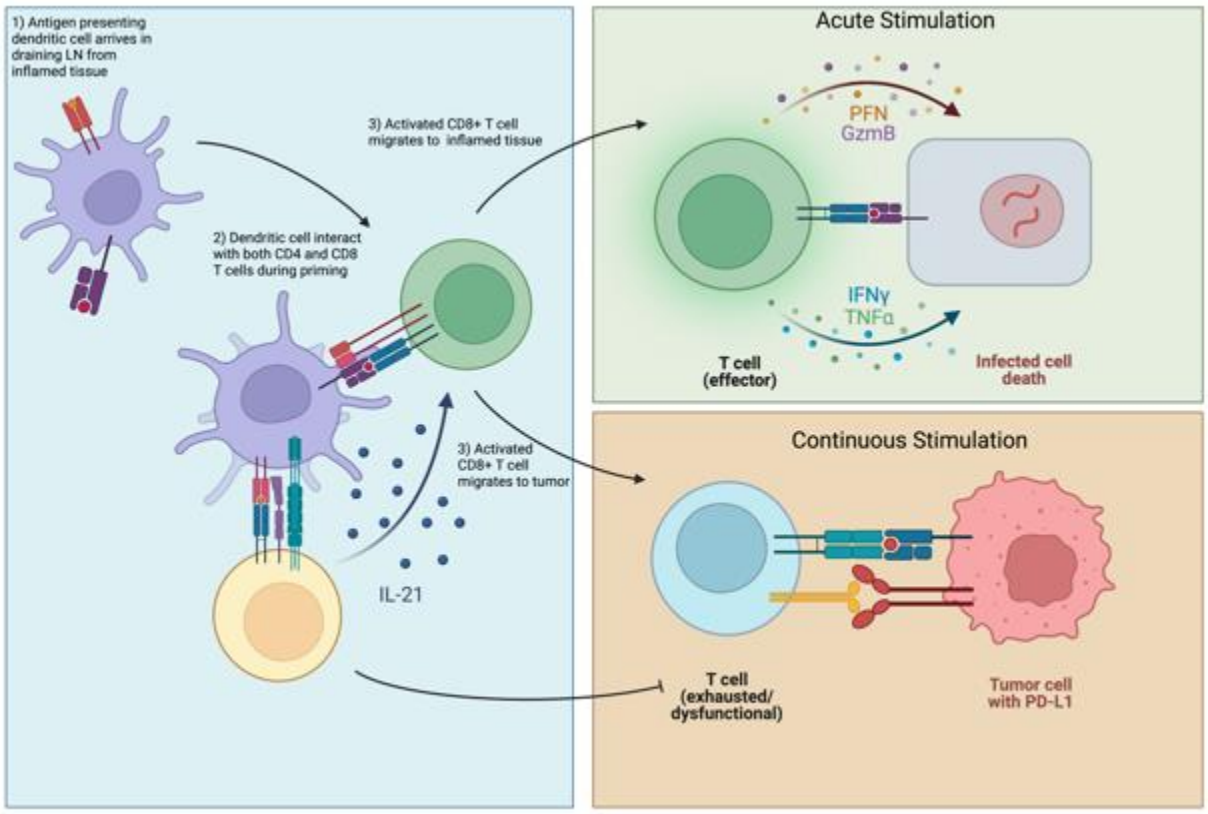

Figure 1. Diagram of CD8$^+$ T Cell Priming and Killing in Acute and Chronic Contexts
Colors: green for functional CD8$^+$ T cell, yellow for CD4$^+$ T cells, and blue for exhausted CD8$^+$ T cell.

1.2.2 Effector and Memory Differentiation in Acute Infections

Understanding the cell fate decisions during CD8$^+$ T cell differentiation is crucial for identifying therapeutic targets, engineering cells for intended therapeutic outcomes, and effective vaccine design. Intriguingly, not all naïve T cells have the same potential upon stimulation and are in fact a heterogeneous pool with distinct activation kinetics and differentiation potential. For example, CD8$^+$ T cells that develop earlier in life are more similar to effector cells, leading to altered differentiation, compared to those T cells that more recently emerged from the thymus, which have increased memory potential (32). Additionally, a variety of signals have been described that influence CD8$^+$ T cell differentiation either towards a memory or terminal effector

fate. Several proposed frameworks incorporate these data and offer explanations for how these decisions are made. However, debates persist regarding which of these models most accurately represents the *in vivo* differentiation process.

As the $CD8^+$ T cell response reaches its peak, two primary progenitor populations can be identified: a short-lived effector (SLEC) population with low expression of IL-7R and high KLRG1; and a memory precursor (MPEC) population with high expression of IL-7R and low KLRG1 (33). Additionally, in the memory phase, there are diverse memory populations with distinct features, including broadly, central memory cells (Tcm), which are more stem-like and circulatory, effector memory cells (Tem), which are less circulatory and have increased effector potential, and tissue resident memory cells, which do not circulate and are the first memory T cells that encounter antigen in the secondary response (34).

Throughout these processes, $CD8^+$ T cells experience various signals, which shape their cell fate decisions. One such signal is the duration and intensity of the TCR signal. Previous work suggests that intermediate-to-high TCR signal strength is necessary for memory, but very high TCR signal strength leads to increased effector differentiation (35). Additionally, cytokine stimulation during priming can also skew these cell fate decisions. Specifically, the cytokines IL-12, IL-2, and type I IFN drive an increased proportion of terminal effector cells with reduced memory potential (36-40). Additionally, different metabolic signals lead to different cell fate decisions, with enhanced glycolysis driving increased SLECs and Tem, while oxidative respiration is associated with stemness and increased proliferative capacity (41). Together, these signals shape the differentiation and functional properties of $CD8^+$ T cells in distinct ways, leading to distinct transcription factor activity and epigenetic landscapes, which specify and maintain the identity of the cells.

Distinct transcription factors are associated with terminal effector vs. memory fates of $CD8^+$ T cells. Indeed, transcription factors associated with "stemness," such as Eomes, Id3, and Bcl6 all have increased expression in memory precursor and memory populations, whereas terminal effector cells have increased expression of T-bet, Id2, and Blimp-1 (25). Expression of these transcription factors is heavily influenced by the signals described above. For example, IL-12 drives expression of T-bet and Blimp-1 via STAT4 activity (42-44). However, transcription factor expression alone is not sufficient for these cell fate decisions, as these factors are expressed in other T cell contexts, such as T cell exhaustion, which will be explored in Chapter 1.2.3.

1.2.3 T Cell Exhaustion

In contrast to effector and memory differentiation, settings of chronic antigen and inflammation drive an alternate pathway of differentiation called T cell exhaustion. Exhaustion was initially observed in chronic viral infections, such as the clone 13 (Cl13) strain of LCMV in mice and hepatitis B virus (HBV) and human immunodeficiency virus (HIV) in humans (45). This state of T cell dysfunction is characterized by reduced or limited effector cytokine production, loss of metabolic capacity, and increased expression of inhibitory receptors (Fig. 2A). Specifically, exhausted $CD8^+$ T cells upregulate PD1, CTLA4, LAG3, and Tim-3, which dampen costimulatory signals and effector functions (46). Importantly, though defined by their loss of function, exhausted T cells maintain some functional capacity, as their total absence in the face of chronic infection has deleterious consequences for the host (47).

Like effector differentiation, exhausted T cells are primed and activated in a similar manner, with antigen-presenting DCs trafficking from the inflamed or infected tissue and interacting with naïve T cells in the secondary lymphoid tissues (Fig. 1, left). After activation, T

cells traffic to the tissue and are exposed to the persistent viral or tumor antigen (Fig. 1, right bottom). Because of these similar early stages, it was initially hypothesized that exhausted cells differentiate from effector cells after being stimulated with persistent antigen within the tissue. However, studies have shown that as early as day 3 after infection, there are transcriptional differences between T cells responding to Cl13, compared to the acute Armstrong (Arm) strain, suggesting that this differentiation decision is made early in the T cell activation, potentially as early as the priming stage (48). In tumors, specifically, some investigators have disputed the effector-to-exhaustion differentiation model, due to the differences in viral infection, compared to the progression of transformed cells into tumors. Differentiation from naïve cells in both pathways is a progressive process with intermediate progenitor stem-like states in both settings. In the effector-memory trajectory, progenitor states have the potential to become different versions of memory cells or terminally differentiate into effector cells (25). However, in exhaustion, progenitor cells progress primarily toward a terminally differentiated dysfunctional state, a process that still remains to be fully understood.

Recently, exhausted $CD8^+$ T cells have been further defined into multiple subsets: a more stem-like, progenitor group, characterized by high expression of TCF1 and Slamf6; and a terminally differentiated exhausted state, characterized by high expression of Tox, as well as expression of inhibitory receptors (specifically Tim-3 and Lag3) and the ectonucleotidase CD39, which cleaves ATP (49, 50). Additionally, an effector-like subset, characterized by high expression of CX3CR1, has recently been described in contexts associated with T cell exhaustion (51-54). While description of these cell fates has improved our understanding of the $CD8^+$ T cell differentiation trajectories, more work remains to be done on which signals, transcription factors, and epigenetic changes may be involved.

Importantly, a variety of signals beyond TCR have been associated with the maintenance of progenitor exhausted populations and differentiation to more effector-like or terminal exhaustion states, including cytokines, which provide the important "signal 3" for T cell activation and differentiation. Common gamma chain cytokines, like IL-2, IL-7, and IL-15, are critical for the maintenance, proliferation, and memory differentiation of $CD8^+$ T cells (55). Thus, treating CAR T cells with IL-7 and IL-15 while expanding them *in vitro* led to increased gene expression of stem- and memory-like genes, as well as decreased expression of terminal exhaustion-related genes, thus promoting the more progenitor-like subset (56). Similarly, IL-2 treatment with αPD1 in chronic viral infection drives a more progenitor-like differentiation (57-59). Immunosuppressive cytokines also directly affect $CD8^+$ T cell differentiation in response to persistent antigen stimulation. IL-10 and TGFβ have both been associated with increased viral persistence and $CD8^+$ T cell exhaustion (60-62). Both of these cytokines also maintain the precursor or progenitor exhausted population of $CD8^+$ T cells, in chronic viral infection (TGFβ) and in tumors (IL-10) (Fig. 2) (63-65). In contrast, Type I IFNs (IFN-Is) play an important role in viral infections and tumor immunity. Traditionally IFN-I contributes to antiviral immunity and is required for T cell expansion and cytolytic function, especially during early infection (66). However, in settings of chronic infection, sustained inflammation from IFN-Is contributes to progressive immune dysfunction. Inhibiting IFN-I signaling shifts the pool of exhausted T cells toward the progenitor subset, suggesting that T cell sensing of sustained IFN-Is promotes exhaustion (109). Finally, $CD4^+$ Tfh-produced IL-21 is crucial for maintaining the antiviral response to LCMV Cl13 by promoting differentiation to the more effector-like $CX3CR1^+$ cells (67). Understanding how cytokines specifically regulate exhausted $CD8^+$ T cells will improve

understanding of how to modulate the differentiation process to improve $CD8^+$ T cell response for immunotherapy.

Another signal that regulates differentiation of exhausted $CD8^+$ T cells is nutrient availability and the distinct metabolic pathways associated with them. Specific metabolic pathways have been associated with $CD8^+$ T cell differentiation in acute infections, with glycolytic pathways driving a terminal effector and effector memory program and oxidative respiration driving memory precursor and central memory differentiation (68). Similarly, mitochondrial oxidative respiration has been associated with progenitor exhausted T cells (69). However, the metabolic programming of terminally exhausted cells is more complex, especially in the context of tumors, where nutrient availability is low. Indeed, many recent studies have described a unique role of metabolic dysfunction in driving terminal exhaustion in the tumor (70-74). Both chronic antigen stimulation and tumor hypoxia support mitochondrial dysfunction in $CD8^+$ TIL, driving differentiation to terminal exhaustion (Fig. 2) (75, 76). Understanding the metabolic changes that occur as these cells differentiate is especially important because metabolites are critical cofactors for making the epigenetic changes necessary for differentiation.

Overall, understanding the signals and molecular pathways involved in $CD8^+$ T cell differentiation is critically important. Immunotherapies aimed at limiting T cell exhaustion, such as ICI and CAR-T, have demonstrated powerful potential to restore antitumor immunity. Thus, an improved understanding of $CD8^+$ T cell differentiation can reveal new signals and pathways to target for preventing (or reversing) differentiation to terminal exhaustion while promoting effector function, further improving the antitumor response.

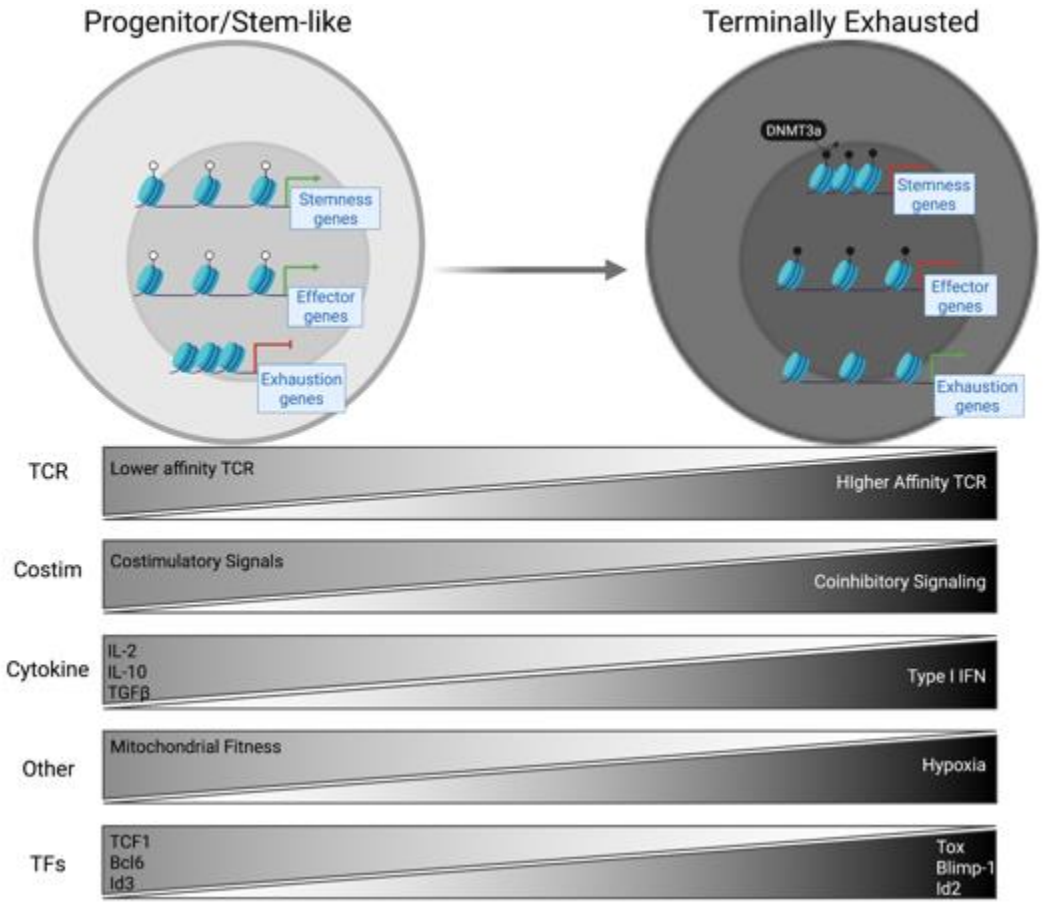

Figure 2. Summary of Signals and Factors Driving T Cell Exhaustion

1.2.4 Transcription Factor Regulation of CD8$^+$ T Cell Exhaustion

Downstream of extracellular signals, transcription factor regulation of gene expression is integral to cell fate decisions. Indeed, many transcription factors have been associated with exhaustion, both for the progenitor and terminally exhausted cells. TCF1 is the prototypical factor associated with the progenitor state; however, it is also expressed in developing thymocytes and other T cell subsets (Fig. 2). TCF1 is regulated by many epigenetic mechanisms in order to drive specific cell fates, including acting as a pioneer factor, mediating chromatin looping, and having intrinsic HDAC activity (77-81). In exhaustion, TCF1 has been proposed to act as a repressor of

pro-exhaustion factors while upregulating Bcl6, a stem factor (82). Bach2 is another transcription factor associated with progenitor cells. Bach2 is a basic leucine zipper factor that acts as a transcriptional repressor with roles in supporting regulatory T cell function and memory $CD8^+$ T cell differentiation in acute infection (83, 84). In chronic viral infection Bach2 was found to enforce stemlike regulatory networks by establishing the epigenetic landscape associated with terminal exhaustion (85).

Another factor of interest is the AP-1 family member BATF, which can heterodimerize with other family members such as c-Jun, or with the IRF family, most notably in T cells IRF4 to bind to AP-1–interferon regulatory factor (IRF) composite elements (AICE). In acute infection BATF is required for effector differentiation by promoting expression of cytokine receptors and the transcription factors T-bet and Blimp-1 (86). However, BATF limited the expression of effector cytokines, suggesting it plays an early role in promoting effector differentiation more than function (86). In chronic viral infection, BATF played a similar role, driving differentiation of a transcriptionally and epigenetically distinct effector-like subset marked by CX3CR1 from the progenitor TCF1 population by maintaining a permissive chromatin state and binding the effector transcription factors T-bet and KLF2 (51). However, the role of BATF in CAR T cells has been more complex. Whereas one study noted that deletion of BATF reduced exhaustion and improved tumor clearance, a second study found that overexpression of BATF led to superior effector function, proliferation in tumors, and tumor clearance (87, 88). Enforced BATF cooperated with IRF4 to induce effector genes associated with increased function (87). Although some BATF was found at newly accessible chromatin regions, the vast majority was not. Furthermore, BATF redistributed IRF4 binding. As both BATF and IRF4 are downstream of TCR, it is possible that TCR signaling dynamics play a key role in the precise function of BATF, perhaps explaining some

differences in these CAR T models between deletion and overexpression of BATF. In line with this finding, overexpression of another AP-1 family member, c-Jun, improved the antitumor function of CAR T cells, further emphasizing the importance of this transcription factor family in the antitumor response (89). Mechanistically, increased c-Jun competed for binding sites with BATF and IRF4, potentially dysregulating expression of exhaustion-related genes. These studies collectively show a clear role for AP-1 family members to alter the differentiation and/or function of exhausted T cells by chromatin modification.

Another transcription factor, Tox, was recently described as a central regulator promoting T cell exhaustion, associating with chromatin modifying enzymes, such as the histone acetyltransferase Kat7, and mediating chromatin remodeling downstream of chronic stimulation of the TCR-dependent molecules calcineurin and NFAT (Fig. 2A) (90, 91). However, Tox is not uniquely expressed in exhaustion; it is also expressed in developing thymocytes as well as effector memory CD8 T cells, where it regulates cytotoxic gene expression (90, 92, 93). Importantly, Tox expression in exhausted T cells increases as cells further differentiate toward a terminal state, but it is nonetheless also expressed at low levels in progenitor populations. Tox belongs to the HMG-box family of transcription factors, but unlike other family members, it does not bind to DNA via a consensus sequence (92). Rather, Tox is thought to bind DNA via a secondary structure, suggesting its function may be in regulating chromatin accessibility or looping (92). Several studies identified and highlighted roles for Tox in exhaustion. Although each study took a distinct approach, several consistent phenotypes were identified. First, Tox played a critical role in the persistence of antigen-specific cells over time. While initial expansion in response to viral infection or tumor antigens was similar in control and Tox-deficient cells, cells lacking Tox failed to persist long term, a consistent finding across several studies. Transcriptome and epigenome

analyses consistently showed that Tox promoted a core exhaustion signature, and loss of Tox led to increases in genes associated with effector function, including cytokine production, expression of transcription factors associated with effector cells, and a decrease in exhaustion genes. There was some discrepancy on the specific effect of the $TCF1^+$ progenitor population. In some studies, Tox overexpression enforced more $TCF1^+$ cells, whereas in others, Tox was required to maintain both $TCF1^+$ and $TCF1^-$ populations. Precisely how Tox controls persistence of the responding population while also driving the exhaustion phenotype is less clear but suggests that Tox may have discrete functions in progenitor cells compared with terminally exhausted cells. This may in part be due to its ability to interact with different partners in different subsets of exhaustion (90, 93, 94). Tox deficiency led to alterations in chromatin accessibility at key genes associated with exhaustion, including *Prdm1* (encoding BLIMP1), *Pdcd1* (PD-1), *Havcr2* (Tim-3), and *Cd38* and transcriptional regulators *Tcf7* (TCF1) and *Id3,* becoming more open at progenitor genes, including *Tcf7*, while also closing chromatin in the absence of Tox at exhaustion genes such as *Havcr2* and *Pdcd1* (95). Given its complex role, precisely how Tox paradoxically supports T cell persistence while promoting exhaustion requires further study.

The nuclear receptor transcription factors NR4A1, NR4A2, and NR4A3 have also been associated with T cell exhaustion. Depletion of all three members in CAR T cells limits exhaustion, and open chromatin regions specific to loss of the NR4A factors were enriched for AP-1 and NF-κB (96). A separate study also found that NR4A1 could antagonize AP-1 binding, and that overexpression of NR4A1 drove increased enhancer activation at super-enhancer regions in activated T cells (97). Furthermore, NR4A factors themselves are targets of NFAT, suggesting that similar to AP-1 and IRF4, TCR signals promote their expression to induce exhaustion (94). NR4A family members likely regulate other exhaustion transcription factors, including Tox and Blimp-

1, the latter of which is a transcriptional repressor associated with exhaustion (98). A recent study deleted Blimp-1 in CAR T cells and although it improved the proliferation and stemlike programs via TCF1, it also drove exhaustion genes, including NR4A3 (99). Knockdown of both Blimp-1 and NR4A3 led to a decrease in exhaustion and improved tumor clearance, suggesting that complex regulatory networks control the chromatin landscape to both drive differentiation and activate effector exhaustion genes.

While the changing expression of various transcription factors is crucial to $CD8^+$ T cell fate decisions, it is important to continue to study how upstream signals, binding partners, and epigenetic changes work in concert to drive differentiation.

1.3 Epigenetic Regulation of Gene Expression

1.3.1 DNA Methylation

DNA methylation is primarily repressive, found in heterochromatin and regulated by families of methyltransferases and demethylating TET enzymes. Methylation occurs at cytosine residues modified to 5-methylcytosine within CpG islands found chiefly at promotors (100). However, differentially methylated regions, defined by gain or loss of DNA methylation, are mostly found in regions distal to promoter (101). Describing dynamic differentially methylated regions has been important in understanding the role of DNA methylation in regulating gene expression beyond heterochromatin. Genome-wide DNA methylation can be measured several ways, including whole-genome bisulfite sequencing, which can identify the precise location of individual methylated cytosine residue (102, 103).

1.3.2 Chromatin Accessibility

Chromatin accessibility distinguishes heterochromatic from euchromatic regions, as the "openness" of chromatin relates to the likelihood of genes to be transcribed. Chromatin accessibility can be measured using DNA cleaving proteins such as DNase and micrococcal nuclease (104). Assay for transposase-accessible chromatin with high-throughput sequencing (ATAC-seq), using the transposase Tn5 to cleave DNA at accessible regions and add sequencing adapters, has been widely applied to CD8 T cells, enhancing efficiency and lowering input required (105, 106).

1.3.3 Histone Modifications

The histone code is a mechanism in which heritable gene expression is stored in the covalent modifications of histones (107). Many covalent modifications have been described, including acetylation, methylation, phosphorylation, ubiquitylation, sumoylation, and citrullination (108). Chromatin-modifying enzymes (writers, erasers) are responsible for adding or removing modifications, whereas readers recognize specific modifications and control transcriptional outcomes.

H3K27me3 and H3K9me3 are the main repressive modifications, associated with facultative and heterochromatin, respectively (109). These modifications are regulated by specific histone methyltransferases (writers), responsible for the addition of methyl groups, and histone demethylases (erasers), which are responsible for their removal. Additionally, the metabolite S-adenosylmethionine (SAM) provides the methyl group for methylation, and alpha-ketoglutarate (aKG) acts as the methyl group acceptor during demethylation. Notably, oxygen is also necessary

for the demethylation reaction. Indeed, availability of these metabolites, as well as levels of S-adenosyl-homocysteine (SAH), which is left after methyl group donation, and succinate, which forms after methyl group addition to aKG, influences the rates of methylation and demethylation within the cell (110). For H3K27, the polycomb repressive complex 2 (PRC2), with Ezh1 or Ezh2 as the catalytic protein, is the primary methyltransferase, whereas Utx and Jmjd3, encoded by the *Kdm6a* and *Kdm6b* genes, are the primary demethylases (111). There is more variety in the methyltransferases for H3K9, each with distinct roles. They include Suv39h1, encoded by *Kmt1a*; Setdb1, encoded by *Kmt1e*, and G9a, encoded by *Ehmt2* (111). For demethylation, the reaction is primarily mediated by the Kdm4 family (112). Overall, the addition and removal of methyl groups at H3K9 and H3K27 is very tightly regulated.

For the active histone modifications, H3K27ac is associated with active enhancers, whereas H3K9ac and H3K4me3 are associated with active gene bodies and promoters (113). H3K4 methylation and demethylation are regulated very similarly to the repressive modifications, but with its own distinct writers and erasers. The Set1 and Kmt2/MLL families of methyltransferases are required for methylation of H3K4, and the Kdm1 and Kdm5 families are the primary histone demethylases (111). Histone acetylation is regulated very similarly to histone methylation, with histone acetyltransferases (HATs) as the writers and histone deacetylases (HDACs) as the erasers. Like methylation, acetylation also requires an acetyl group donor, which is provided by the metabolite acetyl-CoA (110). The primary acetyltransferases associated with transcriptional activation are p300 and CREB-binding protein (CBP), which act as transcriptional co-activators (114). There are a broad variety of HDACs of four different classes. The sirtuin proteins, or class III HDACs, are a prominent group of HDACs, which require nicotinamide adenine dinucleotide (NAD) for deacetylation (115). Both have been associated with acetylation of both H3K9 and

H3K27. These histone modifications work together with DNA methylation and the transcriptional machinery to regulate gene expression.

Chromatin immunoprecipitation (ChIP) sequencing (ChIP-seq) was the first widely used technology to explore histone modifications genome-wide (116). Recent adaptations of this strategy improved efficiency and reduced cellular input, including indexing-first ChIP (iChIP) and multiplexed, indexed T7 ChIP (Mint-ChIP), which rely on multiplexed pooling strategies, and CUT&RUN and CUT&Tag, which cleave DNA using micrococcal nuclease or Tn5 (117-120).

1.3.4 3D Chromatin Conformation

Finally, chromatin is organized into gene regulatory loops or compartments, called topologically associating domains, which are marked by CTCF (121). CTCF and cohesion play an important role in promoter-enhancer looping, a mechanism by which distal enhancers regulate gene expression (122). Because distal enhancers can operate from huge distances from the gene promoter, three-dimensional chromatin conformation can inform how we interpret histone modification and accessibility data. Several methods have been developed to determine the frequency of interactions from two known regions (3C) all the way to an unbiased view of all chromatin interactions (Hi-C) (123-125). More recently developed assays have combined a ChIP-based approach with Hi-C (chromatin interaction analysis by paired-end tag sequencing [ChIA-PET], HiChIP, and capture Hi-C [CHi-C]) to explore the relationship of histone modifications or DNA-binding proteins with looping (126-128).

1.4 Epigenetic Regulation of CD8$^+$ T Cells

1.4.1 Epigenetic Regulation of Effector and Memory CD8$^+$ T Cells

It is the coordinated changes in histone modifications and chromatin accessibility that drive differentiation and gene expression upon activation. Histones are actively modified by a host of histone modifying enzymes that are recruited to specific sites by transcription factors. For example, the *GzmB* locus must first become accessible to allow for AP-1 binding by increasing H3K9ac and H3K4me3, followed by RNA polymerase II (RNA pol II) binding, before finally leading to expression of granzyme B transcripts (129-131). Similarly, the *Ifng* locus must be remodeled prior to expression. However, some effector genes, like *Tnf,* can be more rapidly expressed and exhibit permissive epigenetic signatures such as high H3K9ac, H3K4me3, RNA Pol II docking and low H3K27me3, allowing for TNF to be produced rapidly upon stimulation (132).

Several of the signals described in activation and differentiation promote both epigenetic and gene expression changes, such as TCR stimulation and IL-12 (133, 134). IL-12- and IFNγ-driven STAT4 and STAT1 promote histone acetylation of key effector genes. Indeed, blocking histone deacetylases (HDACs) promotes expression of effector genes activated by IL-12 (135). Further, IL-12-driven expression of the transcription factor Batf plays a key role in differentiation of effector cells by actively binding to and promoting gene expression at genes such as T-bet and Blimp-1, as well as the downregulation of the HDAC Sirt1 which limits acetylation of effector genes prior to activation (86, 136). Indeed, Batf forms a key transcription factor network, working with Irf4, Runx3, and T-bet to modify the epigenetic landscape of T cells upon stimulation (137). Indeed, stimulation-driven Runx3 expression is critical in changing chromatin accessibility and driving effector and memory cell fate by repressing stemness genes during terminal differentiation,

as well as regulating T-bet expression whereas Runx1 and T-bet cooperate to regulate stable epigenetic changes upon stimulation (138-140). Runx3 also directly affects levels of H3K27me3 at stemness genes upon terminal effector differentiation (138).

Alterations in expression of histone modifying enzymes also contribute to the differentiation process. HDAC3 is required for the persistence of effector $CD8^+$ T cells, and HDAC3-deficiency skews cells primarily to the terminal effector fate, leaving few cells with potential to differentiate into memory (141). Polycomb repressive complex 2 (PRC2) deposits H3K27me3 at memory genes and is required for effector differentiation, as well as the proliferative burst that occurs after activation (142). Similarly, Suv39h1 which regulates H3K9me3 is necessary for repression of stemness genes (143). Demethylation of H3K27 via Kdm6a and Kdm6b has similar effects on the burst and effector differentiation of $CD8^+$ T cells, with important roles in demethylating genes necessary for those processes (144-146).

Like changes in DNA and histone methylation, increased acetylation of histones and chromatin accessibility are associated with epigenetic memory, and inhibition of histone acetyltransferase activity prevents expression of effector genes (131, 147). Acetylation of histone H3 increases in memory cells and is associated with improved recall responses (148). Memory cells also have reductions in nucleosome density and H3K27me3 at effector genes (149). Intriguingly, comparison of chromatin accessibility in memory and effector T cells reveals both similarities and distinctions. There is increased chromatin accessibility at effector gene regulatory regions in both effector and memory; however, the size of the peaks are diminished in memory cells over time (150).

Thus, signals encountered during T cell activation drive key transcription factors that act together to alter the epigenetic landscape and promote gene expression as cells transition to effector

or memory cells. Cells with chromatin landscapes that have increased accessibility or potential at stem genes and limited potential for effector genes appear to be more likely to form memory precursor populations that persist as bona fide memory cells, with the potential to respond to secondary infection. In contrast, enhanced TCR, co-stimulation and inflammatory cytokine signals lead to cell states with chromatin landscapes with limited proliferative potential and increased expression of effector molecule, driving effector cells fated for apoptosis.

1.4.2 Role of Epigenetic Modifications in $CD8^+$ T Cell Exhaustion

Through use of the tools described in chapter 1.3, there has been an explosion in our understanding of the epigenetic landscapes associated with $CD8^+$ T cell exhaustion. Initial studies demonstrated that exhausted T cells were epigenetically distinct from effector or memory cells responding to acute infection, confirming that exhaustion was a distinct $CD8^+$ T cell state (151-153). These distinctions are acquired early after T cell activation, suggesting that commitment to exhaustion versus effector is driven by signals specific to chronic viral infection or tumor microenvironments (93, 154-156). The process of differentiation to exhaustion is progressive; initially, cells display a stemlike, precursor, or progenitor state that has some features of memory precursor cells in acute infection, followed by populations of cells that exhibit a more terminal state of exhaustion with reduced effector function more distinct from effector or memory populations of cells (157, 158). These populations are identifiable by increased expression of inhibitory receptors such as PD1 and Tim-3 on terminally exhausted cells, as well as the transcription factor Tox, whereas precursor exhausted cells express the transcription factor TCF1 (encoded by the gene *Tcf7*). The progressive nature of this process has been confirmed by adoptive transfer studies where precursor cells can give rise to terminal cells, but not vice versa (158). In

precursor populations, the chromatin states of stem and memory-associated genes are in an open confirmation, including *Tcf7*, *Bcl6,* and *Id3*. In addition, effector genes are accessible and active, as are cell cycle programs and metabolic enzymes that support metabolic capacity. In contrast, in terminal exhaustion, accessibility of effector and stem genes are lost, whereas the accessibility at exhaustion-associated genes such as inhibitory receptors, *Tox,* and others are increased (158). In studies of bulk populations, smaller ATAC peaks indicate that as a population, stem genes are less "open," whereas exhaustion-associated genes become more "open." Recent single-cell studies, however, have demonstrated heterogeneity of cell populations as progenitor cells move toward terminal exhaustion, identifying several populations that can be defined as either precursor or intermediate, and one of several differently defined terminal populations. Thus, genes that appear less open via bulk analysis are in fact the result of heterogeneity, as chromatin openness at any given region in a single cell is ternary, existing in one of three states: open at both alleles, one allele open and one allele closed, or closed at both alleles (93, 154, 159, 160).

Like chromatin accessibility, changes in DNA methylation drive and maintain T cell exhaustion. *De novo* methylation is controlled by DNA methyltransferase 3a (DNMT3a) while DNA methyltransferase 1 (DNMT1) is the canonical maintenance methyltransferase, re-establishing the methylation landscape after DNA replication (161). In chronic viral infection, DNMT3a methylates and represses stem genes including *Tcf7* and effector genes, including *Ifng*, *Ccr7*, *Tbx21*, and *Eomes*. Deletion of DNMT3a limits the development of exhaustion and promotes retention of effector ability, and thus *de novo* methylation via DNMT3a drives stable epigenetic silencing to enforce the differentiation process toward terminal exhaustion (151). A recent study in CAR T cells found that deletion of *DNMT3A* limited exhaustion and improved antitumor activity via enhanced proliferation and upregulation of IL-10. Similarly, stem genes including

TCF7 and LEF1 were targeted for silencing in CAR T cells by DNMT3a (162). Thus, DNA methylation plays an important role in silencing effector and stem genes as cells progress toward exhaustion.

Finally, histone modifications are another level of regulation that has been recently explored. Previously limited by technical requirements for large cellular input, assessing the histone landscape in exhaustion has lagged compared with DNA methylation and chromatin accessibility. ChIP-seq of H3K27ac of effector cells from acute infection compared with both precursor and terminal cells in exhaustion demonstrated distinct profiles of terminally exhausted cells, as well as between memory precursor cells in acute infection with precursor cells in exhaustion (93). Thus, transcriptional profiles of exhaustion are supported epigenetically by accessibility, DNA methylation, and histone modifications.

These observations are supported by studies that explored epigenetic modulation to improve the antitumor response of adoptive cell transfer (ACT) therapies. HDAC inhibitors improved the ACT response by making the cells more proliferative and functional (163, 164). In contrast, blocking bromodomain and extraterminal domain (BET) proteins, which recognize acetylated lysines, limited the efficacy of ACT (165). These studies suggest that restoring function by epigenetically modifying genes needed to promote effector function may be a beneficial therapeutic avenue.

As outlined above, a variety of epigenetic changes occur as $CD8^+$ T cells differentiate. However, our knowledge of chromatin modifiers and transcription factors that contribute to this process has also grown recently. As direct regulators of the transcriptome, these proteins represent potential targets for therapy particularly in CAR T cells that already undergo genetic modulation by introduction of the CAR. Efforts to define key regulators of exhaustion from progenitor to

terminally differentiated have used CRISPR screens to identify critical chromatin modifier complexes that are required for the process of differentiation to exhaustion. Several studies have identified the BAF and Mediator complexes as critical for these processes (166-169). BAF is a chromatin remodeling complex composed of many subunits that can form multiple distinct complexes (170). For example, Arid1a is known as a key component of the canonical BAF complex. In one study, Arid1a loss led to a decrease in exhaustion gene expression and increased effector cell potential in models of tumor-mediated exhaustion (Fig. 1B) (170). By contrast, another study showed that Arid1a deletion was detrimental for the early responses in both acute and chronic viral infections, whereas deleting Arid2 (part of the PBAF complex) greatly improved stemness and survival of exhausted cells, leading to improved response in the settings of ACT and anti-PD1 therapy (169). Intriguingly, BAF function was also associated with driving effector cells in acute infection, and Arid1a loss at early T cell activation and CAR T cell induction favored memory cell development, in line with its role in modifying chromatin as cells differentiate (171).

Similarly, in models of CAR T cell-driven tumor clearance, CRISPR screens identified the Mediator complex as central to promoting effector function and antitumor immunity (172). Mediator is also composed of many subunits and binds to enhancer-associated transcription factors to bridge binding to RNA polymerase II at promoters (172). Specifically, CRISPR screens in CAR T cells identified Med12 and CCNC, which encode proteins in the Mediator kinase module, as key regulators of exhaustion (168). Deletion of Med12 increased proliferation, cytokine production, and tumor clearance of CAR T cells but did not promote a more stemlike program. Rather, loss of Med12 drove Mediator to more locations in the chromatin, suggesting that Med12 aids in the regulation of the specific enhancer-promoter contacts that drive exhaustion. Indeed, Med12 loss increased enhancer activity at places where STATs and AP-1 binding sites are found, in line with

enhanced effector genes driven by IL-2/STAT5 signaling. Thus, whereas some chromatin modifiers act to remodel chromatin directly, others regulate chromatin looping to control effector gene transcription.

While the epigenetic changes underlying $CD8^+$ T cell differentiation have been explored, they have been limited by technological constraints, primarily the cell input required for these assays. With recent advancements and the improved understanding of the importance of T cell differentiation within solid tumors, it is now very important to explore the epigenetic changes underlying T cell dysfunction to improve cancer immunotherapies and provide new potential targets.

2.0 Transcriptional Changes of Tumor-Infiltrating CD8$^+$ T Cells

Cytotoxic CD8$^+$ T cells play a crucial role in the immune response to tumors. As CD8$^+$ T cells are continuously stimulated by tumor antigen, they differentiate to the dysfunctional cell fate of exhaustion. T cell exhaustion was initially defined in chronic viral infection, with the following characteristics: low cytokine and cytotoxic molecule production, high levels of co-inhibitory receptor expression, low proliferative capacity, highly prone to apoptosis. Dysfunctional tumor-responsive CD8$^+$ T cells have many similar features to exhausted CD8$^+$ T cells responding to chronic viral infection; however, it is contentious whether the differentiation in response to a growing tumor and a viral antigen is the same.

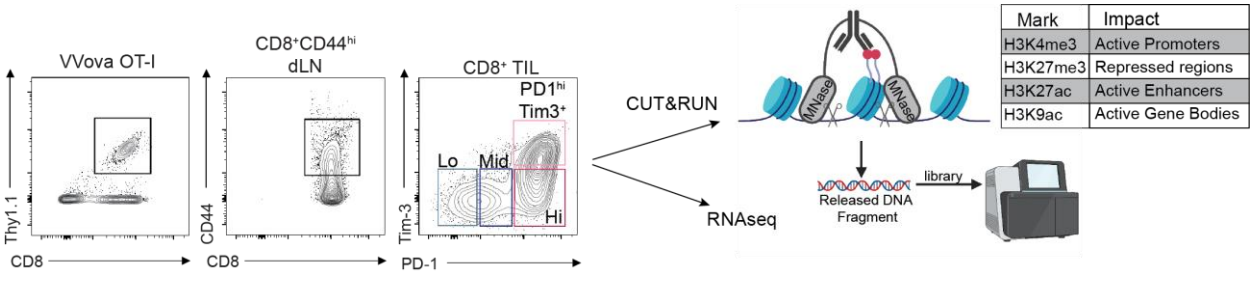

Figure 3. Experimental Scheme.
Sort strategy of Thy1.1$^+$ Vaccinia-Ova-responding effector cells, CD44hi CD8$^+$ T cells from the dLNs in B16 melanoma tumor-bearing mice, and CD8$^+$ T cells sorted from within the B16 melanoma tumor for RNA-seq and CUT&RUN analysis. TILs sorted by PD1 and Tim-3 expression.

Here, we explored how tumor-infiltrating CD8$^+$ T cells (TIL) change their histone modifications and gene expression as they progressively differentiate within the tumor. We sorted the cells based on the expression of the coinhibitory receptors, PD1 and Tim-3, with the assumption that the CD8$^+$ T cells with low (PD1^{lo}) or intermediate (PD1^{mid}) levels of PD1 expression would be progenitor exhausted CD8$^+$ T cells and the CD8$^+$ T cells with high levels of PD1 (PD1^{hi}) and co-expression of both receptors (PD1^{hi}Tim-3$^+$) would be terminally exhausted

(Fig. 3). RNA sequencing was then performed on these sorted cell populations. Advances in low cell input assays have overcome the technical hurdles in assessing the epigenetic landscape of tumor-infiltrating immune cells by histone modifications. Using cleavage under targets and release under nuclease (CUT&RUN), we also determined the histone modifications underlying the changes in gene expression in tumor-infiltrating T cells.

Data in this chapter have been previously published in Science Immunology. Manuscript information: Ford, BR, Vignali, PD, Rittenhouse, NL, Scharping, NE, Peralta, R, Lontos, K, Frisch, AT, Delgoffe, GM, & Poholek, AC. Tumor microenvironmental signals reshape chromatin landscapes to limit the functional potential of exhausted T cells. Science Immunology 2022, 7 (74). Creative commons license: https://creativecommons.org/licenses/by/4.0/legalcode

2.1 Introduction

RNA sequencing (RNAseq) has revolutionized the field of genomics by enabling comprehensive analysis of the transcriptome. Prior to RNAseq, early multiplexed RNA assays, such as RNA microarray, allowed researchers to measure the abundance of specific RNA transcripts in a sample, which provided important insights into gene expression changes in different cell types, but they were limited to a select number of known genes (173). Serial analysis of gene expression (SAGE) was an unbiased RNA quantitation assay, not requiring prior sequence information; however, it was low throughput (174). These technologies provided valuable insights into gene expression patterns, but with the advent of next-generation sequencing (NGS) technologies, researchers realized the potential of NGS for transcriptome analysis. RNAseq

leverages the power of NGS to provide comprehensive and unbiased profiling of RNA transcripts in a sample.

Additionally, NGS technology has been used to understand epigenetic changes underlying gene expression, interrogating chromatin accessibility with assay for transposase-accessible chromatin (ATACseq) and DNA binding proteins, like histones and transcription factors, with chromatin immunoprecipitation (ChIPseq). Methods to distinguish the heterochromatic, inaccessible regions from euchromatic, accessible regions with active transcription have been valuable tools to understand the underlying conformational changes leading to gene expression (104). Chromatin-modifying enzymes are responsible for adding or removing modifications, while chromatin readers recognize specific modifications and control transcriptional outcomes. H3K27me3 and H3K9me3 are the main repressive modifications and are associated with facultative and heterochromatin, respectively (109). H3K27ac is associated with active enhancers, whereas H3K9ac and H3K4me3 are associated with active gene bodies and promoters (113).

These technologies have been widely used to characterize molecular changes and key regulatory proteins as $CD8^+$ T cells differentiate in response to antigen. Early studies characterized effector and memory differentiation in response to acute infection, but RNAseq and microarrays have also been instrumental in describing exhausted $CD8^+$ T cells in chronic viral infection and tumors. While ATACseq and RNAseq have previously been published in these contexts, no study exploring histone modifications in tumor-infiltrating $CD8^+$ T cells ($CD8^+$ TIL), due to the technical limitations described above. We used RNAseq and CUT&RUN to describe the changes in histone modifications underlying gene expression as these cells differentiate. We show that the gene program in these $CD8^+$ TIL conform to published exhausted T cell gene programs, and the histone modifications are largely consistent with their published active and repressive roles.

2.2 Results

2.2.1 Tumor Infiltrating CD8$^+$ T Cells Are Transcriptionally Distinct

While subsets of exhausted cells have been well described, bulk and single-cell RNAseq and ATACseq have shown that progenitor and terminally exhausted CD8$^+$ T cells in chronic viral infection and tumors have distinct transcriptomes and chromatin accessibility, suggesting they have distinct CD8$^+$ T cell differentiation paths (158, 175-181). However, the changes in histone modifications as these cells transition from progenitor to terminally exhausted have not been explored. We used B16-F10 melanoma (B16), an aggressive murine tumor cell line that promotes T cell exhaustion and is insensitive to PD1 blockade, to better understand the relationship between the epigenome and transcriptome of CD8$^+$ TIL as they differentiated from progenitor (PD1^{lo}Tim-3$^-$) to terminally exhausted (PD1^{hi}Tim-3$^+$) (Fig. 3).

CD8$^+$ T cells isolated from B16 tumors were sorted into four populations based on expression of PD1 and Tim-3 (PD1^{lo}, PD1^{mid}, PD1^{hi}, and PD1^{hi}Tim-3$^+$). Antigen-experienced CD8$^+$ T cells (CD44^{hi}) from paired draining lymph nodes (dLNs) were isolated as controls (Fig. 4A). Additionally, we compared TIL subsets with "bona fide" effector CD8$^+$ T cells generated using antigen-specific effector CD8$^+$ T cells (OT-I T cells) responding to acute viral infection, *Vaccinia* virus expressing ovalbumin (*Vaccinia*-OVA) (Fig. 4B). TILs segregated away from both LN CD44^{hi} and effector cells, and progenitor and terminally exhausted T cells separated from each other (Fig. 4A-B). Transcriptome analysis confirmed the distinction between TIL subsets and activated CD44^{hi} CD8$^+$ T cells in the dLN (Fig. 4C). PD1^{lo} and PD1^{mid} TILs were closely related, whereas PD1^{hi} and PD1^{hi}Tim-3$^+$ cells were more similar, suggesting a transition between PD1^{mid}

to PD1^{hi} cells discriminating progenitor and terminally exhausted states (Fig. 4A). Analysis of differentially expressed genes (DEGs) revealed similarity of gene expression among PD1^{lo} and PD1^{mid} TIL and CD44^{hi} cells from the dLNs, as well as separation from PD1^{hi} and PD1^{hi}Tim-3^{+} cells (Fig. 4C).

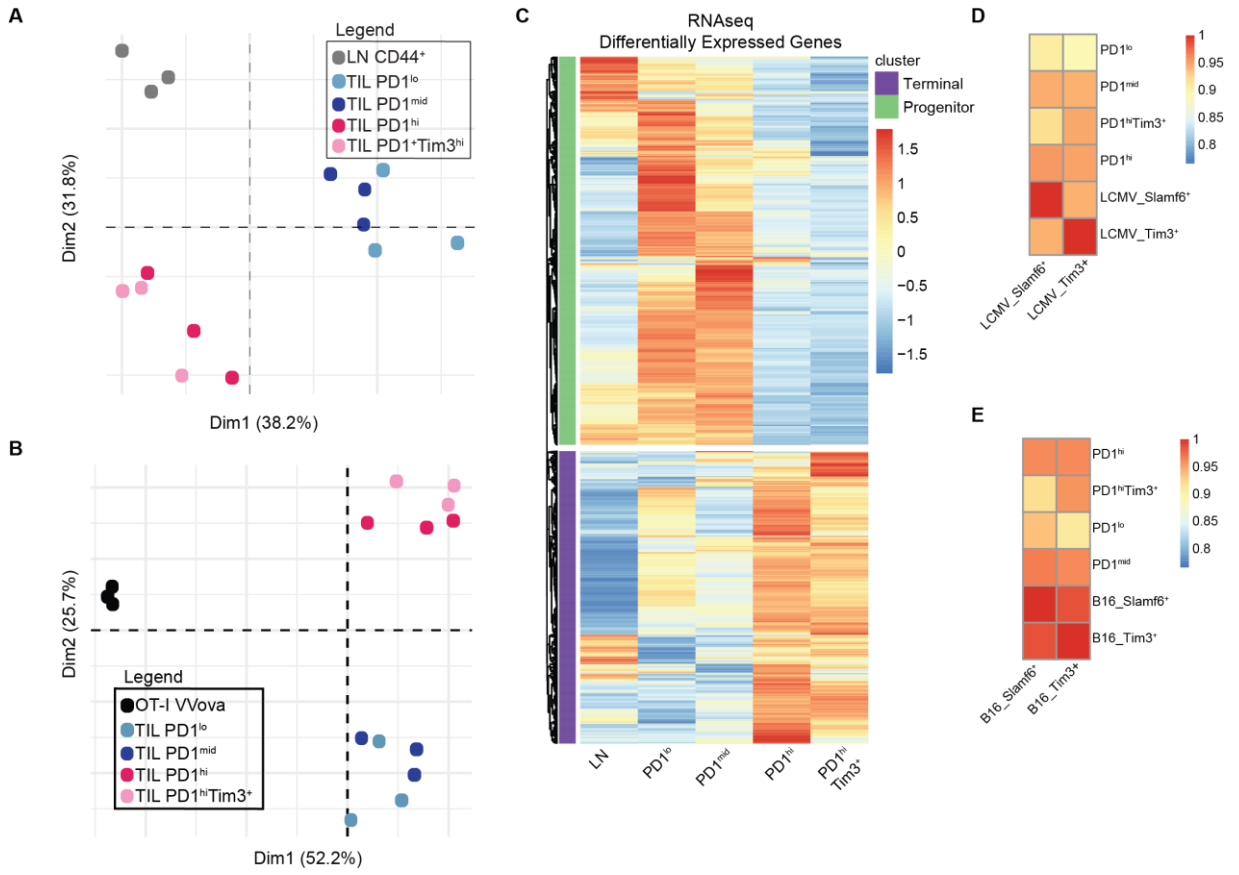

Figure 4. Distinct Clusters of CD8^{+} Tumor-Infiltrating T Cells.
(A and B) Principal component analysis of transcriptomes of LN CD44^{hi} CD8^{+} T cells (A) and Vaccinia-OVA CD8^{+} effector T cells compared to TIL subsets. (C) DESeq2 of transformed log2 (TPM) normalized transcript expression of DEG between LN CD44^{hi} CD8^{+} T cells and TIL subsets. (D and E) Pearson correlation comparing our transcriptome data to publicly available data of progenitor and terminally exhausted CD8^{+} T cells from LCMV (D) and B16 melanoma (E).

We also compared the transcriptome data of the CD8^{+} TIL subsets to publicly available datasets with progenitor (PD1^{+}Slamf6^{+}) and terminally exhausted (PD1^{+}Tim-3^{+}) CD8^{+} T cells from both LCMV Cl13 and B16 melanoma (Fig 4D-E) (158). Intriguingly, when comparing to LCMV Cl13, we found that the Slamf6^{+} and Tim-3^{+} populations were less correlated to each other

than in B16 melanoma. Otherwise, we found similar trends when comparing our subsets to both of their systems—PD1^{hi}Tim-3^{+} cells were more similar to the Tim-3^{+} population than the Slamf6^{+} population, PD1^{hi} and PD1^{mid} cells have similar degrees of correlation to both of their sorted populations, and the PD1^{lo} cells have the least in common with their sorted populations.

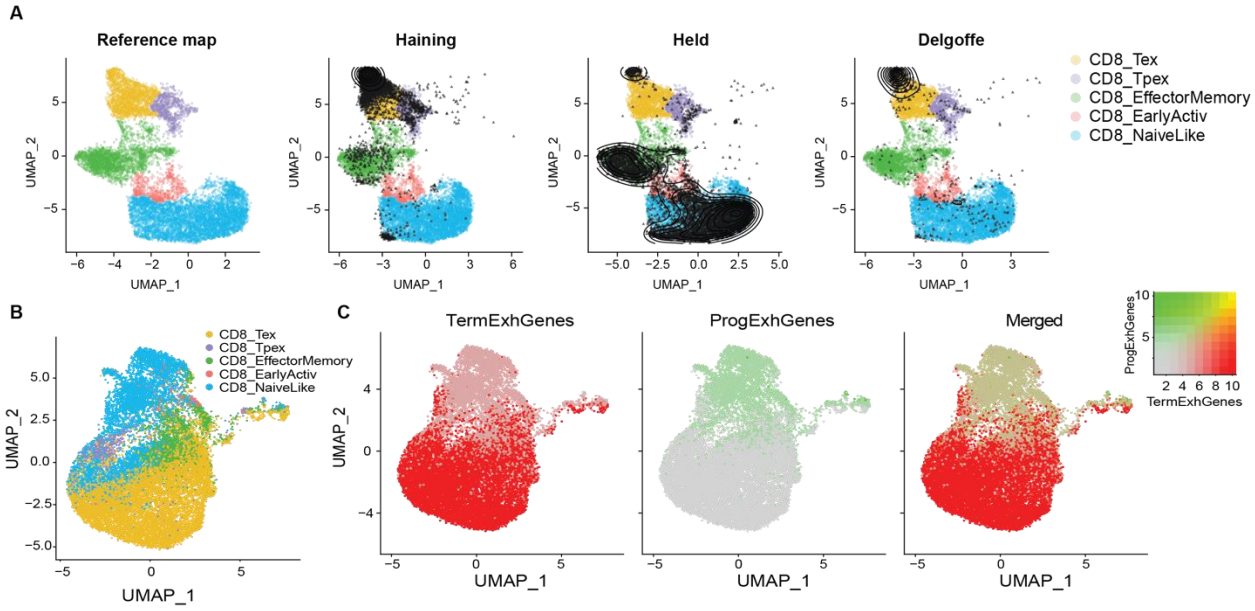

Figure 5. Signatures from Bulk RNAseq Align with Single Cell RNAseq
(A) Three B16 melanoma datasets were projected onto same space, and CD8^{+} T cells were annotated using ProjecTIL. Datasets are named by last name of the corresponding author. (B) B16 datasets were integrated and re-clustered with Seurat and annotated using ProjecTIL. (C) Plots showing expression of the terminal-specific and progenitor-specific DEGs identified in Fig. 2C.

Further, we used two publicly available and an internal single cell RNA sequencing (scRNAseq) datasets to determine how our sorted populations compared to the unbiased clustering that the single cell technology enables (158, 182). The internal Delgoffe scRNAseq was not enriched for a given cell type, so the number of CD8^{+} T cells was limited. We first used ProjecTIL to project and annotate these datasets onto a CD8^{+} T cell reference atlas that includes CD8^{+} T cells from a variety contexts, including MC38 tumors, to determine whether their reference atlas could be used to annotate the B16 CD8^{+} TIL (Fig. 5A) (183). We found that the terminal exhaustion annotation (Tex) was clear in each of the datasets, but there was a lack of a clear progenitor

exhausted population (Tpex) in any of them. Instead, the more progenitor-like $CD8^+$ TIL from B16 melanoma were annotated to the effector/memory and naïve-like clusters, especially in the Held dataset. These findings suggest that the progenitor exhausted cells in B16 melanoma and MC38 tumors may be more transcriptionally distinct from each other than the terminally exhausted clusters in these two tumor models. We next integrated the datasets using Seurat and again annotated using ProjecTIL (Fig. 5B). After integrating the data, we confirmed that there was no batch effect (not shown). To compare our bulk RNAseq to the scRNAseq, we created gene scores of our progenitor and terminally exhausted DEGs and plotted them on the annotated B16 $CD8^+$ TIL (Fig.5C). We found that the terminally exhausted-specific genes were highly enriched in the Tex clusters of the scRNAseq data, but the progenitor exhausted-specific genes were not as highly enriched. These results further confirm that our sorting strategy for $CD8^+$ TIL accurately identifies stem-like progenitor and terminally exhausted populations.

To better understand the DEGs identified between the progenitor and terminally exhausted clusters, we performed gene ontology (GO) analysis using Metascape (184). For the progenitor exhausted cluster, the analysis showed enrichment of GO terms that are generally associated with T cell activation and function, as well as GO terms known to be associated with these more migratory, stem-like cells, notably positive regulation of cell migration and chemotaxis (Fig. 6A). For the terminally exhausted cluster, the analysis showed enrichment of GO terms associated with proliferation, metabolism, and the DNA damage response (Fig. 6B). Additionally, we compared the DEGs that we identified to gene sets known to be associated with each of these $CD8^+$ T cell states (Fig. 6C-D). $PD1^{lo/mid}$-specific genes confirmed a signature similar to one described for progenitor exhausted cells (*Slamf6*, *Tcf7*, *Bcl6*, *Id3*, *Lef1*, and *Tnf*), whereas $PD1^{hi}Tim\text{-}3^+$ cells had a signature consistent with terminal exhaustion (*Lag3*, *Tox*, *Ifng*, *Prdm1*, and *Id2*). Thus, PD1 and

Tim-3 expression identified progenitor and terminal states of exhaustion that transition from the PD1^{mid} to the PD1^{hi} stage.

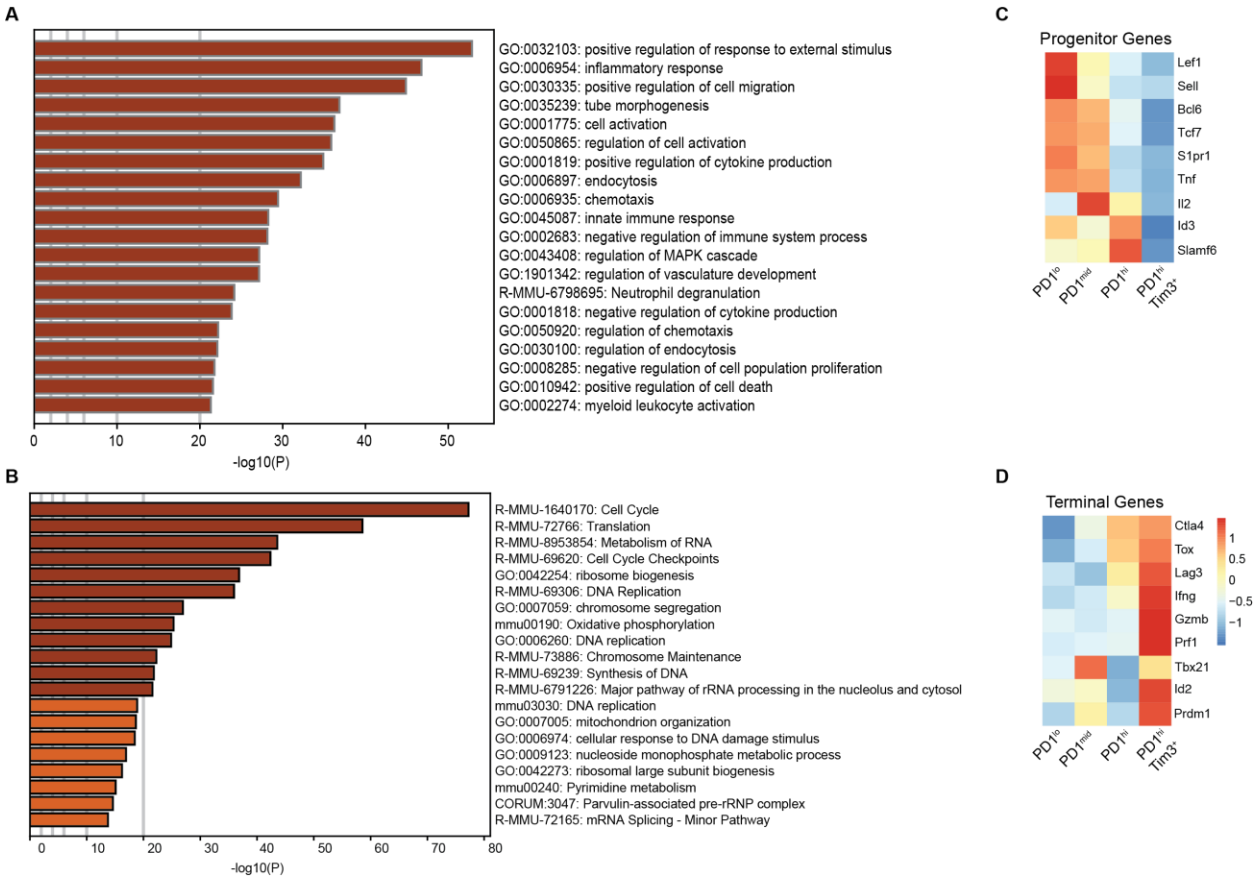

Figure 6. Progenitor and Terminally Exhausted Tumor-Infiltrating CD8$^+$ T Cells Express Associated Gene Sets
(A and B) Metascape gene ontology analysis of progenitor (A) and terminally (B) exhausted clusters. (C and D) Gene expression of known genes associated with T cell stemness (C) and terminal differentiation (D).

2.2.2 Histone Modifications Underlying Transcriptional Changes

We used CUT&RUN to generate a foundational map of chromatin states to assess active chromatin (H3K4me3, H3K9ac, and H3K27ac) and repressed chromatin (H3K27me3) (Fig. 3). To determine whether chromatin states of the sorted populations were consistent with gene expression, 20-kb regions of chromatin around the transcription start site (TSS) of DEG up-regulated in PD1^{lo} progenitor cells or PD1^{hi}Tim-3$^+$ terminal cells were assessed to include

proximal and more distal elements regulating gene expression. Genes upregulated in PD1^{lo} cells displayed increased active histone modifications (H3K4me3, H3K27ac, and H3K9ac) compared to terminally exhausted cells and had less of the repressive modification (H3K27me3) (Fig. 7A-B). Terminally exhausted cells (PD1^{hi}Tim-3^{+}) exhibited a bimodal distribution of H3K27me3 at progenitor-specific genes, with some having increased H3K27me3 (i.e.,Tcf7), indicative of chromatin repression as cells differentiated to a terminal state. Yet some genes remained low for H3K27me3 (i.e., Ppargc1a), suggesting that loss of active histone modifications may be sufficient to down-regulate gene expression (Fig. 7C). A similar pattern was observed for genes specific to terminal exhaustion, with increased active histone modifications (H3K4me3, H3K27ac, and H3K9ac) at genes upregulated in PD1^{hi}Tim-3^{+} (Fig. 7D-E). In contrast to the bimodal distribution at progenitor-specific genes, H3K27me3 at terminal-specific genes was considerably increased in PD1^{lo} cells and reduced in PD1^{hi}Tim-3^{+}, suggesting the progression to terminal exhaustion requires H3K27 demethylation for genes to become up-regulated (Fig. 7E). For example, at the Tox locus, H3K27me3 was reduced in PD1^{hi}Tim-3^{+} cells, whereas active marks were increased (Fig. 7F). We next determined whether changes in chromatin accessibility measured by ATAC-seq in publicly available datasets had similar alterations based on DEGs (5). Unexpectedly, we found limited changes in chromatin accessibility, suggesting that changes in histone modifications provide a more nuanced view of epigenomic control of transcriptional programs for states of exhaustion (Fig. 7G). These data suggest that gene expression alterations during the progression to exhaustion are due to epigenetic changes that regulate transcriptional control of gene expression.

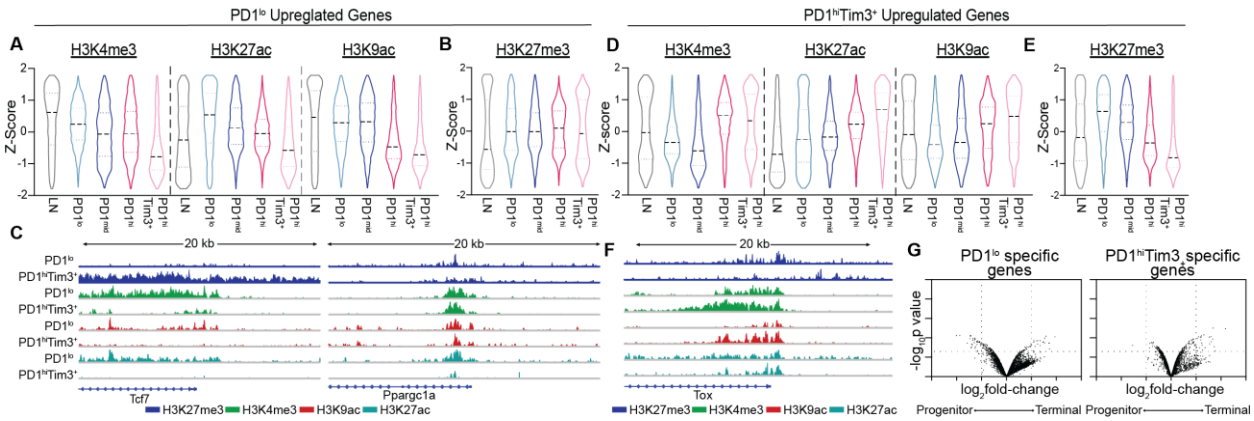

Figure 7. Expressed Genes Are Associated with Increases in Active and Decreases in Repressive Histone Modifications
(A) H3K4me3, H3K27ac, H3K9ac H3K27me3 coverage of genes up-regulated in PD1^{lo} cells. Z score of tag counts per million (CPM) of 10 kb regions surrounding the TSS. (B) Genome browser views of Tcf7 and Ppargc1a in indicated subsets. (C) H3K4me3, H3K27ac, H3K9ac, and H3K27me3 coverage of genes up-regulated in PD1^{hi}Tim-3^{+} cells. Z score of CPM of 10-kb regions surrounding the TSS. (F) Genome browser views of Tox. (G) Volcano plots of chromatin accessibility data, showing differential ATAC peaks from progenitor (left) and terminally exhausted (right) CD8^{+} T cells.

We next compared our CUT&RUN datasets with previously published chromatin immunoprecipitation sequencing (ChIP-seq) analysis of naïve, effector, and memory CD8^{+} T cells (185). Interestingly, H3K4me3 in effector CD8^{+} T cells had similarities to terminal exhaustion, whereas naïve, memory, and memory precursor cells had distinct profiles of active promoters (Fig. 8A). In contrast, active enhancers marked by H3K27ac showed little correlation between TIL subsets and effector, memory, or naïve cells (Fig. 8B). Repressed chromatin regions were similar between memory and progenitor exhausted cells, suggesting a shared landscape of repressed genes (Fig. 8C). Thus, states of exhaustion in TILs are distinct from naïve, effector, and memory CD8^{+} T cells responding to infection at both the transcriptome and epigenome.

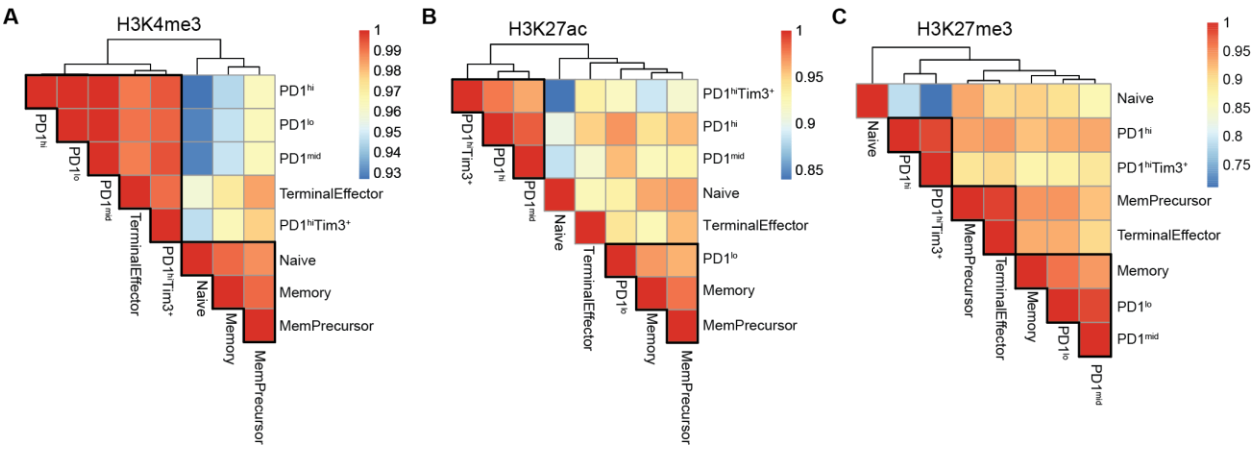

Figure 8. Histone Modifications of Tumor-Infiltrating CD8$^+$ T Cells Are Distinct from Effector and Memory. (A-C) Pearson correlation comparing histone modifications H3K4me3 (A), H3K27ac (B), and H3K27me3 (C) between naïve, terminal effector, memory precursor, memory, and tumor-infiltrating CD8$^+$ T cell populations.

2.3 Discussion

Transcriptional analyses of T cell subsets have provided extraordinary depth to our understanding of how T cells develop and differentiate. Ours and others' analyses of the transcriptional changes underlying differentiation leading to exhaustion have defined clear progenitor and terminally exhausted CD8$^+$ T populations in both chronic viral infection and within solid tumors.

2.3.1 Exhausted CD8$^+$ TIL from B16 Melanoma Have Features of Exhaustion Program

It has become clear that while there are shared features in the different contexts where exhaustion has been described, distinct microenvironmental signals influence gene expression. Indeed, our transcriptional analyses have shown that our sorted progenitor and terminally exhausted cells contain many of the same features and gene signatures that have been reported for

exhausted cells, but when we compared our sorted $CD8^+$ TIL to sorted $CD8^+$ T cells LCMV Cl13, we found that there was a reduced correlation in TILd, relative to LCMV. Intriguingly, when we used ProjecTIL to project B16 scRNAseq datasets onto the ProjecTIL reference map, which uses T cells from MC38 tumors to define progenitor and terminally exhausted cells, we found that the projected cells from B16 melanoma are primarily enriched in a specific part of the Texh cluster, suggesting that the population is more homogeneous. Future work should confirm these inferences and address whether these cells are more terminally differentiated compared to analogous cells in MC38 tumors. Additionally, the more progenitor-like populations were not identified in the Tpex cluster but instead were found primarily in the effector/memory and naïve-like clusters. Notably, MC38 tumors are responsive to αPD1 therapy, which specifically targets progenitor exhausted T cells, whereas B16 melanoma tumors are not (158, 186-189). The transcriptional differences in $CD8^+$ T cell subsets between these two tumor types may contribute to our understanding of why only one is responsive to αPD1, which act on progenitor exhausted cells to drive a more effector-like differentiation.

We also used GO analysis to obtain an unbiased overview of the types of genes that were enriched in the progenitor and terminally exhausted subsets. Unsurprisingly, this revealed distinct gene programs enriched in each subset. Progenitor exhausted cells were enriched in genes that were more associated with immune function, suggesting that while TCF-1^+ cells in chronic viral infection and tumors are committed to exhaustion, they still have the capability to drive effector responses, as has been shown by other groups (157, 188, 190, 191). Intriguingly, terminally exhausted $CD8^+$ T cells were enriched primarily in gene programs associated with cell cycling, DNA replication, and DNA damage. Indeed, we have shown that these cells are more proliferative than the progenitor exhausted cells (data not shown). However, reduced proliferative capacity is a

well-established hallmark of T cell exhaustion (45). These contrasting findings are primarily due to the differences in the context they are considered in and the comparators. When reduced proliferative capacity was defined as a hallmark of exhausted cells, the comparison was between effector cells in acute infection and exhausted cells. Additionally, these cells do not have increased proliferation upon αPD-1 therapy, unlike the progenitor exhausted cells (187). Other studies have primarily examined cell number or population doublings to define the reduced proliferative capacity of terminally exhausted T cells (72). This approach is problematic because it does not actually define the proliferative capacity but rather the proportion of proliferation to the amount of cell death. Our findings indicate that terminally exhausted cells undergo a high degree of non-productive proliferation, with an amount of cell death that is greater than or equal to the increased proliferation.

2.3.2 Active and Repressive Histone Modifications Are Associated with Increased and Decreased Expression, Respectively

After defining differentially expressed genes, we explored how four histone modifications were changing at these gene loci, the active H3K27ac, H3K4me3, and H3K9ac and the repressive H3K27me3. Unsurprisingly, we found that the active modifications were increased in progenitor exhausted cells in known progenitor exhausted-specific genes, while H3K27me3 was lower in progenitor exhausted cells (Fig. 5A-B). Intriguingly, the amount of H3K27me3 in terminally exhausted cells at progenitor-specific genes was bimodal, suggesting that the removal of the active histone modifications is sufficient to decrease gene expression. For terminally exhausted cells, we found similar trends, with increases in active modifications associated with the increased expression in terminal exhaustion-specific genes (Fig. 5C). However, H3K27me3 was found at

high levels in progenitor exhausted cells; this is a mark that must be removed for gene expression during differentiation (Fig. 5D). These findings broadly confirm what has long been understood about how these histone modifications regulate gene expression (107).

2.3.3 Conclusions

Our studies confirm what others have shown that progenitor and terminally exhausted T cells are transcriptionally unique. Indeed, we find that progenitor exhausted cells maintain more stemness and functional capacity, whereas terminally exhausted cells have increased expression of genes associated with terminal differentiation. Intriguingly, we also show that terminally exhausted cells also express high levels of genes associated with cell cycling and proliferation. Finally, we confirm the known roles of active and repressive histone modifications in regulating the differentially expressed genes in these populations.

3.0 Anticorrelated Genes in Terminally Exhausted Tumor-Infiltrating CD8$^+$ T Cells

Cytotoxic CD8$^+$ T cells play a crucial role in the immune response to tumors. However, prolonged exposure to tumor antigens leads to a state of functional impairment, known as exhaustion. T cell exhaustion was initially described in the context of chronic viral infections, by increased co-inhibitory receptor expression, reduced functionality, and increased susceptibility to apoptosis. While dysfunctional CD8$^+$ T cells responding to tumors share many similarities with exhausted CD8$^+$ T cells from chronic viral infections, there remains debate regarding whether the differentiation processes triggered by tumor antigens and viral antigens are identical.

Here, we explored how tumor-infiltrating CD8$^+$ T cells (TIL) histone modifications change throughout the genome as they progressively differentiate within the tumor, independent of changes in gene expression, again using our CUT&RUN data. We performed differentially enriched peak analysis (DEP) on each of the three histone modifications associated with active chromatin, H3K27ac, H3K4me3, and H3K9ac, followed by nearest peak-to-gene annotation to identify how the corresponding gene expression was changing. This inverse look at the epigenetic changes in exhausted CD8$^+$ TIL enabled us to understand how these modifications were changing, independent of DEG changes and to identify a chromatin feature unique to terminally exhausted cells. Additionally, we performed motif analysis to predict which transcription factor binding sites are enriched in progenitor and terminally exhausted subsets. Finally, we treated tumor-bearing mice with α-PD1 blocking and α-41BB agonist antibodies to determine how gene expression changes after treatment.

Data in this chapter have been previously published in Science Immunology. Manuscript information: Ford, BR, Vignali, PD, Rittenhouse, NL, Scharping, NE, Peralta, R, Lontos, K,

3.1 Introduction

As described in chapter 2, histone modifications are essential epigenetic marks that shape the chromatin landscape and regulate gene expression. We profiled three well-studied active histone modifications, H3K27ac, H3K4me3, and H3K9ac, which have key roles in transcriptional regulation and gene activation. H3K27ac is a mark of active enhancers, whereas H3K9ac and H3K4me3 are marks of active gene bodies and promoters, respectively (113). Enhancers play a critical role in regulating cell type-specific gene expression. The interaction between enhancers and target genes is responsible for fine-tuning gene expression patterns. One primary mechanism by which enhancers drive increased gene expression is through the looping of H3K27ac-marked active enhancer regions, which can be found quite distally, to the target gene promoter via the Mediator complex (192). This process brings key transcription factors to the basal transcriptional machinery and is necessary for the initiation of transcription (193). The association of H3K4me3 and active gene promoters has been widely accepted, but only recently was it shown that H3K4me3 is actually necessary for nascent transcription, by release of RNA polymerase II (pol II) from initiation to elongation (194). H3K9ac, which is often found at similar genomic regions to H3K4me3, is also crucial for release of RNA pol II from initiation to elongation (195). These histone modifications have been clearly associated with increased transcription, with H3K27ac-

marked active enhancers primarily affecting the initiation of transcription, and H3K4me3 and H3K9ac playing a role in the initiation-to-elongation transition.

The role of epigenetic changes in regulating $CD8^+$ T cell differentiation has been widely explored, using chromatin accessibility, histone modifications, and DNA methylation to define cell type-specific regulatory regions (196, 197). Indeed, changes in each of these modalities is necessary for effector/memory differentiation, as well as exhaustion. This report describes the increased proportion of active chromatin that does not have corresponding increases in gene expression, identifying a chromatin feature that is unique to terminally exhausted cells. Additionally, it explores the role of the AP-1 transcription factor family in regulating this chromatin feature and proposes a new target for cancer immunotherapy.

3.2 Results

3.2.1 Active Chromatin in Terminally Exhausted Tumor-Infiltrating $CD8^+$ T Cells Have Low Correlation with Transcription

To identify active enhancers specific to progenitor or terminal states, we performed differentially enriched peak (DEP) analysis of H3K27ac across TIL subsets (Fig. 9A). Enhancers promote gene expression, so we interrogated transcription of genes found closest to enhancers specific for each population of cells. In progenitor cells, most active enhancers (~85%) correlated with increased gene expression, which decreased as cells differentiated to terminal exhaustion (Fig. 9B-J). In contrast, in terminally exhausted T cells, only ~55% of active enhancers correlated with gene expression; an extensive fraction (~45%) had anticorrelated gene expression (Fig. 9C-K).

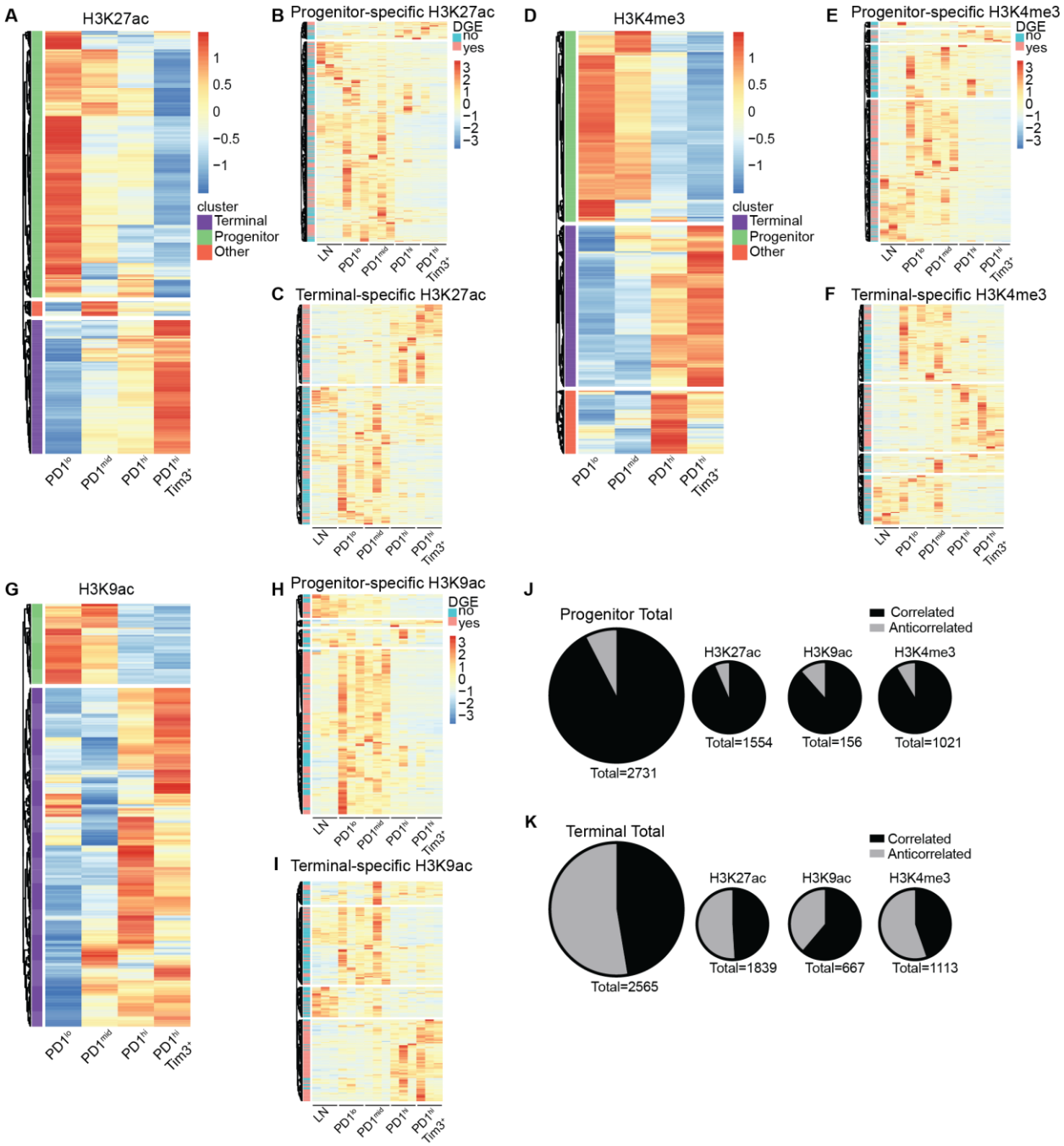

Figure 9. Progenitor and Terminally Exhausted Cells Have Distinct Profiles of Active Histone Modifications
(A) Tag counts (normalized per million) of H3K27ac at differential peaks between TIL subsets (DESeq2). (B and C) Normalized expression of genes nearest to progenitor-specific (B) and terminal-specific (C) H3K27ac peaks. Genes that meet DEGs cutoffs (fold change > 2, P < 0.05) in pink to the left of heatmap. (D) Tag counts (normalized per million) of H3K4me3 at differential peaks between TIL subsets (DESeq2). (E and F) Normalized expression of genes nearest to progenitor-specific (E) and terminal-specific (F) H3K4me3 peaks. Genes that meet DEGs cutoffs (fold change > 2, P < 0.05) in pink to the left of heatmap. (G) Tag counts (normalized per million) of H3K9ac at differential peaks between TIL subsets (DESeq2). (H and I) Normalized expression of genes nearest to progenitor-specific (E) and terminal-specific (F) H3K9ac peaks. Genes that meet DEGs cutoffs (fold change > 2, P < 0.05) in pink to the left of heatmap. (D and E) Number of genes with and without corresponding expression in progenitor (D) and terminally exhausted T cells for (E) H3K27ac, H3K9ac, H3K4me3, and the total of all three.

Although distal enhancers may account for a fraction of these, it is unlikely that enhancer distance would be vastly different in TIL populations (Fig. 9J-K). Additionally, we explored how H3K9ac and H3K4me3, marks associated with the gene body and promoter, respectively, related to gene expression in TIL populations (Fig. 9D-I). Like active enhancers, progenitor-specific H3K4me3 and H3K9ac primarily correlated with gene expression, whereas terminal-specific H3K4me3 and H3K9ac had a substantial fraction of genes that were not correlated (Fig. 9J-K).

Additionally, enhancer activity correlated with other marks of active chromatin (H3K9ac and H3K4me3) at both correlated and anticorrelated genes (Fig. 10A-D). The combined presence of multiple active chromatin marks had no correlation with increased gene expression, as similar amounts of H3K9ac and H3K27ac were associated with H3K4me3-specific peaks in both correlated genes and anticorrelated genes (Fig. 10A-B). These trends were also seen when specifically looking for correlated genes (*Havcr2*, *Prdm1,* and *Ifng*) and anticorrelated genes (*Il10*, *Runx2*, and *Irf8*) (Fig. 10C-D). In contrast, OT-I effector T cells responding to Vaccinia-OVA primarily had correlated gene expression at active promoters, suggesting that the presence of active chromatin with anticorrelated gene expression was specific to terminal exhaustion (Fig. 11A-B). Thus, accumulation of active chromatin marks alone is insufficient to predict gene expression in terminally exhausted TILs. Although expression of exhaustion-associated molecules PD1 and Tim-3 reliably identify tumor antigen–specific $CD8^+$ T cells, sorted $PD1^{lo}$ T cells may be contaminated by so-called “bystander” T cells that display an activated cell signature without T cell receptor (TCR) engagement in tumors (198).

To determine whether correlated and anticorrelated gene expression were preserved in tumor-specific T cells, we performed RNA-seq on adoptively transferred TCR-Tg pmel-1 T cells

specific for the melanoma antigen gp100. By day 12, most transferred pmel-1 T cells displayed high

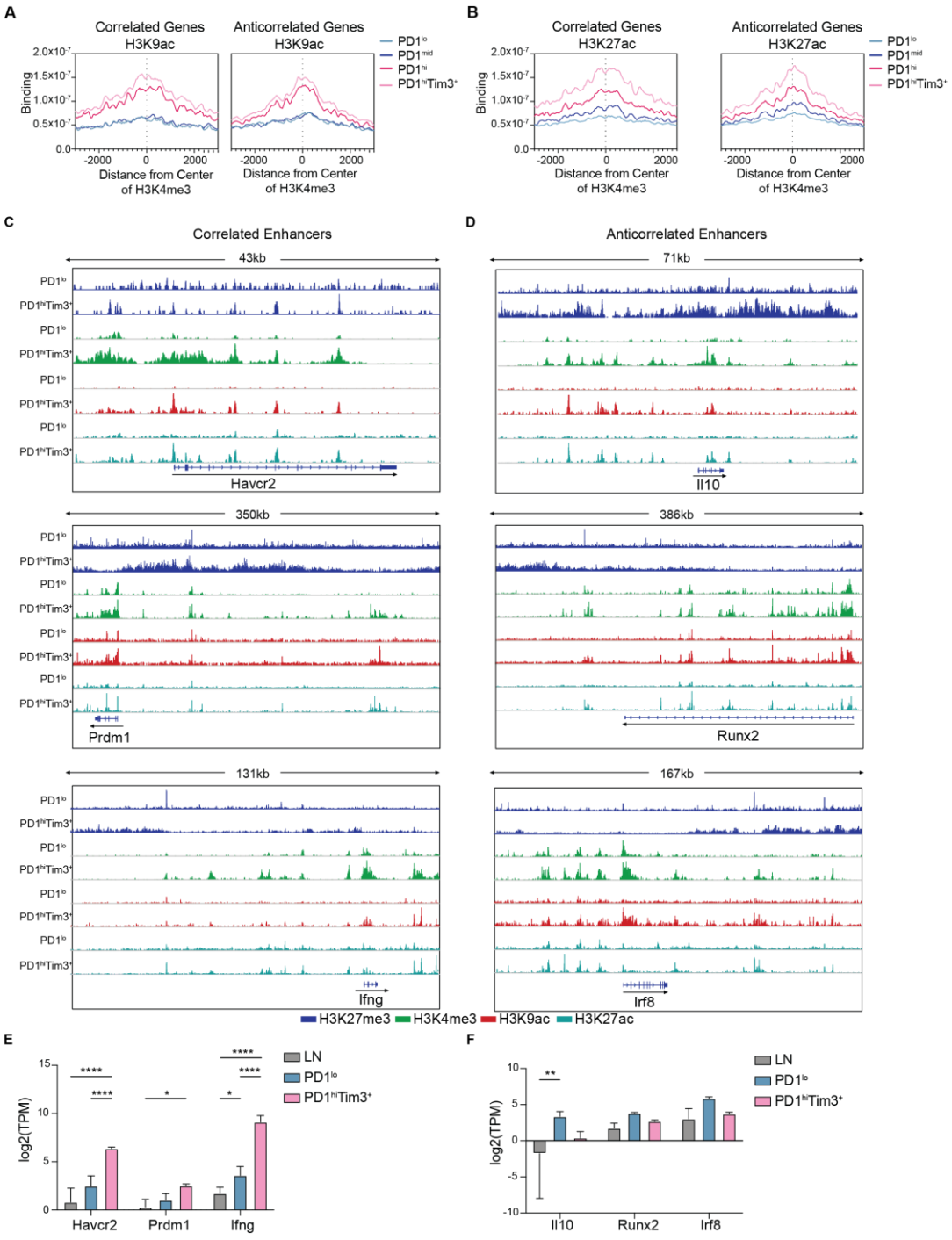

Figure 10. Overlapping Active Histone Modifications In Progenitor and Terminally Exhausted T Cells
(A) Histograms showing H3K4me3 coverage at correlated and anticorrelated H3K9ac terminal exhaustion specific peaks. (B) Histograms showing H3K4me3 coverage at correlated and anticorrelated H3K27ac terminal exhaustion specific peaks. (C) Representative IGV plots showing changes in H3K27me3, H3K4me3, H3K9ac, and H3K27ac at

the correlated genes Havcr2, Prdm1, and Ifng. (D) IGV plots showing changes in H3K27me3, H3K4me3, H3K9ac, and H3K27ac at the anticorrelated genes Il10, Runx2, and Irf8. (E) Log2 normalized gene expression (mean and SD) of the correlated genes Havcr2, Prdm1, and Ifng. p value (DESeq2); *p<0.05, **p<0.01,***p<0.001,****p<0.0001. (F) Log2 normalized gene expression (mean and SD) of the correlated genes Il10, Runx2, and Irf8. p value (DESeq2); *p<0.05, **p<0.01,***p<0.001,****p<0.0001.

Expression of PD1 and Tim-3. Thus, we staggered transfers of pmel-1 T cells 12 and 7 days before sacrifice and used congenic Thy1.1 expression to identify differentiated PD1^{hi}Tim-3^{+} pmel-1 T cells transferred early in tumor progression and newly infiltrating PD1^{lo} pmel-1 T cells transferred later (Fig. 12A). PD1^{hi}Tim-3^{+} pmel-1 T cells exhibit increased expression of correlated genes, compared with PD1^{lo} pmel-1 T cells, whereas genes defined as anticorrelated were unchanged and enriched in expression in PD1^{lo} pmel-1 T cells (Fig. 12B-C). Thus, the presence of anticorrelated genes is likely not due to a difference in responsiveness to tumor antigens and is a hallmark of terminal exhaustion.

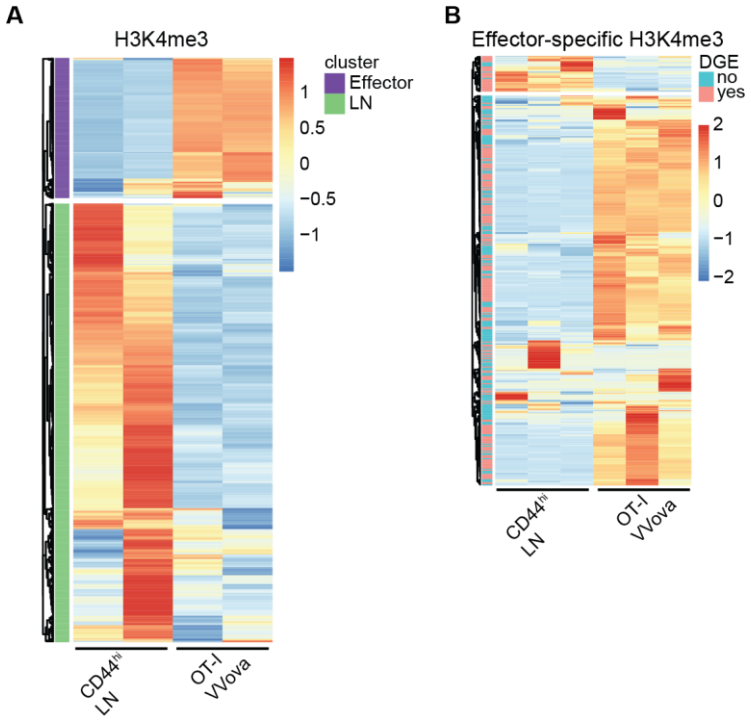

Figure 11. Effector-Specific Active Chromatin Is Not Associated with an Increased Proportion of Anticorrelated Genes

(A) Heatmap shows DESeq2 log2 normalized tag counts of H3K4me3 differential peaks between CD44^{hi} LN and OT-I effector cells. (B) Heatmap of log2 normalized expression of genes nearest to effector-specific H3K4me3 peaks. Those genes that meet differentially expressed genes cutoffs (FC >2, p val < 0.05) marked in pink on the left side of heatmap.

Finally, we explored transcriptional pathways associated with progenitor-specific and terminal-specific active chromatin regions, breaking terminal-specific active chromatin into correlated and anticorrelated genes. Gene Ontology (GO) pathway analysis demonstrated both overlapping and distinct pathways to each group of genes, including T cell activation and lymphocyte or leukocyte pathways, PD1 signaling, cell adhesion, and cell migration (Fig. 13A). Genes involved in T cell activation/function were among those specifically expressed in progenitor- and terminal-specific regions of active chromatin (Fig. 13B-C). Together, these data reveal genes critical for T cell activation and function that were not up-regulated in exhausted T cells, despite the presence of multiple active chromatin marks. Thus, terminally exhausted TILs have a unique chromatin landscape characterized by the presence of active histone modifications but without corresponding active gene transcription.

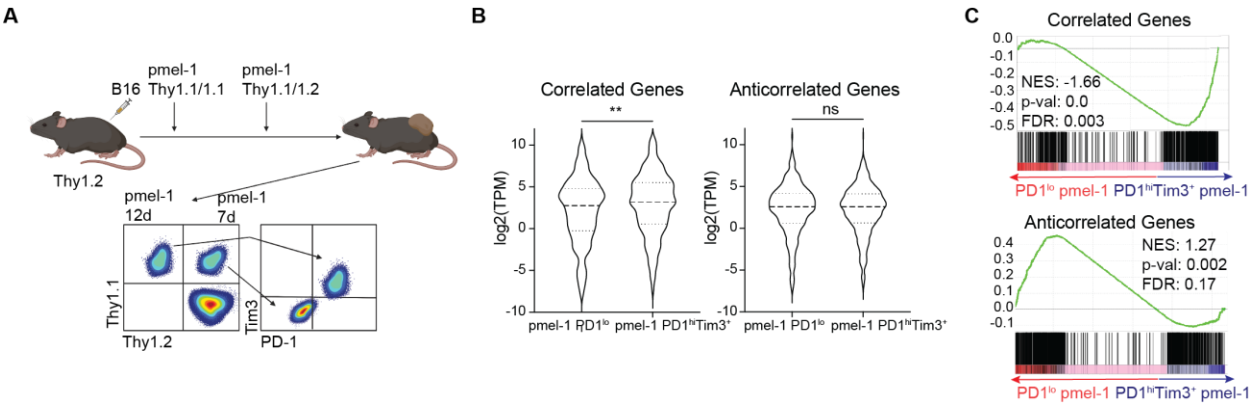

Figure 12. Lack of Corresponding Gene Expression at Anticorrelated Genes Is Antigen-Independent
(A) Experimental design of transcriptome analysis of tumor-specific progenitor and terminally exhausted pmel-1 CD8 T cells in B16 melanoma. (B) Log2 normalized expression of correlated genes (left) and anticorrelated genes (right) identified in Fig 3. p value (DESeq2, generated by one-way ANOVA); *p<0.05, **p<0.01,***p<0.001,****p<0.0001. (C) Gene set enrichment analysis of tumor-specific pmel-1 progenitor and terminally exhausted T cell transcriptomes for correlated or anticorrelated genes defined in Fig. 6.

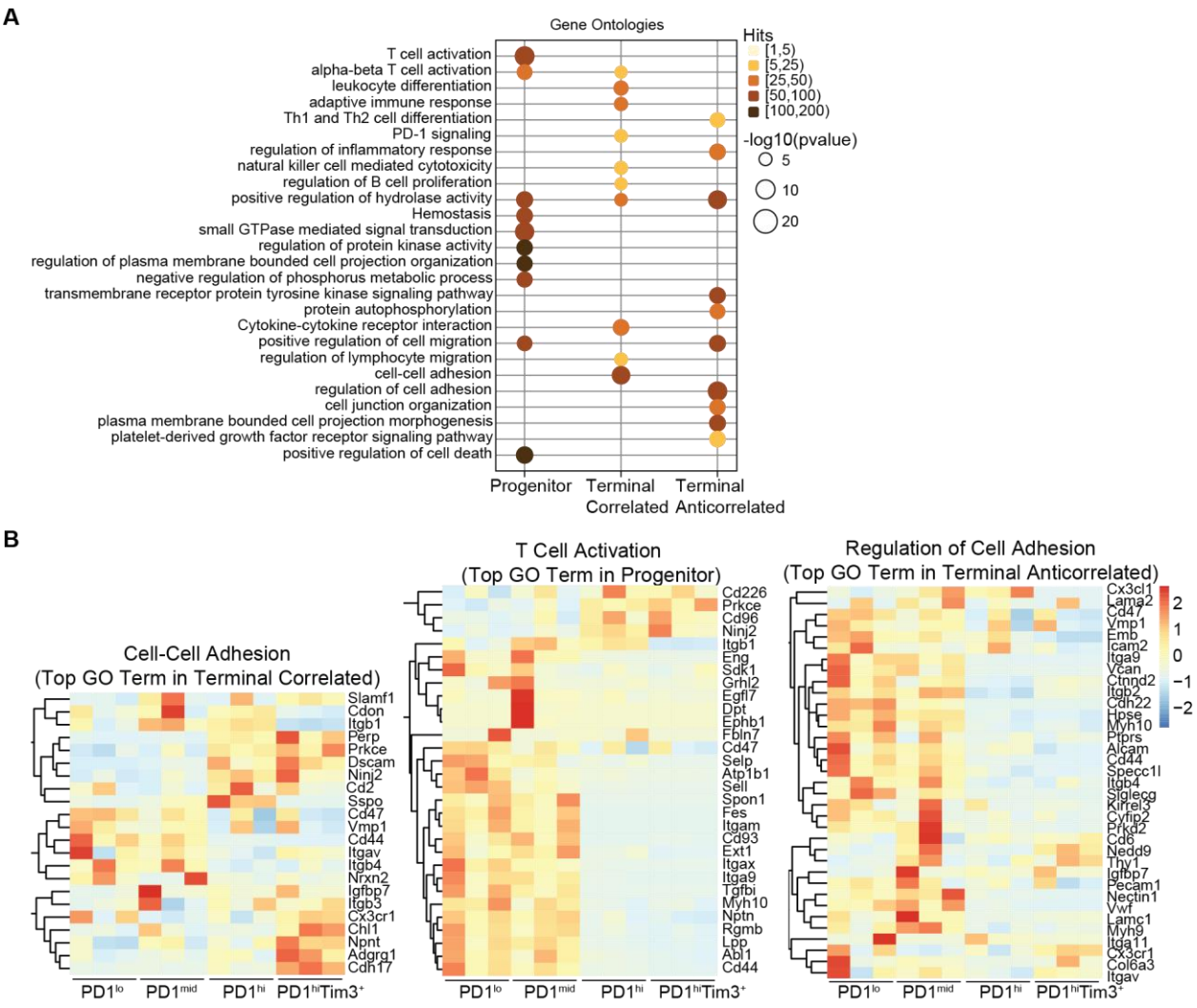

Figure 13. Gene Ontology of Progenitor, Terminal Correlated, and Terminal Anticorrelated Genes
(A) Enrichment of GO terms via Metascape in genes with active chromatin landscapes in indicated groups. (B) Log2-normalized expression of select genes enriched in GO pathways in (A). FDR, false discovery rate; NES, normalized enrichment score.

3.2.2 Anticorrelated Genes Are Enriched in AP-1 Binding Motifs

We next sought to understand why a significant fraction of genes in terminally exhausted cells maintain active chromatin but lack gene expression. Increased H3K27me3 might repress these genes; however, the levels of this mark were similar at correlated and anticorrelated genes

(not shown). Active chromatin is permissive, but transcription factors are required to recruit machinery to drive

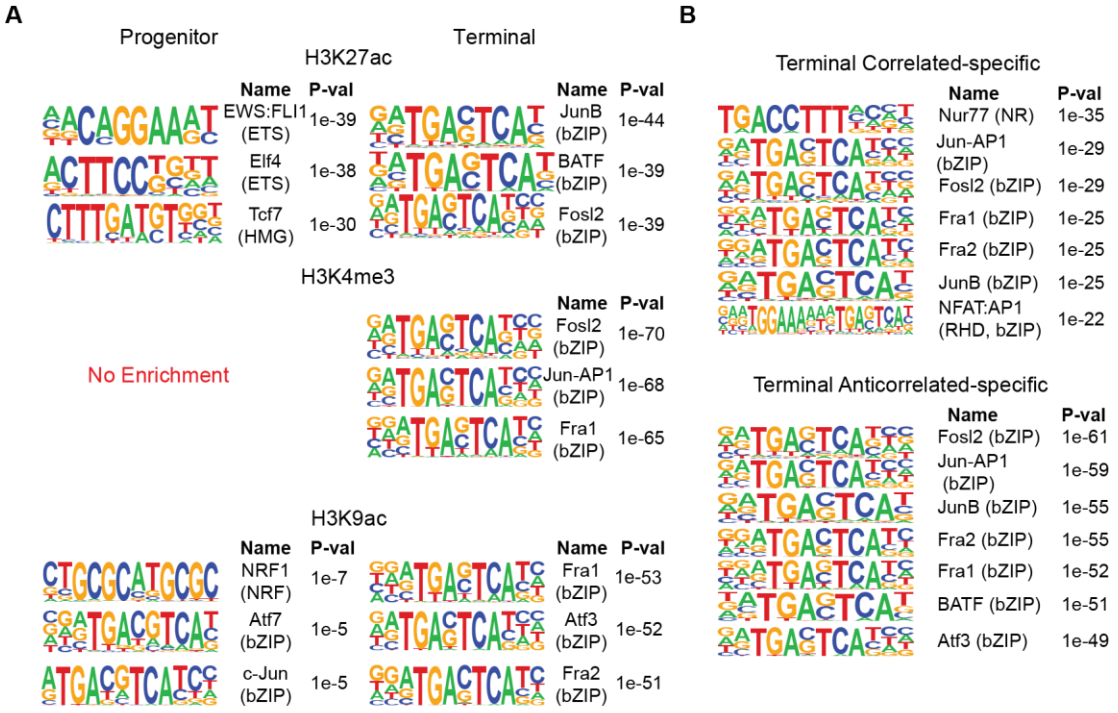

Figure 14. Active Chromatin in Terminally Exhausted Tumor-Infiltrating CD8$^+$ T Cells Is Enriched for AP-1 Family Motifs

(A) Top results from HOMER motif analysis of DESeq2-defined H3K27ac, H3K4me3, and H3K9ac differential peaks in progenitor or terminally exhausted T cells. Terminally exhausted–specific peaks used as background for progenitor exhausted–specific analysis and vice versa. (B) Top results from HOMER motif analysis of correlated and anticorrelated peaks compiled for each mark. Progenitor exhausted–specific peaks used as background for both correlated and anticorrelated analyses. (C) Fold change in PageRank score (y axis) and fold change in gene expression (x axis) for transcription factors. H3K4me3, H3K27ac, gene expression data, and HOMER.

gene expression (199). Progenitor-specific enhancers were enriched for motifs from the erythroblast transformation specific (ETS) family and TCF1, whereas terminal-specific enhancers had enrichment for the basic leucine zipper domain (bZIP) consensus sequence bound by activator protein 1 (AP-1) family members (Fig. 14A). Terminal-specific H3K4me3 and H3K9ac peaks were also enriched for bZIP motifs, whereas progenitor-specific H3K4me3 and H3K9ac peaks had less specific enrichment of any motifs. bZIP motifs were also enriched in enhancers of both correlated genes and anticorrelated genes; however, two notable motifs were enriched only in

correlated genes: Nur77 and the composite nuclear factor of activated T cells (NFAT):AP-1 motif (Fig. 14B). Nur77 (encoded by *Nr4a1*) activity correlates with recent TCR stimulation, and

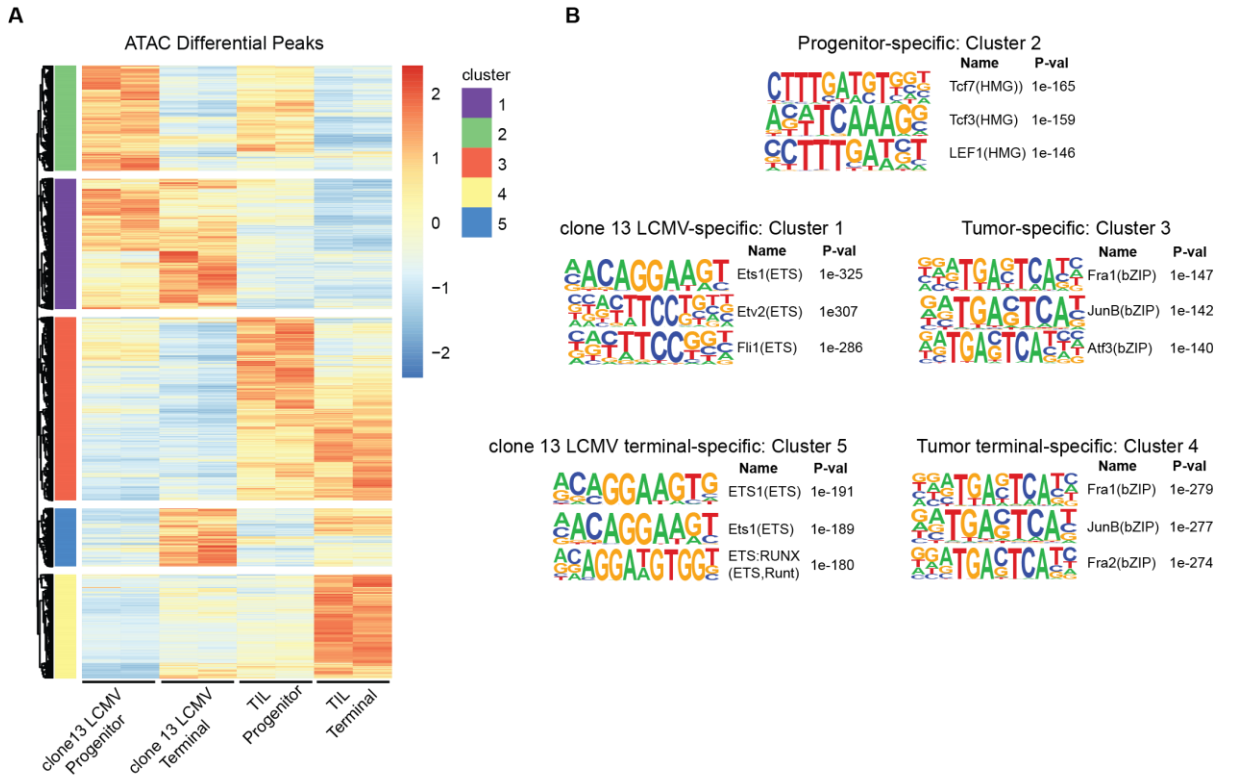

Figure 15. AP-1 motif enrichment in exhausted cells is tumor-specific
(A) Heatmap shows DESeq2 log2 normalized tag counts of defined differentially accessible peaks between exhausted subsets from chronic LCMV and B16 melanoma (GSE123235). (B) HOMER motif analysis for each cluster defined in (A). Default background was used for all motif analyses.

NFAT:AP-1 complexes occur in response to TCR and costimulatory signaling, suggesting that, consistent with prior work, activating signals promote expression of terminal exhaustion–specific genes (200, 201). Exhaustion is driven by continuous antigen receptor stimulation; thus, altered TCR signaling may contribute to the loss of gene expression despite the presence of active chromatin. Chronic antigen stimulation–driven exhaustion also occurs in the context of chronic viral infection; therefore, we sought to determine whether bZIP motifs were enriched in terminally exhausted $CD8^+$ T cells responding to chronic virus. We used published ATAC-seq datasets of progenitor and terminally exhausted $CD8^+$ T cells isolated from both chronic (clone 13)

lymphocytic choriomeningitis virus (LCMV) and B16 tumor models from the same study as above (158). We identified five clusters that could be distinguished as progenitor specific (cluster 2), LCMV specific (cluster 1), tumor specific (cluster 3), LCMV terminal specific (cluster 5), and tumor terminal specific (cluster 4) (Fig. 15A). Motif analysis identified Tcf7 and Lef1 consensus sequences specific to progenitor cells (cluster 2), whereas bZIP motifs were highly enriched in tumor-specific and tumor terminal–specific clusters (clusters 3 and 4) (Fig. 15B). In contrast, ETS motifs were enriched in LCMV-specific and LCMV terminal–specific clusters (clusters 1 and 5) (Fig. 15B). Thus, enrichment of bZIP/AP-1 motifs in terminal active chromatin regions was specific to tumor-mediated exhaustion.

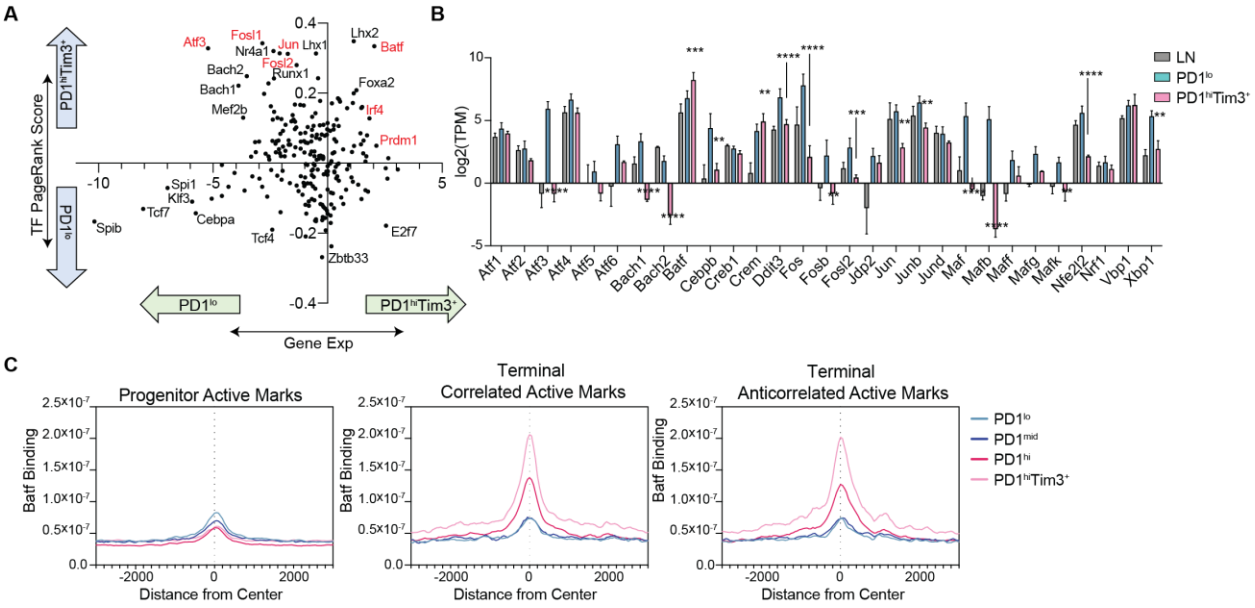

Figure 16. AP-1 Activity Is Not Responsible for Lack of Expression of Anticorrelated Genes
(A) Fold change in PageRank score (y axis) and fold change in gene expression (x axis) for transcription factors. H3K4me3, H3K27ac, gene expression data, and HOMER motif list were provided to Taiji. (B) Expression of AP-1 family members in LN, PD1^{lo}, and PD1^{hi}Tim-3^{+} (mean and SD). P value (generated by a Wald test in DESeq2); **P < 0.01, ***P < 0.001, and ****P < 0.0001. (C) Batf coverage (n = 1) at progenitor, correlated, and anticorrelated active peaks defined by presence of H3K27ac, H3K9ac, or H3K4me3.

To further identify transcription factors that play a role in gene regulation, we performed Taiji PageRank analysis, which uses an integrative "multiomics" framework to identify regulatory networks and candidate driver transcription factors (20, 23). Highly ranked transcription factors in

progenitor cells correlated with increased expression of those factors (Fig. 16A). In contrast, many of the transcription factors highly ranked in terminally exhausted cells were decreased in expression, with notable exceptions (Batf, Prdm1, and Irf4) (Fig. 16A). Many of these down-regulated but highly ranked factors were AP-1 family members (Atf3, Jun, and Fosl2). Most bZIP transcription factors were down-regulated in terminal cells, with few exceptions including Batf (Fig. 16B). CUT&RUN revealed that Batf was not bound at sites of active chromatin (H3K27ac, etc.) in progenitor cells but was highly enriched in terminally exhausted cells (Fig. 16C). No differences were noted between correlated gene and anticorrelated genes. These data suggested that the AP-1 family member Batf was bound specifically in terminal cells at places where active chromatin is present.

3.2.3 Costimulatory Signaling Drives Expression of Anticorrelated Genes

Our results suggest that exhausted T cells harbor enhancers defined by AP-1 binding sites not actively promoting transcription. AP-1 is driven by co-stimulation, and NFAT in the absence of AP-1 drives programs like anergy and exhaustion (201). Exhausted T cells express high levels of both inhibitory and costimulatory receptors (45), most notably 4-1BB (CD137, encoded by Tnfrsf9) (202). Agonistic antibodies to 4-1BB are under intense clinical investigation, and we and others have shown that 4-1BB agonists restore function in exhausted T cells (203). 4-1BB signaling promotes activation of AP-1 family members (204). Thus, we asked whether checkpoint blockade or costimulatory agonist therapy could restore transcription at the defined anticorrelated loci. B16-bearing mice were treated with either anti-PD1 (blocking) or anti–4-1BB (agonist) immunotherapy, and progenitor or terminally exhausted subsets were sorted for RNA-seq (Fig. 17A). Only anti–4-1BB treatment led to increased expression of AP-1 family members, including

Atf3, Batf3, and Mafb (Fig. 17B), yet both immunotherapies increased inflammatory response genes (not shown). Terminally exhausted cells isolated from anti-PD1–treated mice were enriched in both correlated

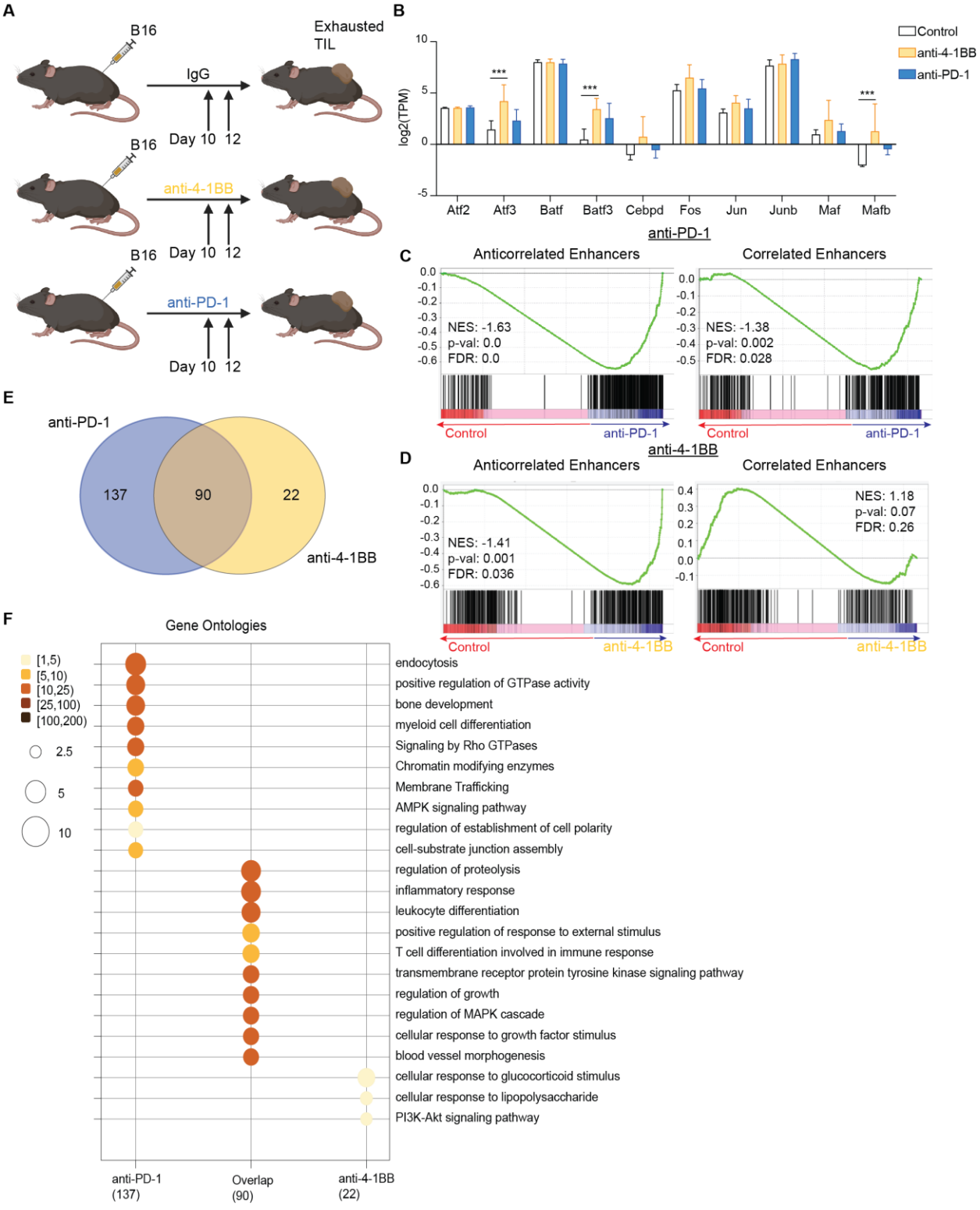

Figure 17. Providing Costimulatory Signaling Restores Expression of AP-1 Family Members and Anticorrelated Genes

Legend continued on next page.

Figure 17 (cont). (A) Experimental design of immunotherapy treatments. (B) Log2-normalized expression (mean and SD) of AP-1 family members in terminally exhausted TILs in IgG−, anti–4-1BB−, or anti-PD1–treated mice. P value (generated by a Wald test in DESeq2); ***P < 0.001. (C and D) Gene set enrichment analysis of transcriptomes comparing terminally exhausted ($PD1^{hi}Tim\text{-}3^{+}$) TILs isolated from tumors in control (IgG) versus PD1-treated (C) and 4-1BB– treated (D) mice. Gene lists of anticorrelated enhancers (left) and correlated enhancers (right) defined as in Fig. 2 (table S1). (E) Terminal anticorrelated genes that change in expression upon treatment. (F) Enrichment of GO terms defined by Metascape in anticorrelated genes modified by treatment with anti-PD1 or anti–4-1BB. RNA-seq data were generated from three individual mice per treatment group sorted into progenitor (PD1lo) or terminal ($PD1^{hi}Tim\text{-}3^{+}$) $CD8^{+}$ TILs. GTPase, guanosine triphosphatase; MAPK, mitogen-activated protein kinase; PI3K, phosphatidylinositol 3-kinase. Figure on previous page. Experiments performed by Nicole Scharping and Paolo Vignali.

and anticorrelated genes, indicating increased expression of genes with active chromatin states (Fig. 17C). 4-1BB–treated terminally exhausted T cells only increased expression of anticorrelated genes, with limited enrichment of correlated genes, suggesting that agonism of 4-1BB increases nuclear AP-1 and restores the expression of genes that retain active enhancers but lack gene expression at the steady state (Fig. 17D). As both anti-PD1 and anti–4-1BB therapies increased expression of anticorrelated genes, we next asked whether the genes restored contained a core signature. Of the 249 restored genes, only 90 genes were commonly restored by both therapies, whereas 137 or 22 genes were of these 90 genes revealed significant enrichment in inflammatory response and leukocyte differentiation pathways, whereas genes affected by anti-PD1 alone were in endocytosis or guanosine triphosphatase pathways, and anti–4-1BB alone regulated responses to glucocorticoids (Fig. 17E-F). Together, anti–4-1BB or anti-PD1 therapy can restore expression of genes primed by an active chromatin landscape in terminally exhausted T cells, but only anti–4-1BB does so by increasing AP-1 family member expression, suggesting that immunotherapies may be capable of “reinvigorating” some effector function of terminally exhausted cells by restoring gene expression of key inflammatory genes. These data support a model whereby coinhibitory receptor signaling reduces transcription by decreasing co-stimulation-driven AP-1 family member activity, which is needed for appropriate gene transcription.

3.3 Discussion

Current immunotherapies are limited by inadequate understanding of the transition from progenitor to terminally exhausted T cells. How tumor microenvironments affect this progression at the epigenetic level is not known, and whether terminally exhausted T cells have therapeutic potential to gain effector capacity is also unclear. By profiling changes in active histone modifications independent of DGE, we uncovered a unique chromatin feature. Thus, we found that a proportion of terminal exhaustion-specific active chromatin that does not have the expected corresponding increase in gene expression, which we have called anti-correlated genes. Although distal enhancers could account for this observation in H3K27ac, it would be unexpected that terminally exhausted cells use more distal enhancers than progenitors. In addition, we found that H3K4me3 and H3K9ac had a similar proportion of anticorrelated. Intriguingly, H3K27ac-marked active enhancers primarily regulate the initiation of transcription, whereas H3K4me3 and H3k9ac both regulate the initiation-to-elongation transition (193-195). Based on these data alone, it was unclear which step of transcription was being impacted, initiation or elongation, as either would results in low levels of transcription. Additionally, differences in mRNA stabilization and degradation could also lead to these results. We suspected that a loss of enhancer-promoter contacts occurs as cells progress to exhaustion, leading to decreased transcriptional initiation. Indeed, our transcription factor motif analysis data suggest that enhancer-promoter loops may be disrupted, due to low levels of bZIP/AP-1 family motifs.

Active chromatin in terminally exhausted T cells was highly enriched for AP-1 family motifs, yet very few AP-1 family members were expressed. The AP-1 family selects cell type–specific enhancers in macrophages and fibroblasts (205, 206). Thus, loss of AP-1 may be sufficient to limit enhancer-promoter contacts. NFAT rendered incapable of binding AP-1 increases

exhaustion; thus, the balance of NFAT downstream of TCR and AP-1 downstream of co-stimulation plays a key part in the progression to exhaustion (201, 207). Interestingly, despite an assumed similar balance of TCR-driven NFAT and co-stimulation-driven AP-1 in chronic viral infection, the chromatin did not have a notable enrichment of AP-1 family members, suggesting the proposed mechanism is unique to terminally exhausted $CD8^+$ TIL. We hypothesize that sustained co-stimulation and AP-1 expression drive productive enhancer looping to promote gene expression; however, studies using chromatin conformation capture and related technologies are needed to formally demonstrate this link.

Immunotherapies that directly agonize co-stimulatory molecules alter AP-1 expression and activity. We reasoned that providing this co-stimulatory signal could restore AP-1 and anticorrelated gene expression. Indeed, we found that 4-1BB agonism specifically altered anticorrelated genes, whereas PD1 blockade increased expression of all genes in terminal cells. One challenge in comparing these two treatments is the difference in cellular targets. αPD1 therapy primarily targets progenitor cells and allows progression to a more terminal state while effector function is maintained, whereas 4-1BB agonist acts on terminally exhausted T cells that exhibit elevated 4-1BB expression (203). We sorted progenitor and terminally exhausted cells separately to account for changes to the cellular phenotype but were unable to further parse these differences. Although both treatments affected anticorrelated genes, the precise genes within that group were not identical, suggesting that PD1 and 4-1BB therapies affect different signaling pathways, leading to increased effector cell programs. PD-1 signaling drives inhibition of a variety of signals downstream of TCR and costimulation, whereas 4-1BB drives a distinct costimulatory pathway. Specifically, blocking PD-1 signaling leads to increases in the PI3K and calcineurin pathways, which are not primary pathways activated by 4-1BB signaling (204, 208). Indeed, downstream

transcription factor activity in aPD-1 therapy is characterized by increases in AP-1, NFκB, NFAT, and FOXO1, whereas 4-1BB agonist drives more specific increases in AP-1 and NFκB (204, 208).

Overall, these data emphasize how altered immunologic signals redirect differentiation to exhaustion and suggest that exhausted T cells remain in their dysfunctional state due to the "memory" of these previous stressors. However, these data also describe an active chromatin state that is primed for gene expression with the appropriate signals and transcription factor activity, without further modifications to the chromatin itself.

4.0 Role of Tox in Terminally Exhausted Tumor-Infiltrating CD8$^+$ T Cells

As transcription factors play a key role in cellular differentiation, efforts to define exhaustion have included studies of a variety of transcription factors, which are responsible for regulating changes in gene expression as cells progress from progenitor to terminal exhaustion. Indeed, TCF1 and Blimp-1, Eomes, and most recently, Tox have all been associated with terminal exhaustion(90, 91, 95, 98, 209). While multiple transcription factors have been defined in progenitor exhausted cells, TCF-1 marks the bifurcation between effector differentiation and exhaustion, shown by the commitment of TCF-1$^+$ cells taken from chronic infection and transferred to acute are committed to dysfunction (157, 210, 211). Understanding the roles of these factors in each step of these cell fate decisions has been critical to progress in our understanding of T cell exhaustion.

We were interested in how Tox binding changed as cells became terminally exhausted. Specifically, we wanted to understand which genes it might directly regulate by binding, in addition to how its binding partners change throughout differentiation. We again sorted out four subsets from B16 melanoma tumors, based on PD-1 and Tim-3 expression, and performed CUT&RUN for Tox (Fig. 1). We performed differentially enriched peak analysis (DEP) to determine how Tox binding changed from progenitor to terminally exhausted cells. We identified progenitor and terminal exhaustion-specific regions that are bound by Tox. In the progenitor exhausted cells, we describe a potential mechanism by which TCF1/Tox dimers promote a progenitor exhausted state that is distinct from the role of TCF1in other stem-like progenitor T cells. In terminally exhausted cells, we identify Batf as a prominent binding partner of Tox and explore the role of Tox in regulating the correlated and anticorrelated genes defined in Chapter 3.

Data in this chapter have been previously published in Science Immunology. Manuscript information: Ford, BR, Vignali, PD, Rittenhouse, NL, Scharping, NE, Peralta, R, Lontos, K, Frisch, AT, Delgoffe, GM, & Poholek, AC. Tumor microenvironmental signals reshape chromatin landscapes to limit the functional potential of exhausted T cells. Science Immunology 2022, 7 (74). Creative commons license: https://creativecommons.org/licenses/by/4.0/legalcode

4.1 Introduction

Tox was recently described as a central regulator promoting T cell exhaustion, associating with chromatin modifying enzymes, such as the histone acetyltransferase Kat7, and mediating chromatin remodeling downstream of chronic stimulation of TCR, calcineurin, and NFAT activity (90, 91). However, Tox is not uniquely expressed in exhausted T cells, but is also expressed in developing thymocytes and effector memory CD8 T cells, where it regulates cytotoxic gene expression (90, 92, 93). Importantly, Tox expression in populations of exhausted T cells increases as cells further differentiate toward a terminal state, but it is also expressed at low levels in progenitor populations. Tox belongs to the HMG-box family of transcription factors; however, unlike other family members, it does not bind to DNA via a consensus sequence (92). Rather, Tox is thought to bind DNA that has adopted a specific secondary structure, as no consensus motif is enriched for Tox binding, further suggesting that its function may be in regulating chromatin structure such as accessibility or looping (92). Several studies identified and highlighted roles for Tox in exhaustion. Although these studies took varied approaches, several consistent phenotypes were identified. First, Tox played a critical role in the persistence of Ag-specific T cells over time. While initial expansion to viral infection or tumor antigens was similar in control and Tox-

deficient cells, cells lacking Tox failed to persist long term across several studies. Transcriptome and epigenome analyses consistently showed that Tox promoted an exhaustion signature such as PD-1, and loss of Tox led to increases in genes associated with effector function, including cytokine production, expression of transcription factors associated with effector cells, as well as a decrease in exhaustion genes. There was some discrepancy regarding the specific effect of Tox on the $TCF1^+$ progenitor population. In some studies, Tox overexpression resulted in more $TCF1^+$ cells, whereas in others, Tox was required to maintain both $TCF1^+$ and TCF1- populations. Precisely how Tox controls persistence of the responding population while also driving the exhaustion phenotype is less clear but suggests that Tox may have discrete functions in progenitor cells compared with terminally exhausted cells. This may in part be due to its ability to interact with different partners in different subsets of exhausted T cells (90, 93, 94). Tox is able open and close chromatin, and Tox deficiency led to alterations in chromatin accessibility at key genes associated with exhaustion. *Prdm1*, *Pdcd1*, *Havcr2*, and *CD38* had decreased accessibility, whereas the transcriptional regulators *Tcf7* and *Id3*, became more open (95). Given its complex role, precisely how Tox paradoxically supports T cell persistence while promoting exhaustion requires further study.

4.2 Results

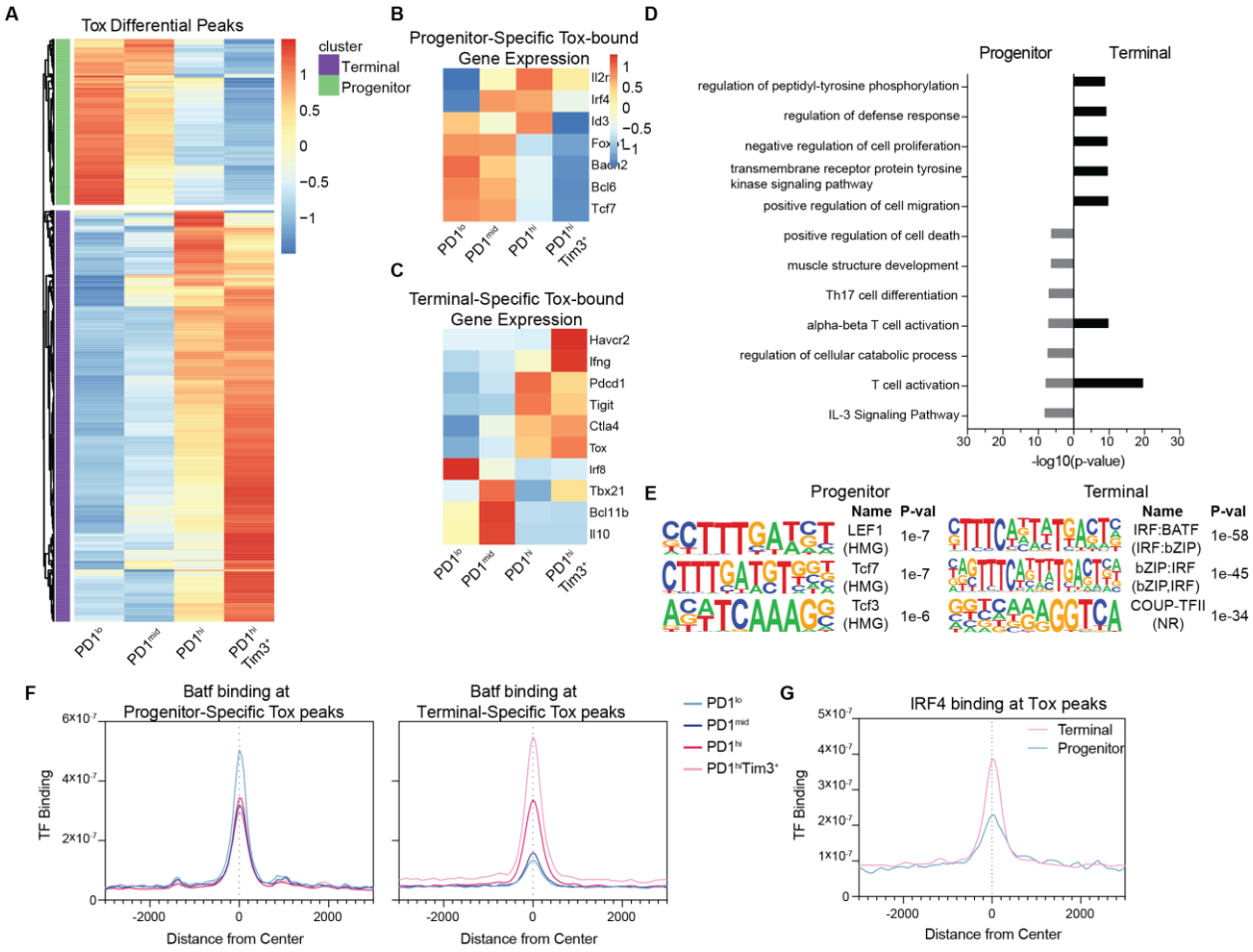

Figure 18. Tox Cooperates with a Vairety of Transcription Factors to Bind Exhausted-Associated Genes in Terminally Exhausted Cells

(A) Normalized CPM of Tox at differential peaks identified between TIL subsets (DESeq2). (B and C) Normalized TPM at selected genes associated with progenitor-specific (B) and terminal-specific (C) Tox peaks. (D) −Log10 (P value) values for GO term pathways identified by Metascape enriched for genes with progenitor and terminally exhausted–specific Tox binding. (E) Top results from HOMER motif analysis of DESeq2-defined Tox differential peaks in progenitor or terminally exhausted T cells. Terminally exhausted–specific peaks used as background for progenitor exhausted–specific analysis and vice versa.) (F) Batf coverage at progenitor and terminal-specific DESeq2-defined differential Tox peaks. n = 1. (G) IRF4 binding (GSE54191) at progenitor and terminal-specific DESeq2-defined differential Tox peaks. IRF4 ChIP-seq is in vitro–activated T cells (86). CUT&RUN for Tox (n = 2) and Batf (n = 1) was performed with 8 to 10 mice pooled per experiment before sorting.

To determine the relationship of Tox binding and the epigenetic landscape in TILs, we performed CUT&RUN for Tox. Although Tox expression increases as cells progress toward terminal exhaustion, Tox is expressed (at low levels) in progenitor T cells (90, 91, 94, 95, 212).

Therefore, we identified DEP of Tox in both progenitor and terminally exhausted $CD8^+$ T cells (Fig. 18A). In progenitor cells, Tox bound several genes associated with the progenitor program, including *Tcf7*, *Bcl6*, *Bach2*, *Foxo1*, and *Id3*, which was mostly associated with increased gene expression, although expression of some genes was decreased, including *Il2ra* and *Irf4* (Fig. 18B). Similarly, in terminally exhausted cells, Tox bound more than 300 genes, many associated with the transcriptional program of terminal cells, including *Havcr2* (encoding Tim-3), *Tbx21*, *Ifng*, *Ctla4*, *Pdcd1*, *Tigit*, and *Tox* itself. Again, Tox binding was associated with both expression and repression (*Irf8*, *Bcl11b*, and *Il10*) (Fig. 18C). Pathway analysis revealed programs in both populations associated with T cell activation, although enrichment was more significant in terminal cells than progenitor cells (Fig. 18D). Motif analysis revealed cell state–specific motifs; in progenitor cells, Tox was associated with Lef1 and Tcf7 motifs, whereas in terminal cells, interferon regulatory factor (IRF) and Batf motifs were strongly enriched (Fig. 18E). IRF4, together with Batf, has been associated with promoting T cell exhaustion. We found that Batf binding significantly overlapped Tox in terminal cells (Fig. 18F). Furthermore, IRF4 was more enriched at regions bound by Tox in terminally exhausted cells than in progenitor cells, confirming enrichment of IRF4:Batf motifs (Fig. 18G).

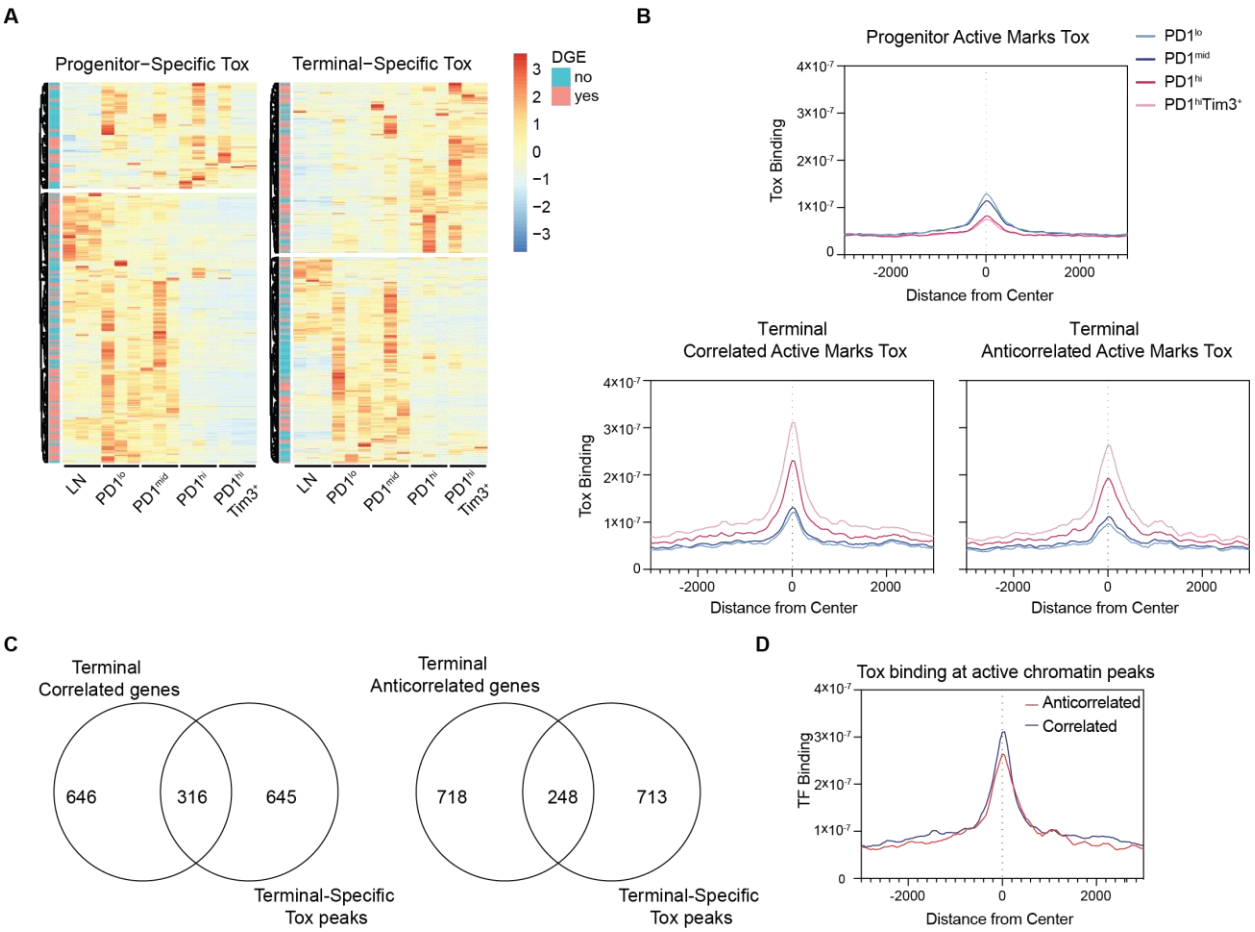

Figure 19. Tox Binds Equally to Correlated or Anticorrelated Genes in Terminally Exhausted Cells
(A) Heatmaps showing log2 normalized expression of genes nearest to progenitor-specific and terminal-specific Tox peaks. Those genes that meet differentially expressed genes cutoffs (FC >2, p val < 0.05) marked in pink on the left side of heatmap. (B) Histograms showing Tox coverage at progenitor, correlated, and anticorrelated active mark peaks. (C) Terminal specific peaks of active chromatin (H3K4me3, H3K27Ac, and H3K9Ac) grouped by those with correlated or anticorrelated gene expression associated with terminal-specific Tox peaks. (D) Tox coverage in terminally exhausted cells at active chromatin defined as having anticorrelated and correlated gene expression as in Fig. 2.

Next, we determined the relationship of Tox to active chromatin (H3K4me3, H3K27ac, and H3K9ac) in terminally exhausted T cells. Tox binding was associated with increases and decreases in gene expression in both progenitor and terminally exhausted cells (Fig. 19A). Indeed, Tox binding was enriched at progenitor, correlated, and anticorrelated active marks, although there was slightly more enrichment in the correlated group (Fig. 19B-D). These data suggest that Tox binds to active chromatin enriched in IRF:Batf composite motifs and works together with IRF4 and Batf to promote expression at key genes associated with terminal exhaustion. In contrast, in

progenitor cells, Tox binds Tcf7 motifs to promote expression of the progenitor exhausted T cell transcriptome.

4.3 Discussion

After Tox was identified as a crucial transcription factor in terminal exhaustion, we performed CUT&RUN to identify Tox binding in our exhausted $CD8^+$ TIL subsets. While others had looked at the effects of Tox deletion on exhaustion, direct Tox binding locations had not yet been identified (90, 91, 95). Furthermore, potential Tox binding sites cannot be identified by Homer motif because Tox does not bind a consensus motif, emphasizing the importance of directly assaying Tox binding (92). Our analysis suggests that Tox has roles in both progenitor and terminally exhausted states (90, 91, 95). Tox is an HMG protein that binds DNA in a sequence-independent manner and regulates chromatin architecture, suggesting that it may play a role in regulating enhancer-promoter looping (92). We found Tox pairs with distinct binding partners in each subset, TCF-1 in progenitor and Batf:IRF [AP-1–interferon regulatory factor (IRF) composite element (AICE)] in terminally exhausted cells (213). TCF-1 can act as a pioneer factor, binding to regions of heterochromatin to promote chromatin accessibility (77). However, intrinsic histone deacetylase activity and repressive function has also been associated with TCF-1, suggesting that either the binding partners or the chromatin landscape affects the precise role of TCF-1 (80).

Both Batf and IRF4 are key transcription factors regulating exhaustion (48, 214, 215). Batf:IRF4 complexes bind to AICE to drive differentiation of Th17 cells, B cells, and dendritic cells (213). We found that Taiji analysis ranked both Batf and Irf4 as highly important and positively correlated with expression, unlike the decreased expression of the other AP-1 family

members (Fig. 14A). Intriguingly, Tox is only moderately more associated with the correlated genes, than the anticorrelated genes identified in Chapter 3, suggesting that Tox binding in terminally exhausted T cells is reliant upon specific transcription factor binding partners. It remains to be determined how Tox may interact with other AP-1 family members to modulate the exhaustion phenotype and effector function in the context of 4-1BB agonist treatment or in AP-1 factor overexpression in CAR T cells (89, 203). Our data suggest that a complex of Batf, Irf4, and Tox is responsible for regulating gene expression in terminally exhausted T cells.

5.0 Bivalent Genes in Terminally Exhausted Tumor-Infiltrating CD8$^+$ T Cells

Regulation of gene promoter activity is a fundamental process governing gene expression. There is a complex interplay of epigenetic mechanisms within the promoter alone that contribute to when and to what extent a gene is activated or repressed. Promoters are regions of DNA located directly upstream of the transcriptional start site (TSS), where the transcriptional machinery binds to initiate transcription of the gene (216). To gain a better understanding of the epigenetic regulation of CD8$^+$ T cell differentiation within the tumor, we interrogated how the histone modifications H3K4me3, found at active promotors, and H3K27me3, found at repressed promotors, change as the cells differentiate.

In this chapter, we show that terminally exhausted T cells have a notable increase in the amount of bivalent chromatin, compared to effector and progenitor exhausted cells. Bivalent chromatin is characterized by the presence of the active mark H3K4me3 and the repressive mark H3K27me3 (217). Bivalency was initially described in embryonic stem cells, where it was found at the promoters of key regulatory genes with low levels of expression (218). Bivalency has largely been described at genes that are poised for either activation or full repression as cells differentiate. Thus, it was intriguing to find an increase in bivalent genes in terminally differentiated CD8$^+$ T cells within the tumor. We describe the role of tumor hypoxia in driving an increase in H3K27me3 and decreasing expression of genes associated with T cell stemness and the effector response as CD8$^+$ T cells progress toward terminal exhaustion. Indeed, we found that enforcing expression of the histone demethylase Jmjd3, encoded by *Kdm6b*, improves CD8$^+$ TIL effector function and the antitumor response.

Data in this chapter have been previously published in Science Immunology. Manuscript information: Ford, BR, Vignali, PD, Rittenhouse, NL, Scharping, NE, Peralta, R, Lontos, K,

5.1 Introduction

Regulation of gene promoter activity is a crucial process that determines when and to what extent a gene is expressed or silenced in a cell. Gene promoters are found upstream of the TSS and are important binding sites for transcription factors and the transcriptional machinery (216). Promotor activity is regulated by DNA methylation, histone modifications, chromatin accessibility, and transcription factor binding. Active promotors have high levels of H3K4me3 and chromatin accessibility, with low levels of H3K27me3 and DNA methylation. Repressed promotors have the opposite, high levels of H3K27me3 and DNA methylation with low levels of H3K4me3 and accessibility. However, some genes are found with both the active modification H3K4me3 and repressive modification H3K27me3, forming a chromatin state referred to as bivalency.

Bivalency is a distinct feature that was initially described in pluripotent embryonic stem cells (218-220). The occurrence of these two opposing histone modifications at bivalent promoters creates a poised state, where genes are primed for either activation or repression (217). RNA polymerase II is found in a paused state at bivalent promotors, which suggested that gene expression could occur more rapidly after activation (221). However, recent studies have shown that bivalent genes are not expressed more quickly than genes with repressed promotors and low levels of H3K4me3 (222). Bivalency had also been thought to contribute to the cellular plasticity

and ability of stem cells to differentiate into distinct cell types. Indeed, the role of bivalency in keeping genes "poised" has been described in various other pluripotent and stem-like cells, including hematopoietic stem cells, thymocytes, and memory T cells (223-226). However, the idea that bivalent promoters resolved into either an active or repressed state by removal of one of the modifications as the cells differentiate has been challenged in recent years (217, 227). Interestingly, bivalency has been associated with low levels of DNA methylation (228). Recently, a role for bivalency in actually protecting these genes from full repression by DNA methylation has been proposed (227). In $CD8^+$ T cells, bivalency plays a role in priming effector $CD8^+$ T cell differentiation, exhibiting bivalent chromatin at effector genes in naïve and memory T cells (229, 230). However, the role of bivalency in exhausted $CD8^+$ T cells is not understood.

5.2 Results

5.2.1 Defining Promoter States of Terminally Exhausted Tumor-Infiltrating CD8$^+$ T Cells

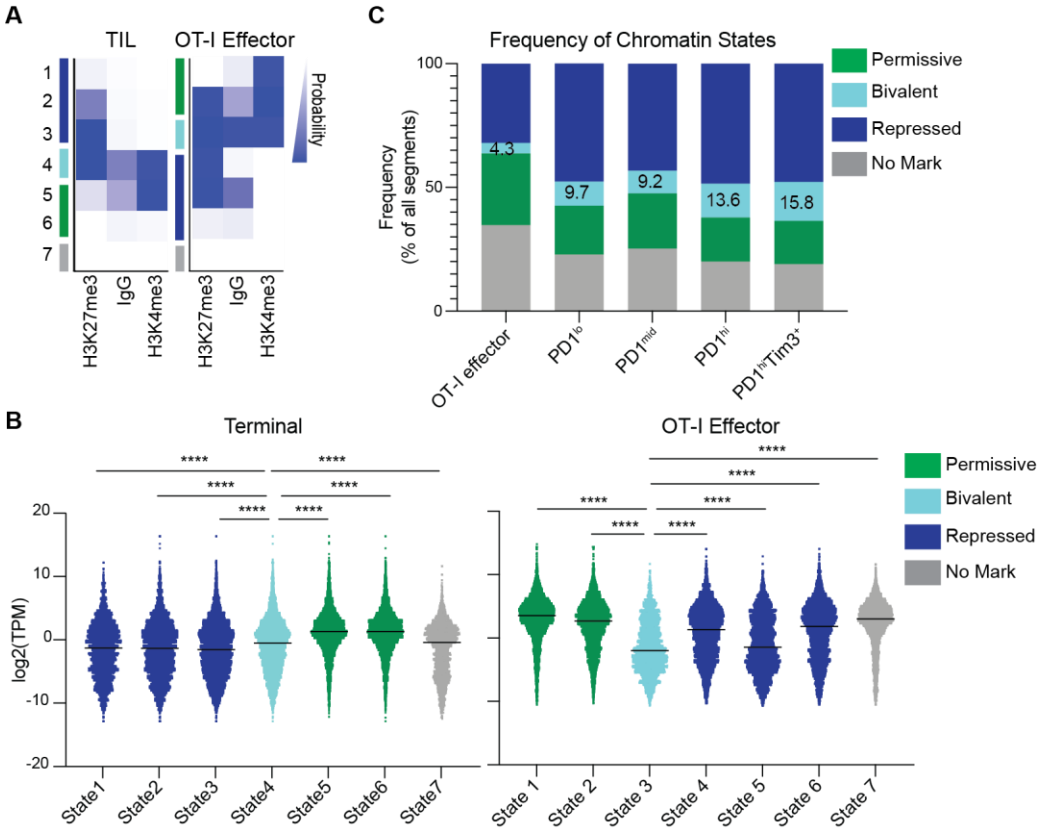

Figure 20. ChromHMM-Assigned Chromatin States Show an Increased Frequency of Bivalent Chromatin in Terminally Exhausted Cells
(A) ChromHMM emission plots depicting defined states in TILs and Vaccinia-OVA effector cells. (B) Frequency of chromatin states identified in (A) in TIL subsets and Vaccinia-OVA effector cells. (C) Log2 normalized expression of genes nearest to the segments defined in (A) in each state in terminally exhausted TIL and Vaccinia-OVA effector cells.

To explore the role of bivalent chromatin, and promotor activity more generally, in tumor-infiltrating lymphocytes, we asked whether there were intrinsic differences in promoter states in progenitor and terminal TILs using ChromHMM, a hidden Markov model developed to identify patterns of chromatin marks (231, 232). We used ChromHMM as an unbiased method to identify promoter states in a peak-independent manner, due to differences in the dynamics and locations of

H3K27me3 and H3K4me3. To identify promoter states, replicates of H3K4me3 and H3K27me3 for TIL samples and OT-I $CD8^+$ effector T cells were merged, and states were identified on the basis of the probability of antibody enrichment of chromatin regions (Fig. 20A). The immunoglobulin G (IgG) control sample was included to eliminate any states enriched as background. An increased probability of IgG binding was typically found in permissive or bivalent chromatin states, in line with nonspecific IgG binding to open chromatin regions. Three states were identified as repressed due to the high probability of binding only H3K27me3. Two permissive states had a high probability of H3K4me3 alone, with state 5 identified as the predominant permissive state. The probabilities of H3K4me3 and H3K27me3 binding were roughly equal in state 4, suggesting bivalency. State 7 had low probabilities for all marks. Seven chromatin states were also identified in OT-I effector cells (Fig. 20A). To determine whether transcription corresponded to the defined states, we assessed gene expression in terminally exhausted and OT-I effector cells using RNA-seq data. Repressive states had reduced gene expression compared with permissive states, and bivalent chromatin had reduced expression compared with permissive chromatin (Fig. 20B) (218). We next compared the frequency of chromatin states among the TIL populations and in effector cells. Whereas all TILs had more bivalent chromatin than effector cells, terminally exhausted cells displayed the highest percentage of bivalent chromatin (Fig. 20C).

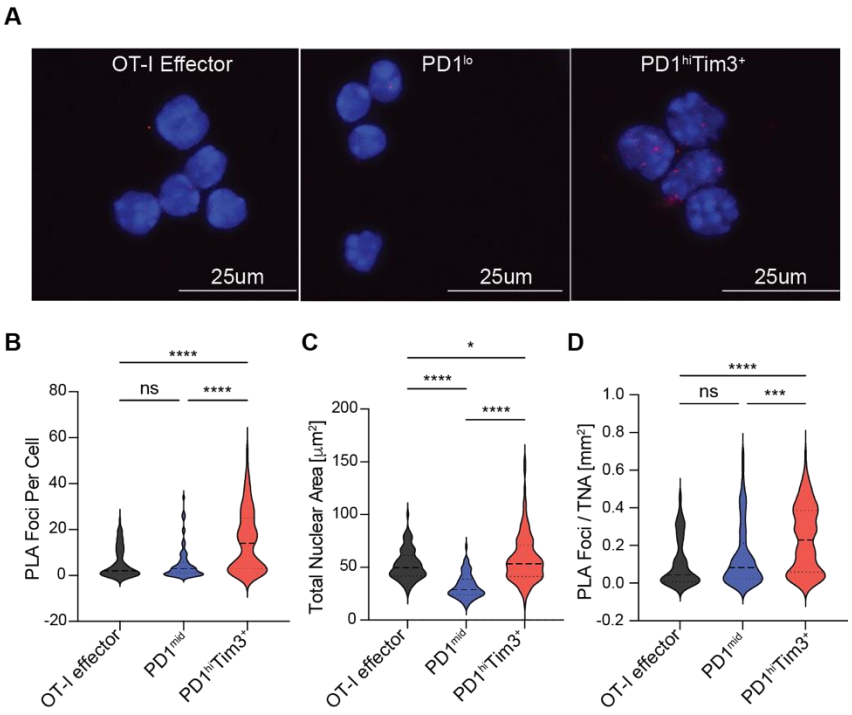

Figure 21. Bivalency Is Increased at a Single Cell Level
(A) Representative images from PLA for H3K4me3 and H3K27me3 in OT-I effector, PD1^{lo} and PD1^{hi}Tim-3^{+} TILs showing PLA foci (red) and nuclear area (DAPI). (B-D) Quantification of PLA Foci per cell (B), total nuclear area (C), and PLA foci normalized by total nuclear area (D) for cell types shown. One-way ANOVA, ***P < 0.001 and ****P < 0.0001.

As CUT&RUN data are from bulk populations of cells, we sought to confirm the presence of both histone marks within close proximity in single cells, indicative of true bivalency and not heterogeneity from cells that were either active or repressed at those loci. Fluorometric proximity ligation assay (PLA) is a highly sensitive and specific single-cell method for identification of two targets in close proximity, such as H3K4me3 or H3K27me3 (233, 234). Consistent with true bivalency, we found a significant increase in PLA foci within PD1^{hi}Tim-3^{+} terminally exhausted T cells as compared with progenitor and OT-I effector CD8^{+} T cells (Fig. 21A-D). Thus, terminally exhausted T cells had an increase in bivalent chromatin, which may represent another mechanism by which transcription is controlled as cells become exhausted.

5.2.2 Identifying Bivalent Genes in Terminally Exhausted Tumor-Infiltrating CD8$^+$ T Cells

We next explored gene programs associated with bivalent chromatin in each TIL subset. We restricted our analysis to bivalent chromatin encompassing a 2-kb region around the TSS and further removed genes that had high expression, as this would not meet the criteria of bivalency. Terminally exhausted cells had an increased number of genes with bivalent promoter regions [4848; PD1^{hi}Tim-3$^+$ (686), PD1^{hi} (856)], compared with effector (398) or progenitor exhausted cells [PD1^{lo} (147), PD1^{mid} (100)] (Fig. 22A). Because gene repression can be a function of chromatin accessibility, we used available ATAC-seq data to explore the relationship between open and closed chromatin and bivalency. We found no changes in chromatin accessibility at terminally exhausted-specific bivalent regions in OT-I effector, progenitor, or terminal cells, despite changes in H3K27me3 and transcript expression (Fig. 22B). Genes identified as bivalent have little overlap with genes described in terminally exhausted cells as having active chromatin but anticorrelated gene expression, in line with comparable H3K27me3 at these regions (Fig. 22C). Terminal exhaustion bivalent genes were enriched for pathways involved in inflammatory response, leukocyte differentiation, and cytokine production (Fig. 22D-E). One such gene, *Klf2,* showed both H3K4me3 and H3K27me3 peaks in terminal cells, whereas LN and progenitor cells had only H3K4me3 (Fig. 22F). *Klf2* had a corresponding decrease in expression from LN and progenitor to terminally exhausted cells (not shown).

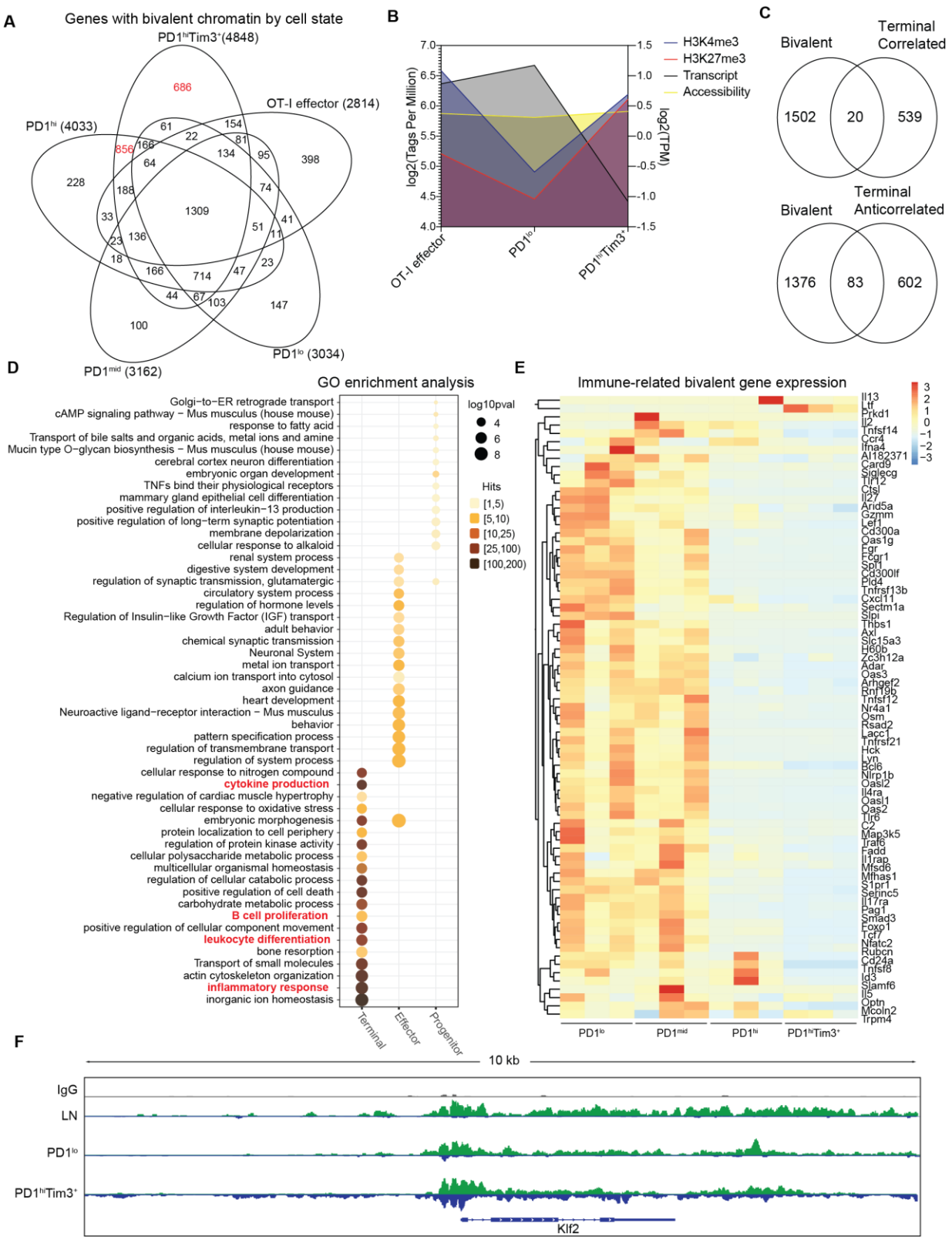

Figure 22. Exhaustion-Specific Bivalent Genes Are Enriched for Immune-Related Genes

Continued on next page.

Figure 22 (cont.) (A) Genes identified in each subset as bivalent defined by both H3K4me3 and H3K27me3 in regions ±1 kb of all TSSs and filtered for expression less than 2 TPM. (B) Summary plot showing changes in H3K4me3, H3K27me3, chromatin accessibility (ATAC-seq, GSE122713), and gene expression of exhaustion-specific bivalent genes identified in (A). Listeria-OVA infection data: GSE95237. (C) Exhaustion-specific bivalent genes compared with correlated and anticorrelated genes defined in chapter 3. (D) Enrichment of GO terms defined by Metascape in effector-, progenitor-, and terminal-specific bivalent genes. (E) Normalized expression of select immune-related genes identified as exhaustion-specific bivalent genes. (F) Representative genome browser (IGV) plots of IgG, H3K4me3 and H3K27me3 peaks determined by CUT&RUN at promoter regions of three select genes Klf2 identified as bivalent in terminally exhausted CD8 T cells in LN, $PD1^{lo}$ progenitor and $PD^{hi}Tim\text{-}3^{+}$ terminally exhausted $CD8^{+}$ T cells.

Expectedly, expression of all bivalent genes, immune-related and otherwise, was also decreased (Fig. 23A). We also confirmed this decrease in gene expression in individual terminally exhausted cells by examining scRNAseq feature plots of the terminally exhausted and bivalent gene signatures. There was distinct expression of the terminally exhausted and bivalent gene signatures, similarly to when we compared to the progenitor exhausted gene signature (Fig. 23B, Fig. 5C). Additionally, we were concerned that bivalency might be an artifact of comparing bystander $PD1^{lo}$ progenitor cells to tumor-specific cells. We used our pmel-1 T cell dataset to determine whether changes in bivalent gene expression were antigen independent. We found that progenitor pmel-1 T cells were significantly enriched for expression of bivalent genes, compared to tumor-reactive terminally exhausted pmel-1T cells (Fig. 23C-D). To determine whether bivalent genes associated with exhaustion were also present in chronic viral infection, we explored their expression in previously published datasets of progenitor and terminally exhausted states isolated from chronic viral infection (LCMV clone 13) or B16 tumors (158). Consistent with our results, expression was significantly decreased in tumor terminal exhaustion. In contrast, no change was observed in chronic viral infection, suggesting that the tumor microenvironment enforces a distinct terminal state in T cells and the increase in bivalent chromatin is specific to tumor-mediated terminal exhaustion (Fig. 23E). These data suggest that tumor-mediated terminally exhausted cells have a selective increase in bivalent chromatin at promoters, leading to decreased gene expression.

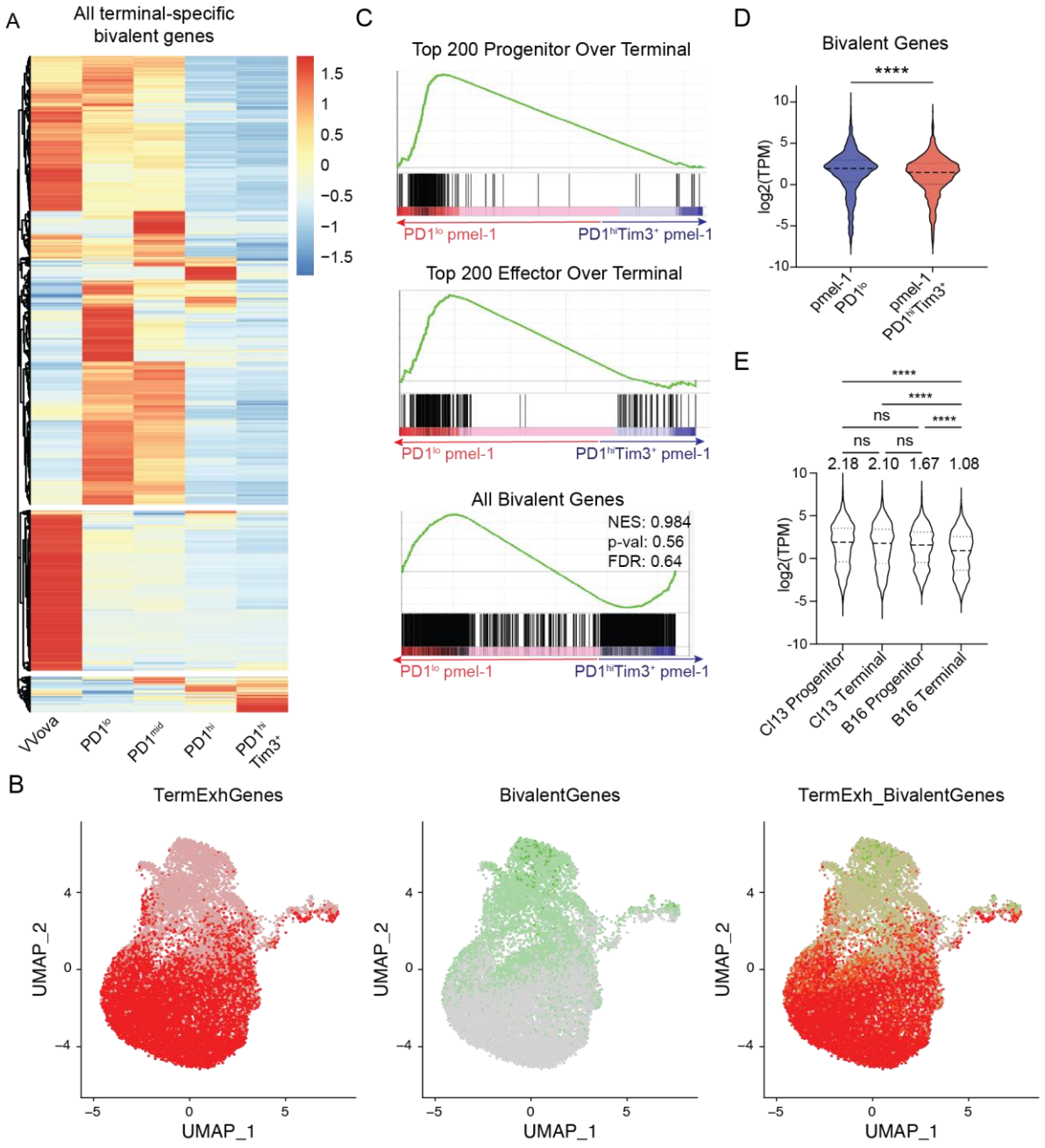

Figure 23. Exhaustion-Specific Bivalent Genes Have Decreased Expression

A) Log2 normalized expression of genes nearest to the segments defined in Fig. 20A in each state in terminally exhausted TIL and VVOVA effector cells. (B) Terminally exhausted-specific genes and bivalent gene signatures displayed and merged on B16 scRNAseq data from Fig. 3. (C) Gene set enrichment analysis of tumor-specific pmel-1 progenitor and terminal exhaustion transcriptomes for top 200 genes that decrease from effector to terminal (top), from progenitor to terminal (middle), or all bivalent genes identified in Fig. 20A. Log2 normalized expression of terminal-specific bivalent genes in pmel-1 PD1lo progenitor or PD-1^{hi}Tim-3^{+} terminally exhausted T cells. (E) Log2-normalized expression of bivalent genes identified in (E) from progenitor and terminally exhausted cells from chronic LCMV or B16 melanoma tumors (GSE122713). Numbers above indicate mean TPM value. p value (DESeq2, generated by one-way ANOVA); *p<0.05, **p<0.01,***p<0.001,****p<0.0001. ns, not significant.

5.2.3 Role of Hypoxia in Regulating Bivalency in Terminally Exhausted Tumor-Infiltrating CD8$^+$ T Cells

Terminally exhausted T cells carry severe metabolic defects, suggesting that exhausted T cell differentiation is due in part to the experience of oxidative stress and elevated reactive oxygen species (76). As oxygen is required for the dioxygenase reactions associated with histone and DNA demethylation, and terminally exhausted cells experience elevated hypoxia relative to progenitor exhausted cells, we asked whether environmental stressors like hypoxia can drive bivalency through alteration of demethylase activity (235, 236). Because these studies had shown global changes in histone methylation level, we first used flow cytometry to assay global changes in histone modifications relevant to bivalency, H3K27me3 and H3K4me3. We found that in terminally exhausted cells global levels of both of these marks were increased, even when the increases in total histone H3 expression were taken into account (Fig. 24A-E). These global increases suggest that the increase in bivalency found in terminally exhausted cells is not due to targeting of these specific regions but to the overall increase in these histone modifications throughout the chromatin.

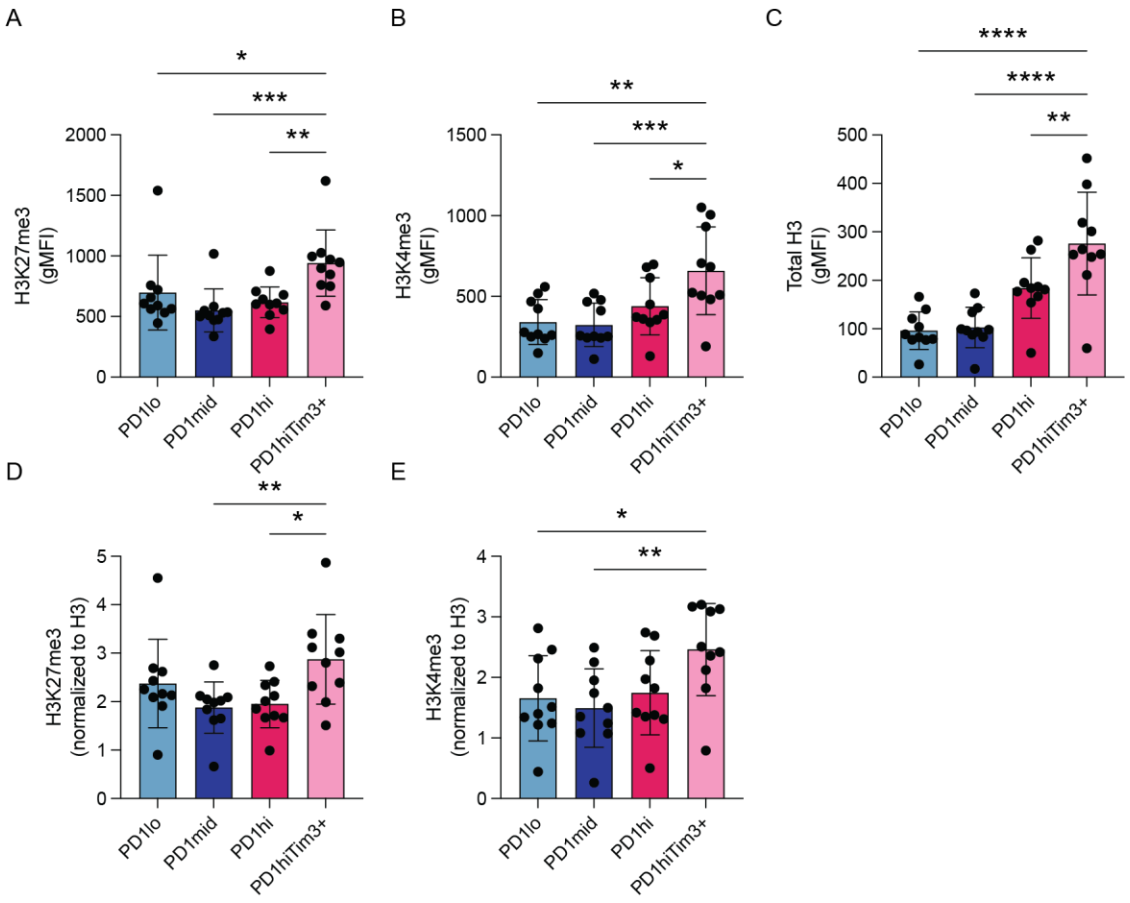

Figure 24. Increased Tumor Hypoxia Is Associated with Increased Methylation Globally
(A-C) Geometric mean fluorescent intensity (gMFI) of H3K27me3 (A), H3K4me3 (B), and total histone H3 (C). (D-E) Levels of H3K27me3 (D) and H3K4me3 (E) normalized per cell for total H3 expression. Flow cytometry plots are representative of 2 experiments. Statistics are an ordinary one-way ANOVA; *p<0.05, **p<0.01, ***p<0.001, ****p<0.0001. ns, not significant.

Because terminally exhausted cells experience more hypoxia than the progenitor exhausted cells, we reasoned that mitigating hypoxia in the tumor could reduce bivalent chromatin and restore gene expression. To test this, we used a genetically modified B16 tumor cell line with a deletion of a subunit of mitochondrial complex I (Ndufs4), resulting in a tumor that consumes less oxygen and produces less hypoxia but maintains baseline proliferation (76). Firstly, we used PLA to determine whether bivalency was changed in these less hypoxic tumors. We found fewer PLA foci formed by proximity of H3K4me3 and H3K27me3 in terminally exhausted cells isolated from tumors with less hypoxia, indicating that decreasing hypoxia was sufficient to decrease bivalent

chromatin (Fig. 25A-B). Bivalent gene expression was partially recovered in terminally exhausted cells isolated from Ndufs4-deficient B16 (Fig. 25C-E). To determine whether this recovery was due to changes in bivalency, we analyzed the presence of H3K4me3 and H3K27me3 in progenitor and terminally exhausted T cells isolated from Ndufs4-deficient and control B16 tumors. Although no significant changes occurred to H3K4me3, we observed a significant decrease in H3K27me3 at bivalent gene promoters in terminal cells isolated from tumors with less hypoxia, despite global changes in both histone modifications (Fig. 25F). Thus, hypoxia promotes bivalent chromatin in tumor-infiltrating terminally exhausted T cells, representing a key microenvironmental signal that alters immune differentiation.

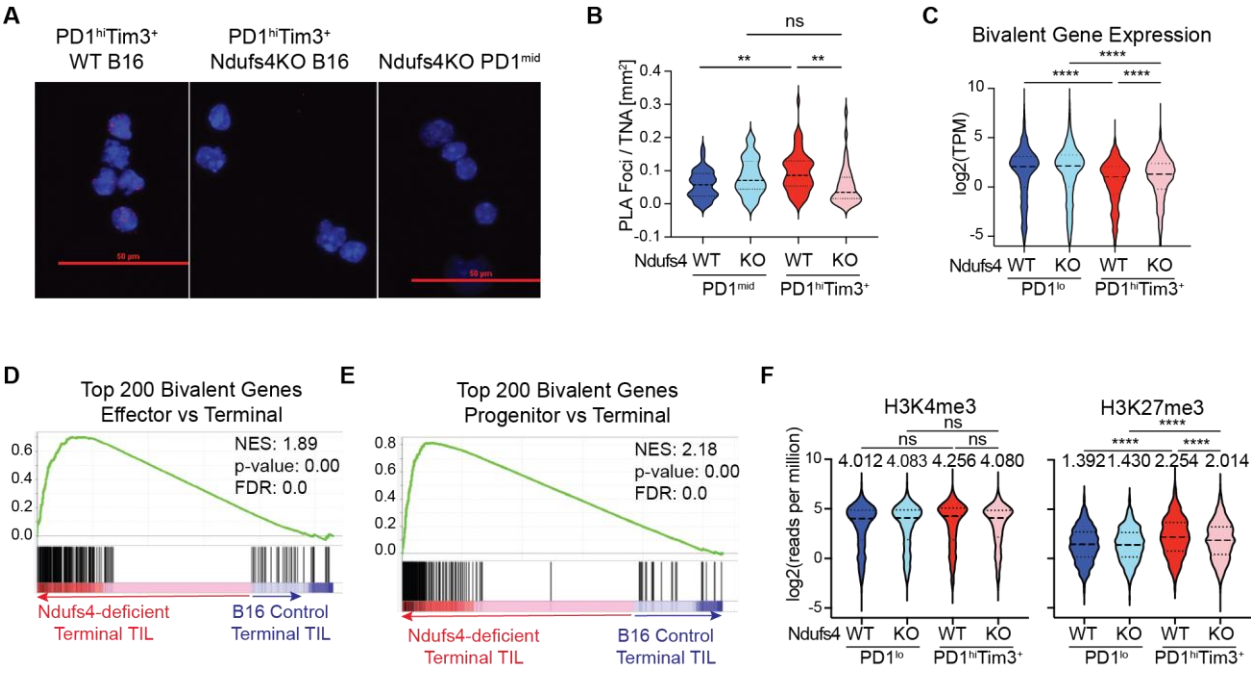

Figure 25. Terminally Exhausted Cells from Less Hypoxic Tumors Have Reduced Bivalency
(A) Representative images from PLA for H3K4me3 and H3K27me3 in PD1lo and PD1hiTim-3^{+} TILs showing PLA foci (red) and nuclear area (DAPI). (B) Quantification of PLA foci normalized by total nuclear area (TNA) shown by DAPI. One-way ANOVA, **P < 0.01. KO, knockout. (C) Log2-normalized expression of bivalent genes identified Fig. 6E. P value (generated by a Wald test in DESeq2); **P < 0.01 and ****P < 0.0001. (D-E) Gene set enrichment analysis of terminally exhausted TIL transcriptomes isolated from Ndufs4-deficient or wild-type (WT) B16 melanoma tumors. Top 200 bivalent genes defined in Fig. 20A that decrease from effector (D) or progenitor (E) to terminally exhausted cells. (F) Log2-normalized coverage of bivalent genes from CUT&Tag data for H3K4me3 and H3K27me3. PLA performed by Paolo Vignali and images were taken by Ronal Peralta.

5.2.4 Enforced Kdm6b Expression Improves Antitumor Response in Adoptive Cell Therapy

UTX and Jmjd3, encoded by *Kdm6a* and *Kdm6b*, are histone lysine demethylases (KDMs) that act on H3K27, whereas Ezh2 methylates H3K27 (237). UTX is a direct oxygen sensor, and hypoxic conditions inhibit KDM activity, either directly or through hypoxia-inducible factor–mediated mechanisms (236). Jmjd3, in contrast, is thought to be less sensitive to oxygen tension and known to affect effector CD8 T cell function and formation of memory (238). Thus, we hypothesized that altered function or expression of H3K27 histone modifiers may be critical to driving bivalency. We found that Kdm6b, the less oxygen-sensitive KDM, is significantly decreased in a hypoxia-dependent manner in terminally exhausted cells (Fig. 26A). In contrast, Ezh2 was increased in terminally exhausted cells and was not altered by hypoxia, suggesting that increased bivalency may be due to the dysregulation of chromatin mediators of H3K27 methylation (239).

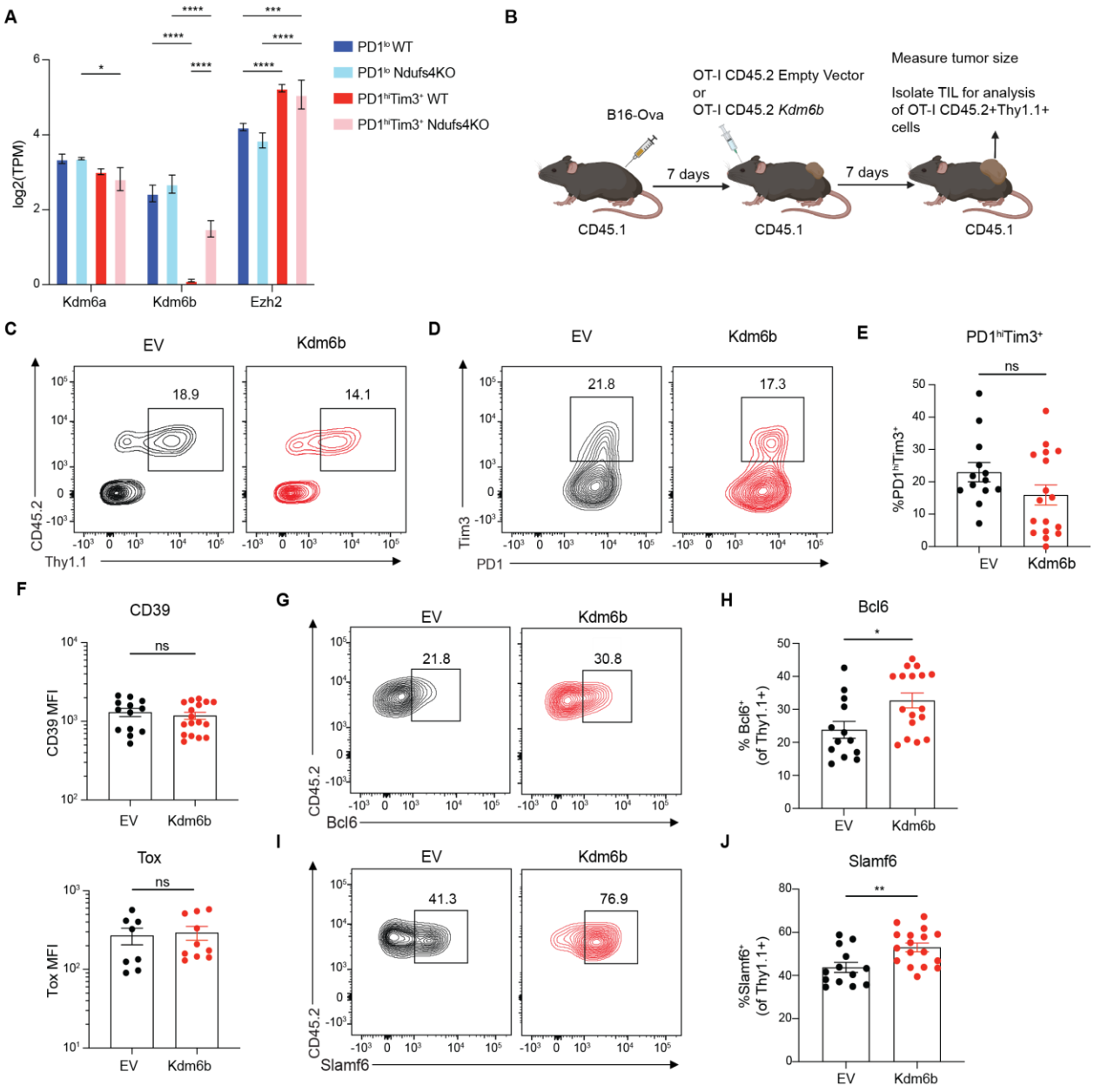

Figure 26. Enforcing Kdm6b Expression in Adoptive Cell Therapy Improves Stemness without Changes in Terminal Exhaustion

(A) Log2-normalized gene expression (mean and SD) of histone modifiers that regulate H3K27me3 from subsets of exhausted TILs from WT and Ndufs4-deficient B16 melanoma. P value (generated by a Wald test in DESeq2); *P < 0.05, **P < 0.01, ***P < 0.001, and ****P < 0.0001. (B) Experimental design of Kdm6b retroviral overexpression studies (C) Representative staining of EV or Kdm6b retroviral overexpression by Thy1.1 staining prior to adoptive transfer into B16-Ove bearing mice. (D) PD1 and Tim-3 expression in EV or Kdm6b expressing OT-I T cells isolated from B16-OVA. (E) Frequency of PD1hiTim-3^{+} cells. (F) Mean fluorescent intensity (MFI) of exhaustion markers CD39 and Tox. (G and I) for Bcl6 (G) and Slamf6 (I) staining gated on transduced OT-I T cells. (H and J) Frequency of Bcl6^{+} (H) and Slamf6^{+} (J) cells. Flow cytometry plots are representative of ≥3 experiments. Statistics are Mann-Whitney (E, F, H, and J) with *P < 0.05, **P < 0.01, ***P < 0.001, and ****P < 0.0001. Experiments performed by Paolo Vignali.

Because Kdm6a is directly inhibited in settings of low oxygen, we hypothesized that restoring histone demethylase activity via enforced expression of Kdm6b, its less oxygen-sensitive counterpart, may limit bivalency and restore function to terminally exhausted cells. We overexpressed Kdm6b in CD45.2 TCR transgenic (OT-I) $CD8^+$ T cells via retroviral transduction (Kdm6b-T2A-Thy1.1) then adoptively transferred these cells into CD45.1 recipients bearing palpable B16 tumors expressing ovalbumin (B16-OVA) (Fig. 26B-C). Kdm6b overexpressing T cells expressed similar levels of the canonical exhaustion markers PD1, Tim-3, CD39, and Tox compared with controls, suggesting that the core differentiation program to exhaustion, likely driven by antigen, was unchanged (Fig. 26E-F). Kdm6b overexpression led to increased expression the bivalent genes, Bcl6 and Slamf6, associated with stemness and memory (Fig. 26G-J). Despite the maintenance of terminal exhaustion-associated proteins, overexpression of Kdm6b improved effector function. Kdm6b-overexpressing T cells displayed markedly increased cytokine production when restimulated with peptide, indicating that although they resembled exhausted T cells, they carried greater effector potential, possibly due to the increased expression of stemness genes (Fig. 27A-D). Tumor growth was also limited in mice receiving Kdm6b-overexpressing OT-I T cells, suggesting that these cells carried greater antitumor activity *in vivo* (Fig. 27E-F). Thus, maintenance of demethylase activity via Kdm6b overexpression limits the acquisition of a dysfunctional phenotype as T cells differentiate in response to persistent antigen, although these cells express canonical markers of exhaustion.

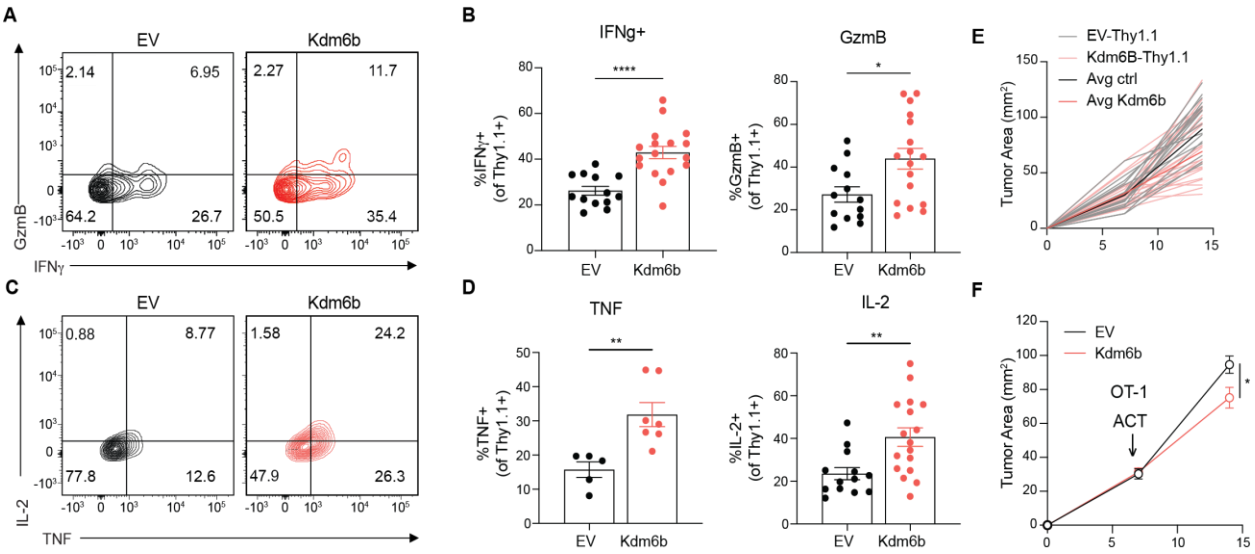

Figure 27. Enforced Kdm6b Expression Drives Increased Effector Function and Antitumor Response
(A) Interferon-γ (IFN-γ) and granzyme B (GzmB) staining gated on transduced OT-I T cells restimulated ex vivo with peptide (SIINFEKL). (B) Frequency of IFN-γ^+ and $GzmB^+$ cells. (C) Tumor necrosis factor (TNF) and IL-2 staining as in (A) and (B). (D) Frequency of TNF^+ and IL-2^+ cells. (E-F) Tumor growth between adoptive transfer of OT-I–transduced T cells at day 7 and termination of experiment at day 14. Flow cytometry plots are representative of ≥3 experiments. Statistics are Mann-Whitney (B, D) and two-way ANOVA (F) with *P < 0.05, **P < 0.01, ***P < 0.001, and ****P < 0.0001. Experiments performed by Paolo Vignali.

Our data support a model in which the hypoxic environment of solid tumors dysregulates the balance of H3K27 methylation, leading to bivalency at genes necessary for a robust effector response. Collectively, our data reveal the environmental burden of the tumor microenvironment upon infiltrating T cells and suggests that targeting hypoxia-mitigating or H3K27me3-regulating regiments to support effective antitumor immune responses for cancer therapy.

5.3 Discussion

Bivalent chromatin is defined as the presence of both positive (H3K4me3) and negative (H3K27me3) histone modifications at the same nucleosome within promoter regions. Primarily found in pluripotent cells and associated with genes that regulate cell fate decisions, bivalent genes are poised for induction or repression upon encounter with appropriate differentiation signals (218,

240). Recent studies have challenged this view, identifying bivalent chromatin in terminally differentiated cells and demonstrating protection from DNA methylation (222, 227). We identified an increase in bivalent chromatin in terminally exhausted cells using two methods: CUT&RUN with ChromHMM and at the single-cell level using PLA. We hypothesize that these are not cell fate genes ready for rapid expression but rather aberrant bivalency due to a loss of demethylase activity. Hypoxia is associated with increased bivalency, and terminally exhausted cells experience the most hypoxia (76, 236, 241). Changing hypoxia *in vivo* altered expression of bivalent genes, and decreasing hypoxia supported H3K27me3. In support of this, we found that enforced expression in an ACT model of JMJD3 (encoded by *Kdm6b*), which demethylates H3K27, increased the function of tumor-specific T cells despite maintaining features of exhaustion such as coinhibitory receptor expression. Accordingly, demethylation of H3K27 by JMJD3 is necessary for memory differentiation, suggesting that its overexpression drives cells to be more memory-like, which has been associated with improved antitumor function in ACT (145, 238). Notably, we did not observe decreased expression of inhibitory receptors or Tox, suggesting that improved effector functionality may be further bolstered with additional checkpoint blockade. Studies exploring DNA methylation via Dnmt3a found that exhausted cells had increased *de novo* DNA methylation at effector genes, which could be relieved by loss of Dnmt3a or DNA-demethylating agents in combination with anti-PD1 therapy (151). As there is interest in combining therapies targeting the epigenome, including Dnmt3a and Ezh2, in combination with checkpoint blockade, our study underscores the need for further exploration of the molecular players driving alterations such as bivalency, to understand how these therapeutic strategies may alter tumor immunity (151, 242).

While describing the role of Kdm6b in improving $CD8^+$ T cell function in the tumor, it does not address how H3K27me3 is being added to the bivalent genes as cells become terminally exhausted. The PRC2 complex is largely responsible for the addition of H3K27me3 via either the Ezh1 or Ezh2 catalytic subunit (243). *Ezh2* is expressed at a much higher level in $CD8^+$ T cells and is upregulated in terminally exhausted $CD8^+$ TIL, so it is the likely catalytic subunit responsible for methylation of H3K27me3 (data not shown, Fig. 26A). The role of PRC2 in regulating H3K27me3 is not fully understood. However, the PRC2 complex has been implicated in acquired bivalency in adult mouse intestinal cells and other adult tissues (244). Thus, PRC2 is the likely mechanism by which H3K27me3, but more work remains to be done to understand if preventing PRC2 activity is sufficient to prevent bivalency and terminal exhaustion.

Although CUT&RUN and CUT&TAG provide a technical advantage for analysis of histone modifications in small cell numbers, it is a bulk method, and thus, we are unable to resolve the level of heterogeneity at the single-cell level. Although single-cell methods may resolve some questions, there are limits of detection at the level of individual histones that are challenging to overcome with current technologies. An additional caveat of our study is that we limited analysis to B16 melanoma for practical reasons; however, although the precise chromatin states may vary somewhat in other tumor lines and in human patients, it is likely that our findings would be consistent for those that are highly infiltrated by immune cells and exhibit hypoxic niches.

Overall, our data highlight the importance of understanding the components of the tumor microenvironment and how they affect the epigenome and thus, differentiation. We have shown that the hypoxic tumor microenvironment is necessary for increased H3K27me3, leading to increased bivalency in terminally exhausted cells. Additionally, enforced expression of Kdm6b,

which removes methyl groups from H3K27me3, drives an improved antitumor response, highlighting it as a potential target for genetic manipulations for ACT, such as CAR T cells.

6.0 Continuous Stimulation and Hypoxia in Epigenetic Regulation of Terminally Exhausted Tumor-Infiltrating CD8$^+$ T Cells

Controlled gene promoter activity is a fundamental mechanism that regulates gene expression. The histone modifications H3K4me3 and H3K27me3 are active and repressive markers for promotor activity, respectively. We were surprised to find that terminally exhausted CD8$^+$ TIL had a prominent increase in hypoxia-driven bivalent promotors, at which both active and repressive histone modifications are found. To further explore the signals involved in increased bivalency in terminally exhausted cells, we used an in vitro system, which recapitulates many of the features of exhaustion, including coinhibitory receptor expression, decreased functionality, and mitochondrial dysfunction identified in terminally exhausted CD8$^+$ TIL (76).

Here, we explore the epigenetic and transcriptional landscapes of in vitro exhausted T cells. We first confirm that the combination of continuous stimulation and hypoxia (CSH) is sufficient to drive phenotypic and functional exhaustion. Indeed, we find that many of the gene programs upregulated in terminally exhausted CD8$^+$ TIL are also upregulated in CSH cells, notably genes related to cell cycling and DNA replication. Interestingly, we find that the both the continuously stimulated in normoxia (CSN) and CSH cells are epigenetically and transcriptionally similar to terminally exhausted CD8$^+$ TIL, whereas acutely stimulated cells in normoxia plus hypoxia (ASN, ASH) are more similar to the progenitor exhausted CD8$^+$ TIL. However, we find the combination of continuous stimulation plus hypoxia, or hypoxia alone, is not sufficient to drive increased bivalency in *in vitro* exhausted T cells.

6.1 Introduction

Due to the complexity of the *in vivo* settings where T cells become exhausted, a variety of reductionist methods that drive an exhaustion-like state *in vitro* have been published (72, 76). All rely primarily on providing continuous TCR signaling, and one such method removes the costimulatory signal (αCD28) after the initial activation period, allowing for the co-inhibitory receptor program to proceed (72). Another leverages a key feature of the tumor microenvironment, continuously stimulating the T cells in a hypoxic environment (76). These studies show that continuously stimulated cells are more like terminally exhausted $CD8^+$ TIL, whereas acutely stimulated cells are more stem like. Additionally, they show that hypoxia supports further progression to phenotypic and functional exhaustion, compared to continuously stimulated cells expanded in normoxia, suggesting that these cells better recapitulate the features of terminally exhausted TIL. We have adapted this protocol to interrogate the sufficiency of these two key signals, continuous TCR signaling and hypoxia, in regulating the transcriptional and epigenetic changes seen in terminally exhausted TIL (Fig. 28).

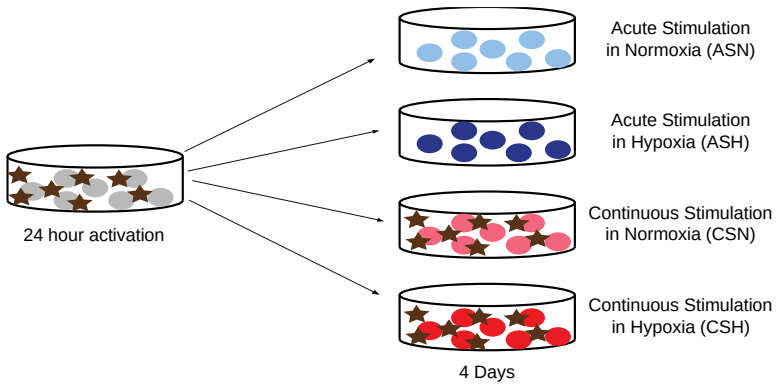

Figure 28. Experimental Setup for *in vitro* Exhaustion System.
Adpated from Scharping et al. (76). Circles represent cells, and stars represent αCD3/CD28 Dynabeads.

6.2 Results

6.2.1 Transcriptional and Epigenetic Features of In Vitro Exhausted T Cells

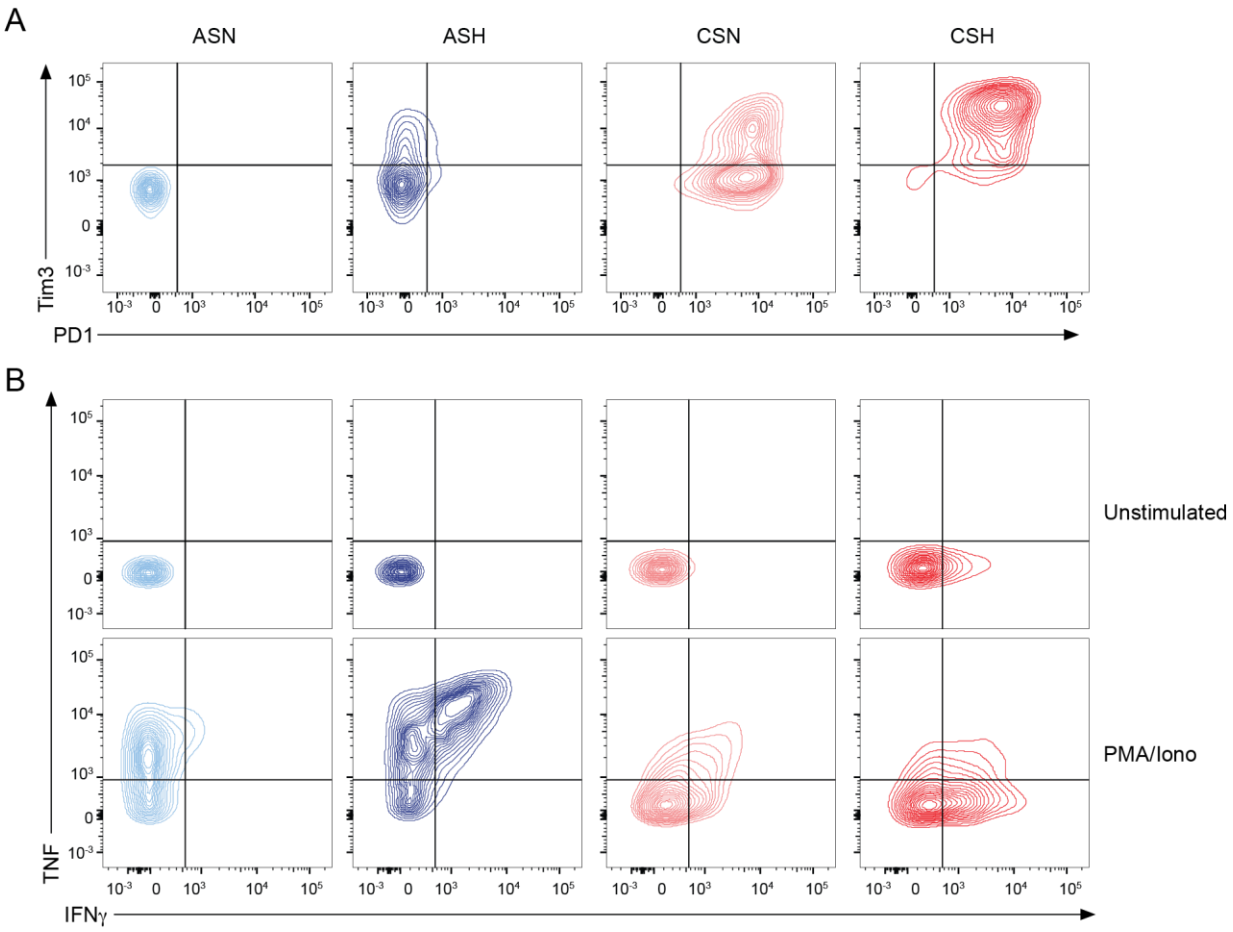

Figure 29. In Vitro Exhausted T Cells Recapitulate the Phenotype of Terminally Exhausted Tumor-Infiltrating CD8⁺ T Cells
(A) Representative flow cytometry plots showing the surface marker phenotype by PD1 and Tim-3 expression in each of the indicated groups. (B) Representative flow cytometry plots or intracellular cytokine staining of IFNγ and TNF expression either unstimulated or with PMA/Ionomycin stimulation. ASN, acute stimulation in normoxia; ASH, acute stimulation in hypoxia; CSN, continuous stimulation in normoxia; CSH, continuous stimulation in hypoxia.

We first confirmed that we indeed see the phenotypic and functional changes that were previously described (76). We found that cells acutely stimulated in normoxia and hypoxia (ASN and ASH, respectively) had low levels of PD1 expression, consistent with a more memory-like differentiation program (Fig. 29A). However, ASH cells did have a consistent increase in the

amount of Tim-3 expression compared to ASN. This increase is likely due to the described role of Tim-3 as a stress response gene (245). Additionally, we did confirm the increased expression of both PD1 and Tim-3 on cells continuously stimulated in normoxia and hypoxia (CSN and CSH, respectively) and showed the increased frequency of $PD1^{+}Tim\text{-}3^{+}$ T cells when expanded in hypoxia (Fig. 29A). We also confirmed the functional defect in these in vitro exhausted T cells by performing intracellular cytokine staining for TNF and IFNγ. We found a reduction in the number of $IFN\gamma^{+}TNF^{+}$ cells in CSH, compared to ASH and CSN (Fig. 29B). Unfortunately, we observed unexpected, consistent low IFNγ production in the ASN cells. The benefit of ASH on effector function had been previously shown, and indeed the cytokine production in ASH cells was consistently higher than in ASN cells (76).

To determine whether cells from CSH were transcriptionally similar to terminally exhausted TIL, we performed bulk RNAseq. Cells from each of the different conditions clustered independently with principal components clearly indicating continuous stimulation and hypoxia as important drivers of the transcriptional state (Fig. 30A). Analysis of DEGs revealed six distinct clusters (Fig. 30B). Cluster 1 was the cluster associated with continuous stimulation, and indeed, the exhaustion-associated genes *Pdcd1*, *Havcr2*, and *Prdm1* were found within this cluster (not shown). Cluster 2 was more associated with acute stimulation, and stemness/memory genes, like *Tcf7*, *Bcl6*, *S1pr1*, and *Sell* were all found within this cluster (not shown). To better understand these transcriptional programs, we again performed GO analysis, which identifies distinct gene programs in each of the six clusters (Fig. 30C). Cluster 1 recapitulated many of the features of terminally exhausted TIL, showing enrichment in genes associated with proliferation, whereas like progenitor exhausted TIL, cluster 2 was much more associated with T cell function. Interestingly, cluster 3 was most enriched for genes involved in the cellular response to hypoxia, including

HIF1α signaling. Clusters 4-6 had enrichment in GO terms associated with other immune-related function, including adhesion, chemotaxis, and proliferation. Finally, we used gene lists associated with stemness and terminal differentiation to show that indeed the acute stimulated genes are more associated with stemness and continuously stimulated with terminal differentiation, like their TIL counterparts (Fig. 30 D-E).

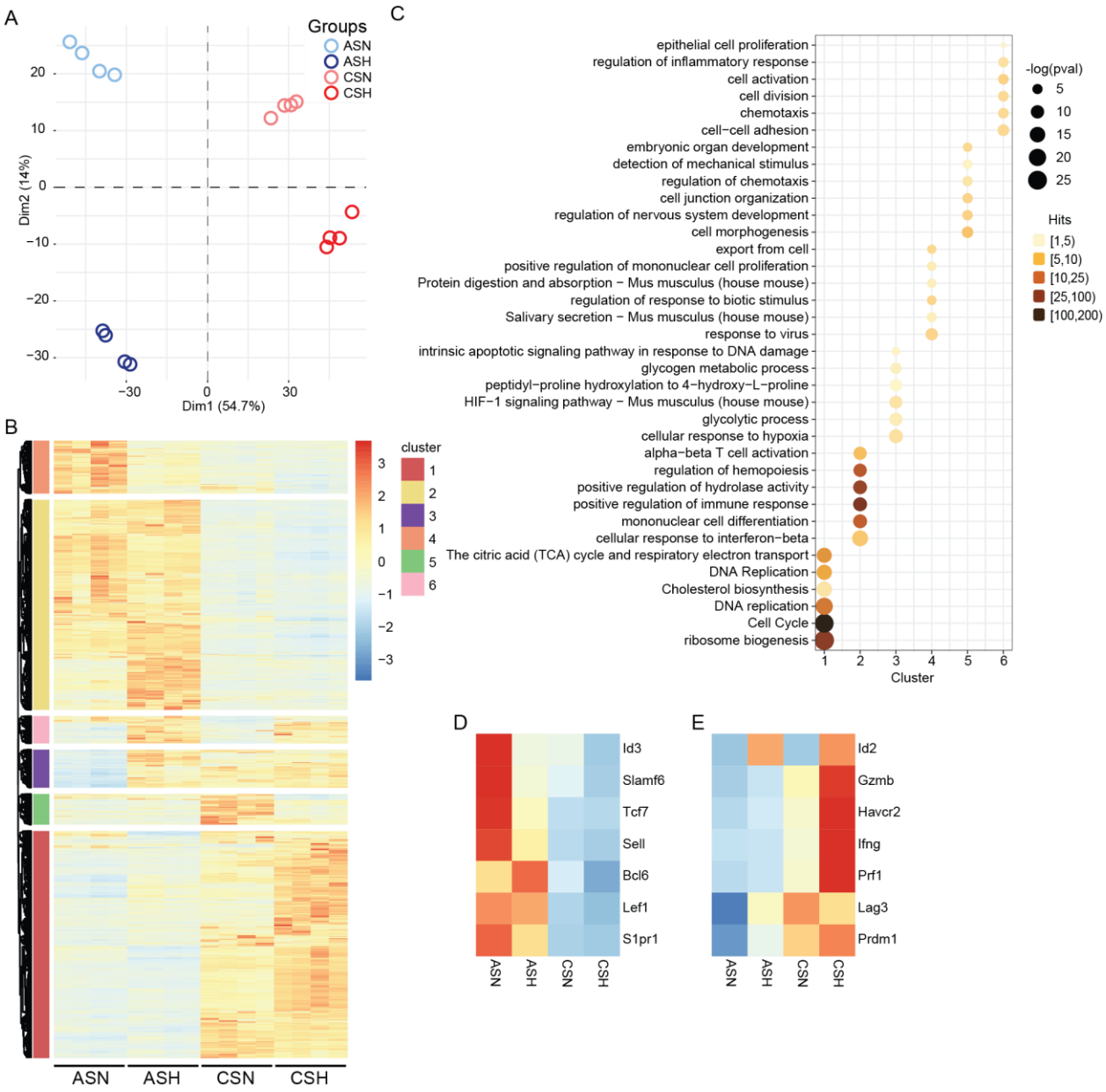

Figure 30. In Vitro Exhausted T Cells Are Transcriptionally Distinct

(A) Principal component analysis of transcriptomes of cells from ASN, ASH, CSN, and CSH. (B) DESeq2 of transformed log2 (TPM) normalized transcript expression of DEG cells from ASN, ASH, CSN, and CSH. (C) Enrichment of GO terms via Metascape in genes with active chromatin landscapes in indicated groups. (D and E) Gene expression of known genes associated with T cell stemness (D) and terminal differentiation (E).

To understand the epigenetic changes underlying the differentiation in these different culture conditions, we again performed CUT&Tag for H3K4me3 and H3K27me3. We found that like the transcriptional data, there were distinct clusters for each condition with clear stimulation and hypoxia-driven principal components (Fig. 31A-B). Analysis of DEPs revealed four distinct clusters for each histone modification, of which cluster 1 for H3K4me3 and cluster 3 for H3K27me3 were associated with continuous stimulation (Fig. 31C-D). Notably, the amount of H3K27me3 in cells from CSN and CSH were more variable than is seen in H3K4me3. Statistically, however, the cluster was robust, not breaking apart even when data was separated into ten clusters.

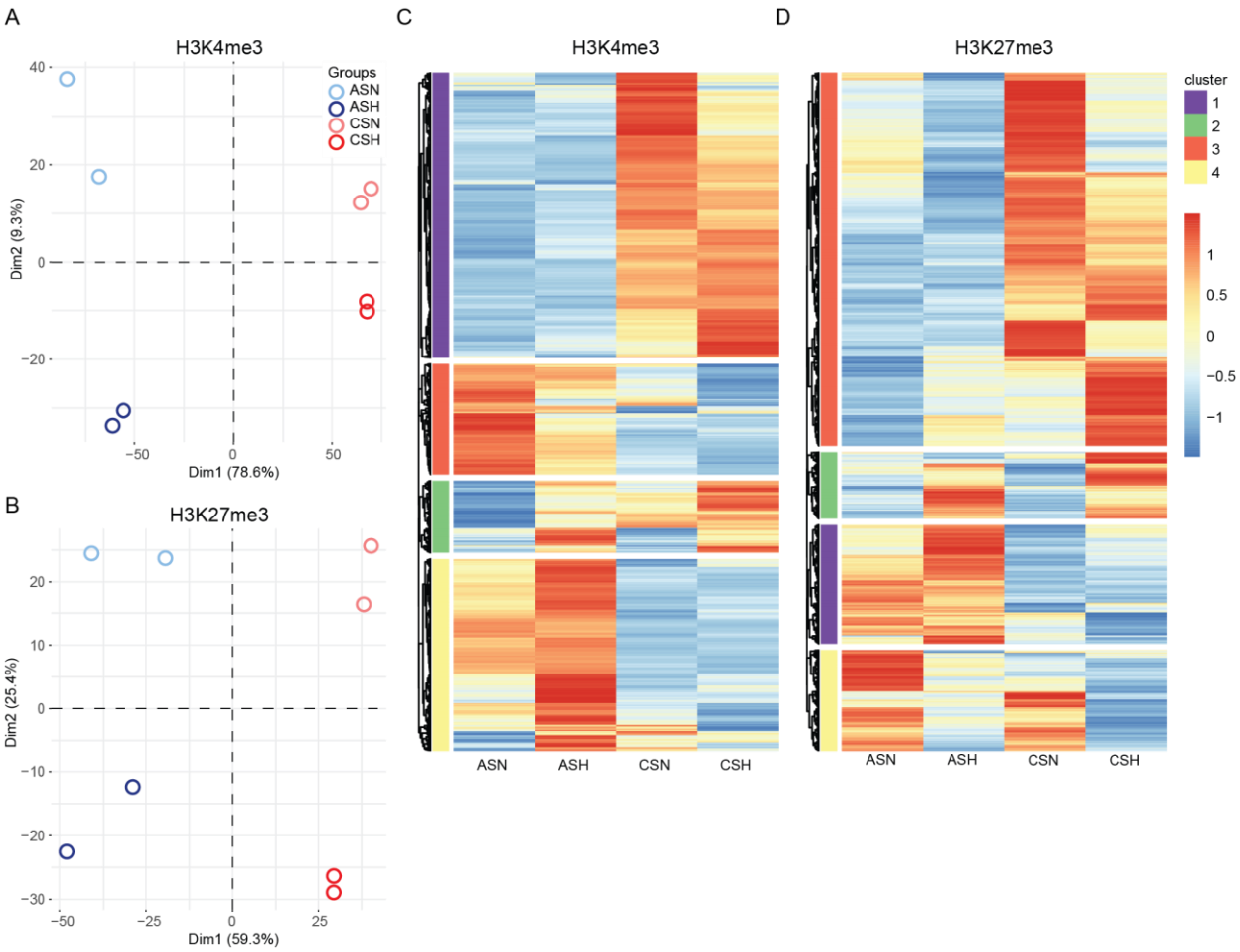

Figure 31. In Vitro Exhausted T Cells Are Epigenetically Distinct from Other In Vitro Cells
(A-B) Principal component analysis of H3K4me3 (A) and H3K27me3 (B) in cells from ASN, ASH, CSN, and CSH. (C-D) Tag counts (normalized per million) of H3K4me3 (C) and H3K27me3 (D) at differential peaks between in vitro conditions (DESeq2).

We were primarily interested in how the changes in gene expression of *in vitro* exhausted $CD8^+$ T cells were related to terminal exhaustion *in vivo*. We compared the transcriptional profiles of tumor-infiltrating lymphocytes from WT and *Ndufs4*-deficient B16 melanoma, which has reduced tumor hypoxia (76). In the transcriptional dataset, all four populations described in previous chapters were sorted. Interestingly, the differences in hypoxia within the TIL were not reflected in the Pearson correlation, with terminally exhausted TIL from both WT and *Ndufs4*-deficient B16 melanoma correlating more with CSH cells, than CSN (Fig. 32A). CSN cells

correlated primarily with the sorted PD1^{hi} population, and ASN and ASH both correlated primarily with the PD1^{mid} populations. Additionally, the sorted PD1^{lo} population was not closely related to any *in vitro* population.

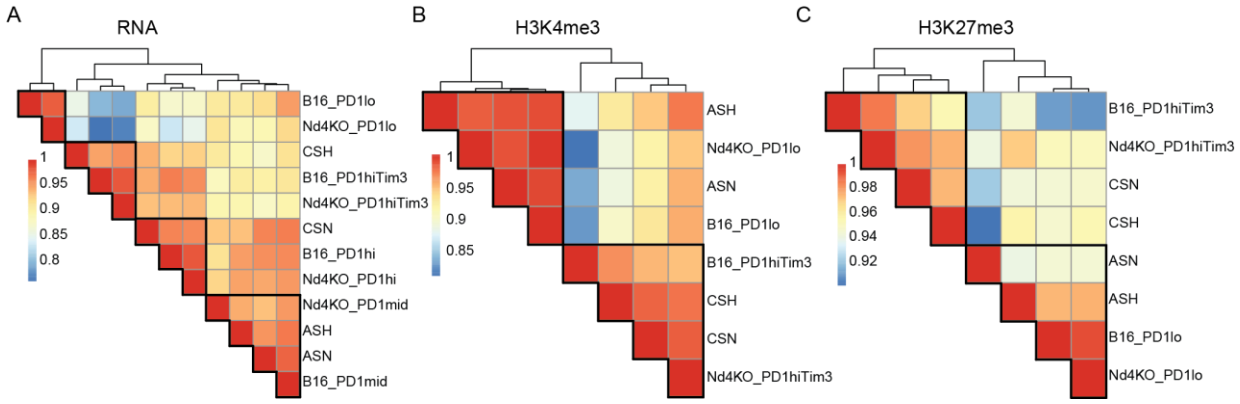

Figure 32. In Vitro Exhausted Cells Are Epigenetically Similar to Terminally Exhausted CD8$^+$ TIL
(A-C) Pearson correlations for RNA (A), H3K4me3 (B), and H3K27me3 (C) for in vivo CD8$^+$ TIL from WT and Ndufs4-deficient B16 melanoma.

We also explored the epigenetic similarities between *in vitro* exhausted T cells and CD8$^+$ TIL. For the tumor data, we sorted out only a PD1$^{lo/mid}$ progenitor population and a PD1^{hi}Tim-3$^+$ terminally exhausted population. The Pearson correlation of these data depicted two clear clusters of promoter activity marked by H3K4me3, one more progenitor, stem-like cluster and another terminal exhaustion cluster (Fig. 32B). Interestingly, for H3K27me3 the scale of correlation was greatly reduced, suggesting more similarity of the repressive modification within the different subsets. These results indicate that these in vitro conditions replicate epigenetic and gene expression features found *in vivo*.

6.2.2 Histone Methylation of In Vitro Exhausted CD8$^+$ T Cells

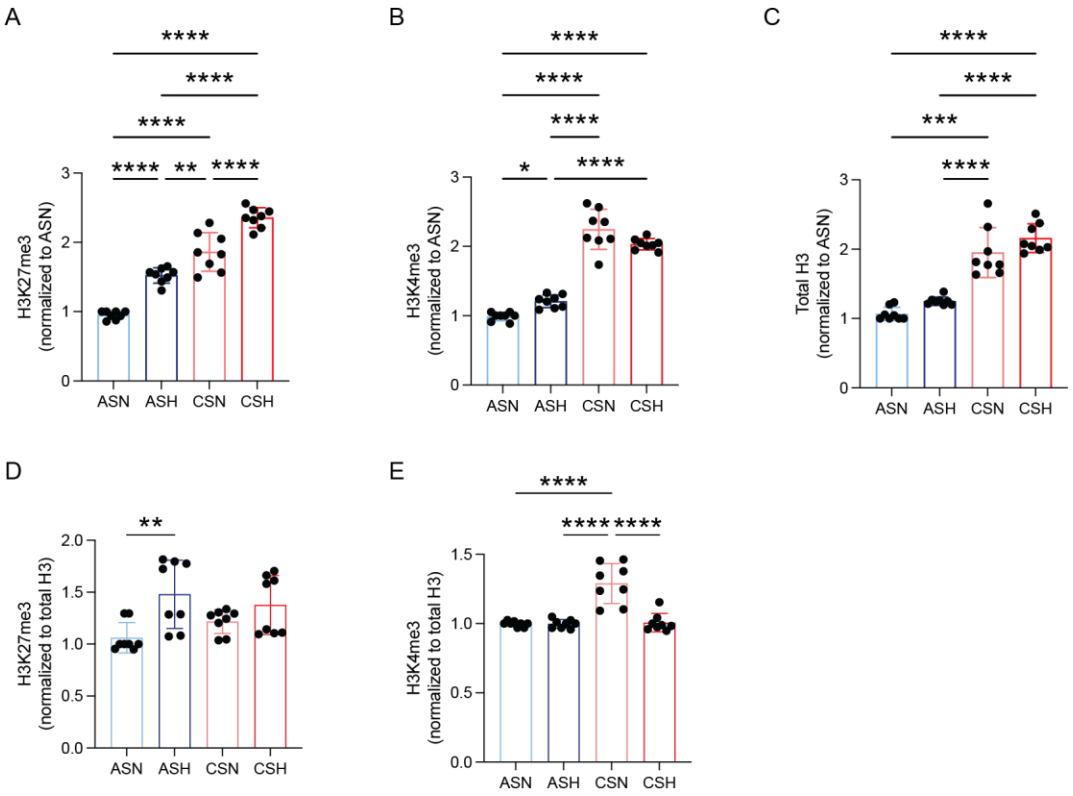

Figure 33. Global Increase in Methylation Is Not Seen in In Vitro Exhausted Cells
A-C) Geometric mean fluorescent intensity (gMFI) of H3K27me3 (A), H3K4me3 (B), and total histone H3 (C). (D-E) Levels of H3K27me3 (D) and H3K4me3 (E) normalized per cell for total H3 expression. Flow cytometry plots are representative of 2 experiments. Statistics are from ordinary one-way ANOVA; *p<0.05, **p<0.01, ***p<0.001, ****p<0.0001. ns, not significant.

Because we had found a global increase in the amount of histone methylation at H3K4 and H3K27 in terminally exhausted CD8$^+$ TIL experiencing more hypoxia, we explored whether hypoxia is sufficient to drive increased histone methylation, as previously described (235, 236). We used flow cytometry to assay global changes in the histone modifications relevant to bivalency, H3K27me3 and H3K4me3, in each cell culture condition. We found that there was a slight increase in H3K27me3 but no change in H3K4me3 in response to hypoxia, when normalized to H3 (Fig. 33A-E). Indeed, both CSN and CSH *in vitro* exhausted T cells had significant increases in the amount of histone H3, which was largely responsible for shifts in measured H3K27me3 and

H3K4me3. The lack of global increases indicate that chronic stimulation and hypoxia are not sufficient for the global increases in histone methylation found in terminally exhausted $CD8^+$ TIL.

6.2.3 Bivalent Genes in In Vitro Exhausted $CD8^+$ T Cells

We were especially interested in whether promotor bivalency was recapitulated *in vitro*, so we used ChromHMM to analyze the H3K4me3 and H3K27me3 CUT&Tag data (232). We again found a distinct bivalent state, state 2, with a high probability of both H3K27me3 and H3K4me3 at these genomic regions (Fig. 34A). However, we did not find a prominent increase in the CSH cells as we expected (Fig. 34B). Interestingly, the most noticeable increase in bivalency was in the CSN cells. Despite this result, we continued our analysis to determine whether these bivalent regions were found at promoters and whether they were primarily shared or unique to each cell type (Fig. 34C). We found that the number of bivalent promoters in these *in vitro* T cells is remarkably lower than in the $CD8^+$ TIL. Additionally, most of these genes were found shared between other groups, with only 83 genes being unique to CSN cells, which had the largest frequency of bivalent chromatin. Finally, we examined the amount of histone methylation at the bivalent genes identified *in vivo*, to explore whether these changes were conserved, despite not seeing changes in bivalency defined by ChromHMM. We found that like $CD8^+$ TIL, there were no significant changes in H3K4me4 in any of the four conditions (Fig. 34D). However, we did find changes in H3K27me3, but these were opposite to what we had expected, with higher levels of H3K27me3 in both ASN and CSN cells compared to ASH and CSH cells. These results suggest that the signals provided within the *in vitro* system are not sufficient to drive bivalency in terminally exhausted cells.

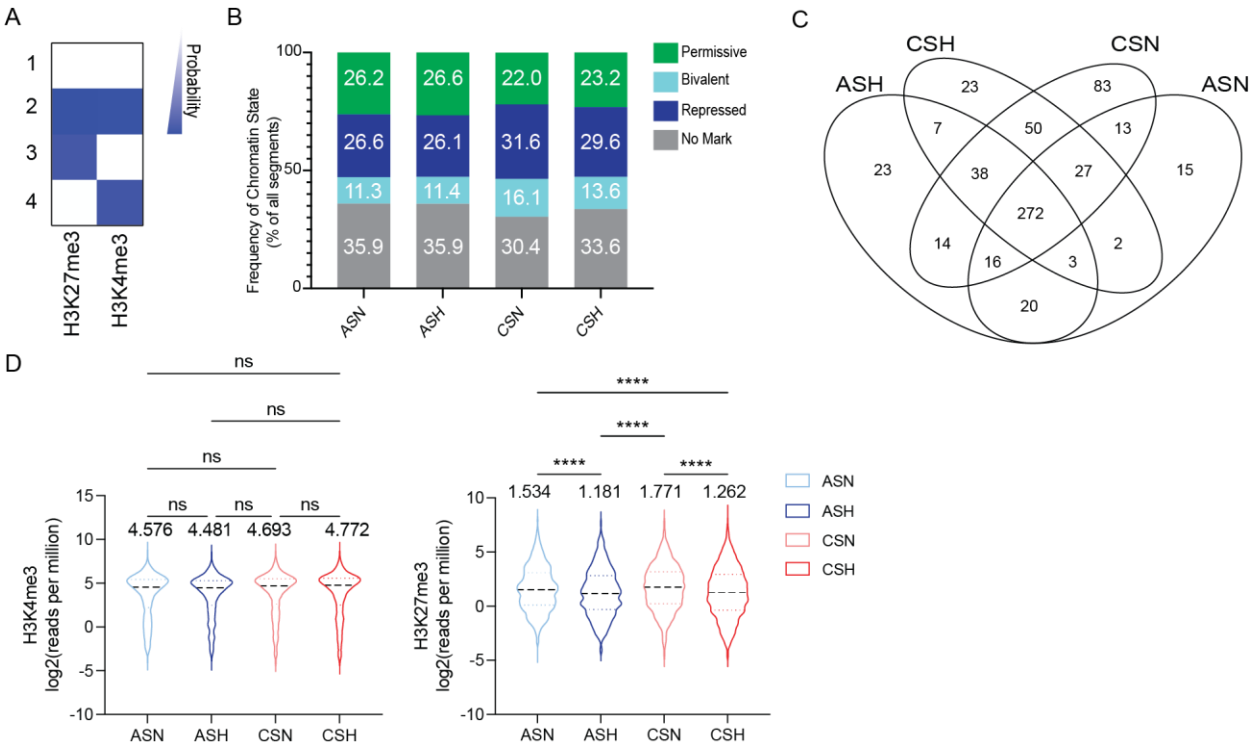

Figure 34. Hypoxia Is Not Suffient to Drive Increased Bivalency in In Vitro Exhausted T Cells

(A) ChromHMM emission plots depicting defined states in TILs and Vaccinia-OVA effector cells. (B) Frequency of chromatin states identified in (A) in TIL subsets and Vaccinia-OVA effector cells. (C) Genes identified in each subset as bivalent defined by both H3K4me3 and H3K27me3 in regions ±1 kb of all TSSs and filtered for expression less than 2 TPM. (D) Log2-normalized coverage of bivalent genes from CUT&Tag data for H3K4me3 and H3K27me3.

6.3 Discussion

Our extensive analysis demonstrates that neither hypoxia alone, nor the combination of continuous stimulation and hypoxia is sufficient to drive bivalency *in vitro*. These findings suggest that while hypoxia supports increased methylation and bivalency *in vivo*, another tumor microenvironmental signal is necessary for bivalency. Interestingly, unlike in terminally exhausted $CD8^+$ TIL, expression of the oxygen-insensitive histone demethylase *Kdm6b* is maintained in CSH, which may explain global levels of H3K27me3 remaining constant (data not shown). While increased expression of *Kdm6b* in TIL from the less hypoxic *Ndufs4*-deficient B16 suggested that

hypoxia inhibits *Kdm6b* gene expression, there may be other changes within these tumors and infiltrating T cells that regulate *Kdm6b*.

Intriguingly, despite not seeing the global increases in methylation or bivalency of in vitro exhausted T cells, we found that the gene expression and locations of H3K27me3 and H3K4me3 were similar to tumor-infiltrating $CD8^+$ T cells from *Ndufs4*-deficient and WT B16 melanoma tumors. Indeed, *in vitro* and *in vivo* hypoxia levels had little correlation at the transcriptional level. However, H3K4me3 and H3K27me3 from CSN cells were more correlated with terminally exhausted $CD8^+$ TIL from *Ndufs4*-deficient vs. WT mice. However, this correlation was also seen for CSH cells. More work needs to be done to directly compare which genes and genomic regions are changing in both these contexts and what is failing to be recapitulated *in vitro*. These future studies could provide further explanation for why changes in global methylation and bivalency are not seen in the in vitro exhausted $CD8^+$ T cells.

Overall, transcriptional and epigenetic profiles of in vitro exhausted T cells have highlighted that these cells recapitulate many of the features of exhausted $CD8^+$ TIL, but continuous stimulation and hypoxia are not sufficient for increased bivalent genes in terminally exhausted $CD8^+$ TIL. Specifically, these studies have further emphasized the potential importance of *Kdm6b* in regulating bivalency. These studies have also indicated a need for deeper analysis of the differences in histone modifications and gene expression in the CSN and CSH groups, compared to the terminally exhausted $CD8^+$ TIL from WT and *Ndufs4*-deficient B16 melanoma to identify hypoxia-dependent changes and potentially other effects of *Ndufs4* deletion on terminally exhausted $CD8^+$ TIL.

7.0 Summary and Future Directions

7.1 Summary

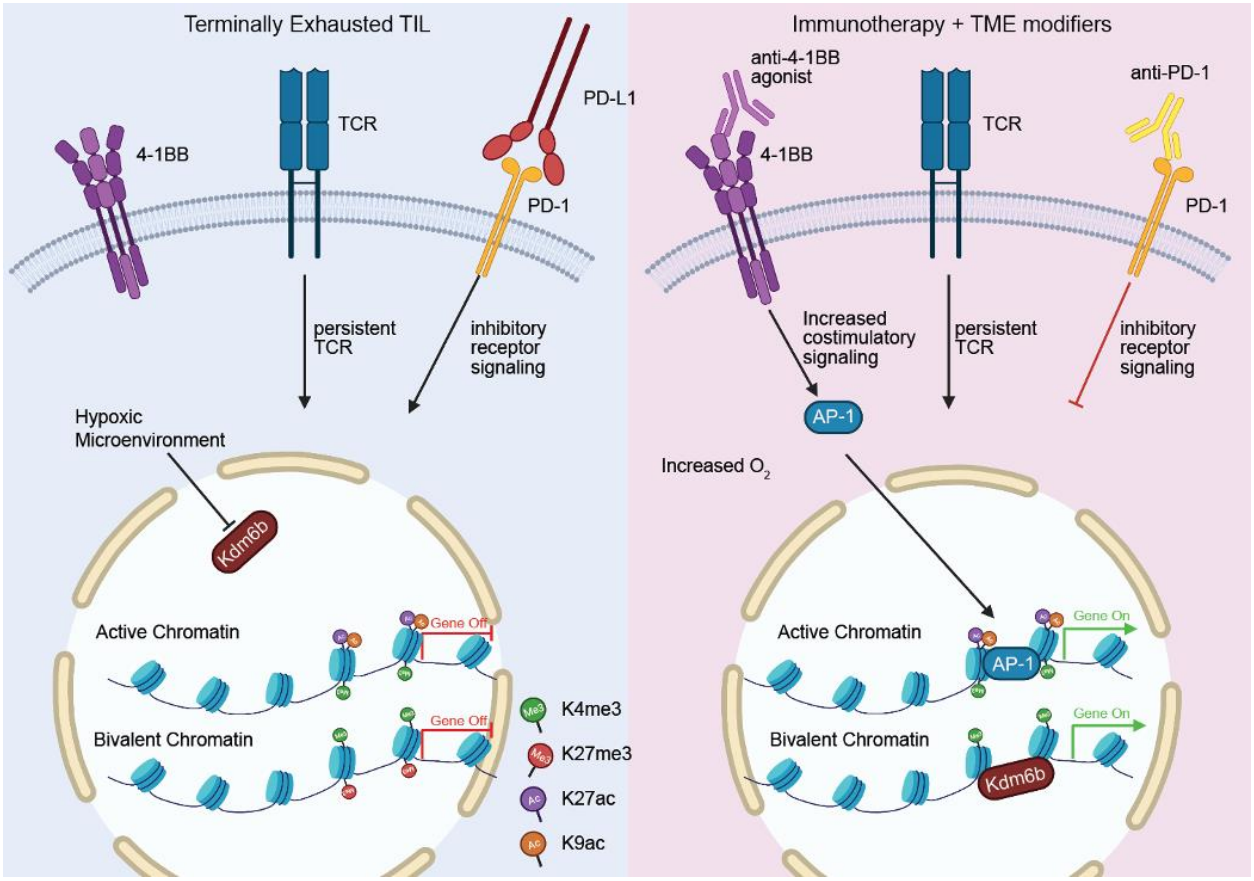

Figure 35. Graphical Summary

Cytotoxic $CD8^+$ T cells are critical in mounting an antitumor immune response. However, as $CD8^+$ T cells are continuously stimulated by tumor antigen, they undergo differentiation to a cell fate called exhaustion, which is characterized by high levels of coinhibitory receptor expression, reduced effector function, and increased susceptibility to apoptosis. The phenomenon of T cell exhaustion was initially described in the context of chronic viral infections but has been

widely described in tumor-infiltrating lymphocytes as well. Indeed, the dysfunctional $CD8^+$ T cells that respond to tumors exhibit many similarities to exhausted $CD8^+$ T cells observed in chronic viral infections. However, there is ongoing debate regarding whether the differentiation of $CD8^+$ T cells in response to a growing tumor and a viral antigen follows the exact same mechanisms.

In Chapter 2, we applied next generation sequencing (NGS) to understand transcriptional changes as $CD8^+$ TIL become terminally exhausted, as well as the changes in histone modifications in the genes changing expression. NGS technologies, especially RNA sequencing (RNAseq), have been extensively used to examine molecular alterations and regulatory proteins involved in the $CD8^+$ T cell differentiation upon antigen stimulation. While early investigations focused on characterizing the differentiation of effector and memory $CD8^+$ T cells during acute infections, RNAseq has also played an instrumental role in elucidating the features of exhausted $CD8^+$ T cells in chronic viral infections and tumor contexts. However, our results in Chapter 2 are novel, based on our characterization of histone modifications. Due to the limitations of chromatin immunoprecipitation sequencing (ChIPseq), which requires roughly one million cells, it was technically infeasible to collect these data on histone modifications. However, with the development of the low-input alternatives CUT&RUN and CUT&Tag, these experiments became possible.

While there are shared features in the different contexts of exhaustion, distinct microenvironmental signals influence gene expression under different conditions. Indeed, our transcriptional analyses showed that progenitor and terminally exhausted cells from the tumor contain many of the same features and gene signatures that have been reported for exhausted cells, but there is a reduced correlation compared to LCMV. Intriguingly, terminally exhausted $CD8^+$ T cells were enriched primarily in gene programs associated with cell cycling and DNA replication,

which while seemingly contradictory to the reduced proliferative capacity described as a hallmark of exhaustion, reflects more on the context of that claim than the reality of these cells. Finally, our studies in Chapter 2 confirm the known roles of active and repressive histone modifications in regulating the differentially expressed genes in these populations.

Our work in Chapters 3 and 5 identify two unique chromatin features in terminally exhausted $CD8^+$ TIL. First, we identify an increased incidence of active chromatin which is not associated with corresponding increases gene expression, which we have called anticorrelated genes (Fig. 35). We show that these active chromatin regions in terminally exhausted cells are highly enriched for the bZIP/AP-1 family of transcription factors, yet these transcription factors are not highly expressed. Indeed, we identify a role of reduced costimulatory signaling in lowering AP-1 gene expression in terminally exhausted cells, and if these cells are provided a costimulatory signal via 4-1BB agonist, AP-1 expression and anticorrelated gene expression is recovered. Additionally, we describe a surprising increase in promotor bivalency in terminally exhausted cells, despite initial descriptions of bivalency in maintaining cellular plasticity in embryonic stem cells and other pluripotent cell types (217, 218). This tumor-specific phenomenon is due to hypoxia-driven aberrant methylation of H3K27 at genes related to T cell stemness and effector function. By restoring the balance between methyltransferase and demethylase activity with enforced expression of the oxygen-insensitive histone demethylase Kdm6b, we improve the effector function and antitumor response. In terminally exhausted $CD8^+$ TIL, these two unique chromatin features are downstream of distinct signals within the tumor microenvironment, e.g. reduced co-stimulation and increased hypoxia. However, both suggest a similar priming of chromatin with high levels of active histone modification and no gene expression. In the case of anticorrelated genes, expression can be recovered by the appropriate costimulatory signal driving

AP-1 transcription factor expression, and for bivalent genes, removal of the repressive histone modification H3K27me3 is sufficient to restore effector function. Indeed, our data collectively suggest that terminally exhausted T cells may be a target for reinvigoration given the right therapeutic interventions, and our study may be helpful in developing combination therapies that take full advantage of all subsets of tumor-infiltrating T cells to eradicate cancer cells.

We also describe the role of direct binding of the transcription factor Tox in regulating both progenitor and terminally exhausted cells using CUT&RUN. While others had looked at the effect of Tox deletion on exhaustion, direct Tox binding locations had not yet been explored (90, 91, 95). We found Tox pairs with distinct binding partners in each subset, TCF-1 in progenitor and Batf:IRF in terminally exhausted cells. TCF-1 can act as a pioneer factor, binding to regions of heterochromatin to promote chromatin accessibility, and these binding sites can greatly be affected by binding partners (77). Thus, Tox may play a crucial role in determining differential TCF-1 binding in progenitor exhausted $CD8^+$ T cells, compared to other stem-like T cells with high TCF-1 expression. Through Taiji analysis, we found that both Batf and Irf4 were ranked as highly important and were positively correlated with gene expression, unlike the decreased expression of the other AP-1 family members. Our data implicate the cooperation of Batf, Irf4, and Tox in promoting expression of the exhaustion program in terminally exhausted $CD8^+$ TIL.

In the final chapter, we use a reductionist *in vitro* system that combines continuous stimulation and hypoxia to drive an exhaustion-like fate *in vitro* (76). Indeed, these in vitro cells have functional and phenotypic similarities to terminally exhausted $CD8^+$ TIL and similar epigenetic and gene expression changes. However, neither hypoxia alone nor the combination of continuous stimulation and hypoxia was sufficient to drive increased global methylation or bivalency, suggesting that another feature of the tumor microenvironment is necessary. Indeed, the

complete ablation of *Kdm6b* expression that we see *in vivo* is not seen in these in vitro exhausted cells, so it is possible that the balance between methylation and demethylation is maintained, unlike within the tumor. Indeed, this work suggests that the application of this *in vitro* system should be restricted to studies that explore the functional and phenotypic changes in exhaustion upon perturbation, rather than those that focus on epigenetic changes.

Overall, with this body of work, we have taken the crucial first steps into understanding how the tumor microenvironment tunes histone modifications and gene expression in $CD8^+$ T cell exhaustion. We have highlighted the primed chromatin in terminally exhausted cells with the potential to reinvigorate these cells, as well as targeting progenitor exhausted cells with αPD1 to take full advantage of each of the subsets of tumor-infiltrating T cells to improve the antitumor response. However, much work remains to be done to understand how these findings relate to human tumors, and further mechanistic studies are required to parse the signals involved in each of the chromatin features we described.

7.2 Future Directions

While these studies have taken important first steps in understanding histone modifications in T cell exhaustion, many questions remain to be answered, ranging from therapy-focused to purely mechanistic. We have proposed a model by which two distinct tumor microenvironment signals, lack of costimulatory signals and hypoxia, drive unique chromatin features in exhausted T cells. Therapeutically, providing a costimulatory signal with 4-1BB and reducing tumor hypoxia has improved the efficacy of αPD1 immunotherapy (203, 246, 247). However, an emerging area of research is targeting epigenetic modifiers in combination with αPD1 therapy, and our findings

suggest that there careful study is necessary to understand which epigenetic therapies may be efficacious due to their effect on $CD8^+$ T cells (248-250). For example, combining αPD1 with histone deacetylase inhibitors (HDACi) has been promising, primarily due to its role within the tumor cells (251-254). However, our finding of an increase in anticorrelated genes associated with high levels of histone acetylation suggest that this approach to directly target $CD8^+$ T cells will be insufficient. Similarly, ablation of the histone demethylase LSD1, which removes methyl groups at H3K4, has been shown to promote expression of endogenous retroviral elements and improve the response to αPD1 (255). Our results show high levels of H3K4me3 at anticorrelated genes, suggesting that this therapy may not improve $CD8^+$ T cell function itself. By contrast, tazemetostat (Taz) has been approved for clinical use in target Ezh2 in cancer cells themselves, and early studies are being performed to determine if Taz plus αPD1 is a valuable treatment strategy (256, 257). Our results showing increased H3K27me3 at immune-related bivalent genes suggest that Taz treatment of $CD8^+$ T cells could improve $CD8^+$ T cell stemness and synergize with αPD1 to promote the antitumor response. Of course, not all successful treatment strategies need to target the $CD8^+$ T cells specifically, but using our distinct chromatin features to understand the potential detrimental effects of non-specific drugs, like chemical inhibitors, on $CD8^+$ T cells is necessary for designing optimal treatment strategies. Thus, we will perform *in vivo* mouse tumor experiments to test these therapies and look at changes in the histone modifications, phenotype, and function to determine the effect that these combinations have on $CD8^+$ T cells. We will also complement this approach with genetic approaches to specifically target T cells. For example, for the combination of Taz and αPD1 treatments, we can use a CD8-specific tamoxifen-inducible deletion of *Ezh2* to determine the direct effects of low Ezh2 activity in $CD8^+$ T cells. We will also utilize our *in vitro* strategy to determine the direct effect that these therapies have on $CD8^+$ T cells when possible. For

all of these experiments, we can come back to our initial described chromatin features and determine whether they are impacted by these therapies, which will greatly inform how we understand differentiation to terminal exhaustion, as well as provide crucial information about whether modulating these epigenetic features is at necessary for improved $CD8^+$ T cell responses to cancer.

Understanding the role of epigenetic modifiers in $CD8^+$ T cell differentiation will be essential in designing epigenetic manipulations for CAR T cells, and other engineered cell therapies. A variety of studies have shown an improved antitumor response upon epigenetic manipulations. For example, deleting the DNA methyltransferase DNMT3a in CAR T cells greatly improves the antitumor response by preventing exhaustion (162). On the other side of DNA methylation regulation, lentiviral disruption of the *TET2* locus in a CAR T cell patient improved the antitumor response (258). These seemingly contrasting results emphasize the importance of a broader understanding of the interplay and targeting of these two proteins to understand how and when each manipulation may be beneficial. Similarly, our studies have shown an improved antitumor response upon enforced expression of *Kdm6b*, but deletion of *Kdm6b* was also shown to promote a more memory-like phenotype, which has long been associated with an improved antitumor response upon ACT (145). Another important stage of ACT is the expansion phase, in which patient T cells are manipulated and expanded *in vitro* prior to transfer. This phase provides a good opportunity for transient manipulations of epigenetic modifiers prior to infusion. Indeed, transient inhibition of Ezh2 with tazemetostat during the expansion phase improves the antitumor response (259). We can take a similar approach outlined above with combination therapies to determine if genetic and transient modulation of epigenetic modifiers has an effect on the chromatin features we have described, as well as exhaustion phenotype and T cell function.

Overall, these results again suggest that understanding how activity of an epigenetic modifier changes during activation and differentiation will be key in designing optimal engineered T cells for ACT. Specifically, it will be necessary to determine when a more transient or permanent manipulation of epigenetic modifiers is necessary for the appropriate immune response.

Our research on bivalent genes has highlighted the importance of H3K27me3 in terminal exhaustion. Increased levels of H3K27me3 have been associated with terminal differentiation (260). Indeed, PRC2-mediated methylation of H3K27 is necessary for terminal effector differentiation (142). The H3K27me3-mediated decreases in expression (via bivalency) of genes associated with T cell stemness and function suggests a similar role for H3K27me3 in terminal exhaustion. We are interested in first determining how methylation of H3K27 specifically drives terminal differentiation, as well as exploring the differing signals and resulting chromatin changes between these two distinct terminal cell fates. Additionally, we are intrigued by approaches for engineering PRC2 for targeting of specific genomic loci (261). Such an approach could be used to determine the sufficiency of sites of interest in driving terminal differentiation. Alternatively, a similar protein could be engineered with Jmjd3, to determine whether demethylation at specific sites is sufficient to prevent or reverse terminal differentiation. Additionally, understanding if and when H3K4me3 is co-deposited with H3K27me3 in terminal differentiation will be necessary in understanding the signals needed to potentially reverse terminal effector or exhaustion differentiation. This improved understanding of the role of H3K27me3 will greatly inform how we understand terminal differentiation in $CD8^+$ T cells, both in exhaustion and effector differentiation.

Our RNA sequencing results from both terminally exhausted $CD8^+$ TIL and *in vitro* exhausted T cells from CSH conditions show a prominent enrichment of genes associated with

cell cycling and DNA replication, despite the known inability of these cells to increase in absolute number (72). This cell state of high cycling and a terminal differentiated state is somewhat unique, as most terminally differentiated cells permanently exit from the cell cycle (262). We are interested in exploring the mechanisms that drive increased cell cycling and proliferation in terminally exhausted $CD8^+$ TIL and the phenotypic and functional consequences. Of course, chronic TCR stimulation is likely the cause of this highly proliferative state. Unfortunately, parsing out the role of TCR itself will be complicated by the fact that continuous TCR stimulation is necessary for the survival of these cells (263, 264). Thus, decoupling changes in proliferation and changes in survival will be challenging. However, modulating the ability of cells to cycle and monitoring changes in exhaustion phenotype and function is relatively straightforward, since *in vitro* exhausted T cells recapitulate this feature. Overall, understanding the role of cell cycling in terminal exhaustion could greatly inform how these cells differentiate, as well as provide future targets and strategies for engineering these cells for therapy.

Since beginning this work, single cell sequencing techniques have become much more widely applied, and indeed, the technology has progressed immensely. Understanding whether and how anticorrelated and bivalent genes are regulated in single cells will greatly contribute to how these chromatin features can be targeted for improved antitumor responses. For anticorrelated gens, joint profiling of histone modifications and RNA within single cells would be especially useful (265-267). Confirming that these anticorrelated genes are found within single cells would allow us to better understand heterogeneity of anticorrelated gene expression and would more directly show the presence of low gene expression despite these active histone modifications within single cells. The description of CUT&Tag-based single cell assays that can interrogate multiple histone modifications in single cells is also especially applicable (268, 269). While

proximity ligation analysis (PLA) has provided evidence that bivalency is not a function of cellular heterogeneity, we have not yet been able to address which genes are bivalent within single cells, which is likely a lower number than what we have described with bulk sequencing data.

Specifically, using these single cell data for network analyses will be crucial in determining whether there are conserved anticorrelated and bivalent gene modules within single terminally exhausted cells or heterogeneity in which genes have these features in which cells. Additionally, the role of these chromatin features will provide unbiased evidence of their importance in terminal exhaustion. Finally, pseudotime or velocity-type analyses of chromatin and RNA changes could provide valuable information regarding the temporal nature of histone changes with respect to RNA and differentiation state in general. Overall, the possibilities of single cell data to further inform how we understand these chromatin features with respect to differentiation and terminal exhaustion are extensive.

8.0 Materials and Methods

8.1 Ethics and Biosafety Information

All research in this study was conducted under the oversight of the University of Pittsburgh IACUC (protocol 21028804). All experiments were performed in University of Pittsburgh Biosafety Level 2 (BSL-2) laboratories. All mouse experiments were performed in BSL-1.

8.2 Study Design

Our research objective was to investigate the epigenetic and transcriptomic landscape of tumor-derived $CD8^+$ T cells. Study design included controlled and observational laboratory experiments. Sample sizes for sequencing studies pooled animals to collect sufficient cell numbers and were repeated two to three times to generate biological replicates. All data were included, and outliers were only removed if there was sufficient evidence of contamination or technical flaws in the experimental process. All animal studies, including tumor endpoints, were approved under Institutional Animal Care and Use Committee protocol 20077737. Analysis of initial datasets were used to form hypotheses on the relationship of hypoxia and costimulatory signaling.

8.3 Cell Lines and Virus

B16-F10 tumor cells were obtained from the American Type Culture Collection. Ndufs4-deficient B16-F10 tumors were generated as previously described (1). Vaccinia-OVA was generated by J. R.Bennink and provided by J. Powell (Johns Hopkins University).

8.4 Mouse Tumor Experiments

Mice were injected intradermally with $2.5x10^5$ B16-F10 cells [B16; American Type Culture Collection (ATCC)], B16-OVA (MO5; from P. Basse and L. Falo at the University of Pittsburgh), or B16-Ndufs4KO (41). TILs and dLNs were harvested on day 14, when tumors were typically 8 to 10 mm in diameter. In immunotherapy experiments, B16 was injected intradermally into mice. On day 10 (5- to 6-mm average diameter), mice were treated with 200 μg of anti-PD1 (J43; BioXCell), 200 μg of anti–4-1BB (3H3; BioXCell), or equivalent isotype control and then a second dose after 48 hours. Tumors were isolated for TIL preparation 24 hours after the second dose.

Tumors were surgically removed and injected repeatedly with a total of 1.2 mL of 2mg/ml collagenase type IV, 2 U/ml of hyaluronidase, and 10 U/ml DNase I in RPMI with 10% FBS and incubated for 30 minutes at 37°C. Tumors were mechanically disrupted between frosted glass slides, filtered, and vortexed for 2 minutes. For sequencing experiments, tumor cells were removed by anti-CD105 negative magnetic bead selection (BioLegend, MojoSort). Lymph nodes and splenic T cells were isolated by mechanic disruption through a 30μm filter.

8.5 *Vaccinia*-OVA Experiments

Mice were simultaneously injected with 10^6 PFU of Vaccinia-OVA intraperitoneally and $1x10^5$ naïve OT-I$^+$Thy1.1$^+$CD8$^+$ T cells retro-orbitally. On day 10, spleens were harvested, and erythrocytes lysed with a 1x solution of RBC lysis buffer (Thermo Fisher). Thy1.1$^+$ T cells were enriched by negative magnetic bead selection using MojoSort Streptavidin Nanobeads (BioLegend) and biotinylated antibodies: anti-TCRγ/δ, anti-CD19, anti-B220, anti-NK1.1, anti-CD49b, anti-CD105, anti-CD32/64, anti-CD11c, anti-CD11b, anti-Ly6G, and anti-CD24. Activation of OT-I CD8$^+$ T cells was verified by flow cytometry.

8.6 In Vitro Exhaustion Experiments

All *in vitro* exhaustion experiments were performed with naïve CD8$^+$ T cells isolated from 6-8 week old mice. Naïve CD8$^+$ T cells were magnetically enriched using the EasySep Mouse Naïve CD8$^+$ T Cell kit (Stem Cell) and were checked for at least 95% purity prior to continuing. Cells were then stimulated for 24 hours with CD3/CD28 Dynabeads (Gibco) at a 1:1 cell-to-bead ratio and 10ng/ml IL-2 (Miltenyi) and 10 ng/ml IL-2 (Miltenyi) in RPMI with 10% fetal bovine serum. After stimulation, cells were split into four conditions, two of which were passaged in normoxia or hypoxia with 10ng/ml IL-2 alone and two of which were continuously stimulated in normoxia or hypoxia with a CD3/CD28 Dynabeads at a 1:10 cell-to-bead ratio. After 48 hours, cells were split in half and topped with fresh media and IL-2, as well as the addition of beads in continuously stimulated conditions to maintain the 1:10 cell-to-bead ratio. After 48 more hours, cells were collected for various readouts. For RNAseq and CUT&Tag experiments a Dead Cell

Removal Kit (Miltenyi) was used to remove dead cells. For flow cytometry, cells were taken and stained directly.

8.7 Flow Cytometry

For flow cytometry, surface stains were performed on live cells in Hanks' Balanced Salt Solution (HBSS) at 4°C. Cells were then fixed with 2% paraformaldehyde (PFA) solution, followed by Foxp3 kit (Invitrogen) fixation/permeabilization overnight. Intracellular antibodies were added to cells in Foxp3 kit permeabilization wash.

8.8 RNA Sequencing

cDNA was prepared from ~1,000 cells using the SMART-seq v4 Ultra Low Input RNA Kit for Sequencing, (Clontech Laboratories). Sequencing libraries were prepared using the Nextera XT DNA Library Preparation kit (Illumina), normalized at 2nM using Tris-HCl (10 mM, pH 8.5) with 0.1% Tween-20, diluted and denatured to a final concentration of 1.8nM using the Illumina Denaturing and Diluting libraries for the NextSeq 500 protocol Revision D (Illumina). Cluster generation and 75-bp paired-end, dual-indexed sequencing was performed on the Illumina NextSeq 500 system.

8.9 CUT&RUN and CUT&Tag

CUT&RUN and CUT&TAG assays were performed as previously described (15, 16). For CUT&RUN, live sorted cells were incubated overnight with concanavalin A beads (Bangs Laboratories Inc.) and antibodies recognizing H3K4me3 (Abcam), H3K27me3 (Cell Signaling Technology), H3K27ac (Abcam), H3K9ac (Abcam), Tox (Abcam), Batf (Brookwood Biomedical), or IgG (Cell Signaling Technology). Protein A–micrococcal nuclease (pA-MNase) was then added, followed by $CaCl_2$ to cleave the antibody-bound chromatin. Phenol-chloroform extraction was then performed to isolate enriched DNA. Two replicates were performed for each antibody (except for Batf). Libraries were prepared using NEBNext Multiplex Oligos for Illumina (New England Biolabs) and either the sparQ DNA Library Prep Kit (Quantabio) or the NEBNext Ultra II DNA Library Prep Kit for Illumina (New England Biolabs). For CUT&TAG, nuclei were extracted from live sorted cells and incubated overnight with concanavalin A beads (Bangs Laboratories Inc.) and antibodies recognizing H3K4me3 (Abcam) and H3K27me3 (Cell Signaling Technology). A goat anti-rabbit secondary antibody (EpiCypher) and pAG-Tn5 (Epicypher) were then added, followed by $MgCl_2$ to fragment the antibody-bound chromatin with Illumina-compatible adapters. After amplification of libraries, DNA was purified using AMPure beads (Beckman Coulter). Libraries were quantified by quantitative polymerase chain reaction (qPCR) using either the sparQ Library Quant Kit (Quantabio) or the NEBNext Library Quant Kit (New England Biolabs) for Illumina. Appropriate library size was confirmed by running amplified qPCR products on an agarose gel. Cluster generation and 75–base pair paired-end, dual-indexed sequencing was performed on an Illumina NextSeq500.

8.10 Proximity Ligation Assay

Sorted T cells were attached to slides using an Epredia Cytospin Centrifuge for 10 min at 2000 rpm, 4°C, followed by immediate 4% paraformaldehyde fixation and serial permeabilization washes with 0.1% Triton X-100 in 1x phosphate-buffered saline. After blocking with Duolink buffer (Sigma-Aldrich), primary antibodies were directed against H3K4me3 (C36B11; Cell Signaling Technology) and H3K27me3 (ab6002; Abcam) and were added to Duolink antibody diluent and incubated on slides overnight at 4°C. Downstream staining was accomplished in accordance with the manufacturer's protocol with Duolink In Situ Orange (Sigma-Aldrich). Slides were imaged with a Nikon 100x 1.40 numerical aperture objective on a Nikon Ti inverted microscope and point scanning confocal scan head. Stacks of 500-nm intervals were captured for 4′,6-diamidino-2- phenylindole (DAPI) and Cy3 channels and refined on NIS-Elements to capture the three-dimensional structure and accurately count PLA foci within the cell nucleus.

8.11 *Kdm6b* Overexpression Experiments

Retrovirus for T cell transduction was generated with the Platinum-E (Plat-E) cell line (ATCC) and used Xfect Transfection Reagent (Takara) per the manufacturer's protocol. Naive OT-I T cells were activated with plate-bound anti-CD3 (5 μg/ml; BioLegend), soluble anti-CD28 (1 μg/ml; BioLegend), and IL-2 (100 U; National Institutes of Health) for 24 hours. Retroviral supernatants were harvested from Plat-E cultures, filtered, and supplemented with polybrene (6 μg/ml) and IL-2 (100 U). Prepared retroviral supernatants were spun onto activated T cells (2200 rpm, 2 hours, 37°C) and then rested at 37°C for an additional 2 hours. T cells were washed

thoroughly and cultured in fresh complete RPMI 1640 with IL-2 (50 U) for 3 days to allow for expansion and expression of vector cassette. After 3 days, 5 million T cells (per mouse) were retro-orbitally injected into CD45.1 mice carrying day 7 B16-OVA tumors (~6x6 mm^2). Transferred T cells were identified by CD45.2 and vector expression by Thy1.1.

8.12 Sequencing Data Processing

FastQC was used to perform a quality assessment on all fastq files. The mouse reference genome (GRCm38) was downloaded from Ensembl. Adaptors were trimmed for both RNA sequencing and CUT&RUN data using cutadapt v1.18. RNA sequencing samples were aligned to using HISAT2 v2.1.0. Raw count values were generated using Subread, and gene expression values were normalized using transcripts per million. CUT&RUN reads were aligned to the reference genome using Bowtie2 v2.3.4.2. Duplicates were removed using Picard, and regions from the ENCODE Blacklist were removed using bedtools intersect.

8.12.1 Peak Calling and Generation of Tag Count Files

For the characterization of reproducible histone modification and transcription factor peaks from CUT&RUN and publicly available ATAC-seq and ChIP-seq datasets, macs2 v2.1.1 was applied. For H3K27ac, a p value cutoff of 0.05 was used. For all other marks and ATAC-seq, a p value cutoff of 0.005 was used. Broad peaks were called for H3K27me3 and H3K4me3, whereas narrow peaks were called for H3K27ac, H3K9ac, ATAC-seq, and transcription factors. Irreproducible discovery rate (IDR) peaks were then found using a threshold of 0.05. IDR peak

files of all TIL samples were then merged to create a master list of peaks for each mark. The master peak list and the alignment files were then used in bedtools coverage to generate tag counts for each replicate.

8.12.2 Differential Peak and Gene Expression Analysis

DESeq2 was applied to raw counts transcriptome data in a pairwise manner to determine differentially expressed genes. These gene lists were compiled to make a master list of all differentially expressed genes. Log2 transformed normalized counts were then displayed as a heatmap to display expression of differentially expressed genes. DESeq2 was applied to raw tag count data for called peaks in a pairwise manner to determine differential peaks. These peak lists were compiled to make a master list of all differential peaks for each mark. Peaks were annotated to the nearest gene using ChIPpeakAnno (Zhu et al 2010).

8.13 Analysis of Bioinformatic Data

Motif enrichment analysis was performed using HOMER findMotifsGenome (60). Differential peak files were used for these analyses to define the specific motifs that were changing. The background file was specified using progenitor as background for terminal analyses and vice versa, unless otherwise specified. All motifs shown are from the known motifs output of findMotifsGenome.

HOMER makeTagDirectory and AnnotatePeaks functions were used to make histograms. Alignment files were used in makeTagDirectories to make tag directories for each replicate.

AnnotatePeaks was used with the peak file of interest and the tag directories to generate magnitude data for each replicate at a given point from the center of the peak. These values were normalized using the read count for each replicate and graphed using GraphPad Prism.

PageRank analysis was performed using Taiji (23). The analysis was performed using H3K4me3, transcriptome, and H3K27ac data to rank the transcription factors. The motifs used were from the Homer database. Fold change between progenitor and terminally exhausted PageRank values was then calculated to determine factors important in each context.

Bivalent chromatin was defined using ChromHMM. Bam files with duplicated and blacklisted regions removed were used in the BinarizeBam function with a bin size of 1000. The LearnModel function was then used with seven states defined and a bin size of 1000. Bivalent states were defined using the presence of both H3K27me3 and H3K4me3 and low gene expression.

8.14 Analysis of Single Cell Data

Matrix, features, and barcodes files were downloaded from NCBI Gene Expression Omnibus (GEO) or provided by collaborators. These datasets were each projected onto the ProjecTIL T cell reference atlas (ref_TILAtlas_mouse_v1) using ProjecTIL and annotated $CD8^+$ T cells alone were isolated for further analysis. All of the annotated $CD8^+$ T cells from these three B16 datasets were combined and dimension reduction and clustering were performed using Seurat. Differential gene expression and bivalent gene lists from bulk sequencing were provided as features for visualization.

8.15 Statistical Analysis

Statistical significance of genomics data was determined using P values given by DESeq2. Any other methods of determining statistical significance are described in the figure legends.

Bibliography

1. Virchow, R. 1989. Cellular pathology. As based upon physiological and pathological histology. Lecture XVI--Atheromatous affection of arteries. 1858. *Nutr Rev* 47: 23-25.

2. Nauts, H. C., W. E. Swift, and B. L. Coley. 1946. The Treatment of Malignant Tumors by Bacterial Toxins as Developed by the Late William B. Coley, M.D., Reviewed in the Light of Modern Research. *Cancer Research* 6: 205-216.

3. Old, L. J., D. A. Clarke, and B. Benacerraf. 1959. Effect of Bacillus Calmette-Guérin Infection on Transplanted Tumours in the Mouse. *Nature* 184: 291-292.

4. Redelman-Sidi, G., M. S. Glickman, and B. H. Bochner. 2014. The mechanism of action of BCG therapy for bladder cancer—a current perspective. *Nature Reviews Urology* 11: 153-162.

5. Rosenberg, S. A. 2014. IL-2: the first effective immunotherapy for human cancer. *J Immunol* 192: 5451-5458.

6. Ehrlich, P. 1908. *Ueber den jetzigen Stand der Karzinomforschung*.

7. Old, L. J., and E. A. Boyse. 1964. Immunology of Experimental Tumors. *Annual Review of Medicine* 15: 167-186.

8. Dunn, G. P., L. J. Old, and R. D. Schreiber. 2004. The Immunobiology of Cancer Immunosurveillance and Immunoediting. *Immunity* 21: 137-148.

9. Dunn, G. P., L. J. Old, and R. D. Schreiber. 2004. The Three Es of Cancer Immunoediting. *Annual Review of Immunology* 22: 329-360.

10. Pagès, F., J. Galon, M. C. Dieu-Nosjean, E. Tartour, C. Sautès-Fridman, and W. H. Fridman. 2010. Immune infiltration in human tumors: a prognostic factor that should not be ignored. *Oncogene* 29: 1093-1102.

11. Ali, H. R., E. Provenzano, S. J. Dawson, F. M. Blows, B. Liu, M. Shah, H. M. Earl, C. J. Poole, L. Hiller, J. A. Dunn, S. J. Bowden, C. Twelves, J. M. Bartlett, S. M. Mahmoud, E. Rakha, I. O. Ellis, S. Liu, D. Gao, T. O. Nielsen, P. D. Pharoah, and C. Caldas. 2014. Association between CD8+ T-cell infiltration and breast cancer survival in 12,439 patients. *Ann Oncol* 25: 1536-1543.

12. Sharma, P., Y. Shen, S. Wen, S. Yamada, A. A. Jungbluth, S. Gnjatic, D. F. Bajorin, V. E. Reuter, H. Herr, L. J. Old, and E. Sato. 2007. CD8 tumor-infiltrating lymphocytes are predictive of survival in muscle-invasive urothelial carcinoma. *Proceedings of the National Academy of Sciences* 104: 3967-3972.

13. He, X., and C. Xu. 2020. Immune checkpoint signaling and cancer immunotherapy. *Cell Research* 30: 660-669.

14. Waldman, A. D., J. M. Fritz, and M. J. Lenardo. 2020. A guide to cancer immunotherapy: from T cell basic science to clinical practice. *Nature Reviews Immunology* 20: 651-668.

15. Larkin, J., V. Chiarion-Sileni, R. Gonzalez, J.-J. Grob, P. Rutkowski, C. D. Lao, C. L. Cowey, D. Schadendorf, J. Wagstaff, R. Dummer, P. F. Ferrucci, M. Smylie, D. Hogg, A. Hill, I. Márquez-Rodas, J. Haanen, M. Guidoboni, M. Maio, P. Schöffski, M. S. Carlino, C. Lebbé, G. McArthur, P. A. Ascierto, G. A. Daniels, G. V. Long, L. Bastholt, J. I. Rizzo, A. Balogh, A. Moshyk, F. S. Hodi, and J. D. Wolchok. 2019. Five-Year Survival with Combined Nivolumab and Ipilimumab in Advanced Melanoma. *New England Journal of Medicine* 381: 1535-1546.

16. Wolchok, J. D., V. Chiarion-Sileni, R. Gonzalez, P. Rutkowski, J.-J. Grob, C. L. Cowey, C. D. Lao, J. Wagstaff, D. Schadendorf, P. F. Ferrucci, M. Smylie, R. Dummer, A. Hill, D. Hogg, J. Haanen, M. S. Carlino, O. Bechter, M. Maio, I. Marquez-Rodas, M. Guidoboni, G. McArthur, C. Lebbé, P. A. Ascierto, G. V. Long, J. Cebon, J. Sosman, M. A. Postow, M. K. Callahan, D. Walker, L. Rollin, R. Bhore, F. S. Hodi, and J. Larkin. 2017. Overall Survival with Combined Nivolumab and Ipilimumab in Advanced Melanoma. *New England Journal of Medicine* 377: 1345-1356.

17. June, C. H., S. R. Riddell, and T. N. Schumacher. 2015. Adoptive cellular therapy: A race to the finish line. *Science Translational Medicine* 7: 280ps287-280ps287.

18. Rosenberg, S. A., J. R. Yannelli, J. C. Yang, S. L. Topalian, D. J. Schwartzentruber, J. S. Weber, D. R. Parkinson, C. A. Seipp, J. H. Einhorn, and D. E. White. 1994. Treatment of patients with metastatic melanoma with autologous tumor-infiltrating lymphocytes and interleukin 2. *J Natl Cancer Inst* 86: 1159-1166.

19. Sadelain, M., R. Brentjens, and I. Rivière. 2013. The Basic Principles of Chimeric Antigen Receptor Design. *Cancer Discovery* 3: 388-398.

20. Porter, D. L., B. L. Levine, M. Kalos, A. Bagg, and C. H. June. 2011. Chimeric Antigen Receptor–Modified T Cells in Chronic Lymphoid Leukemia. *New England Journal of Medicine* 365: 725-733.

21. Neelapu, S. S., F. L. Locke, N. L. Bartlett, L. J. Lekakis, D. B. Miklos, C. A. Jacobson, I. Braunschweig, O. O. Oluwole, T. Siddiqi, Y. Lin, J. M. Timmerman, P. J. Stiff, J. W. Friedberg, I. W. Flinn, A. Goy, B. T. Hill, M. R. Smith, A. Deol, U. Farooq, P. McSweeney, J. Munoz, I. Avivi, J. E. Castro, J. R. Westin, J. C. Chavez, A. Ghobadi, K. V. Komanduri, R. Levy, E. D. Jacobsen, T. E. Witzig, P. Reagan, A. Bot, J. Rossi, L. Navale, Y. Jiang, J. Aycock, M. Elias, D. Chang, J. Wiezorek, and W. Y. Go. 2017. Axicabtagene Ciloleucel CAR T-Cell Therapy in Refractory Large B-Cell Lymphoma. *New England Journal of Medicine* 377: 2531-2544.

22. Maude, S. L., T. W. Laetsch, J. Buechner, S. Rives, M. Boyer, H. Bittencourt, P. Bader, M. R. Verneris, H. E. Stefanski, G. D. Myers, M. Qayed, B. De Moerloose, H. Hiramatsu,

K. Schlis, K. L. Davis, P. L. Martin, E. R. Nemecek, G. A. Yanik, C. Peters, A. Baruchel, N. Boissel, F. Mechinaud, A. Balduzzi, J. Krueger, C. H. June, B. L. Levine, P. Wood, T. Taran, M. Leung, K. T. Mueller, Y. Zhang, K. Sen, D. Lebwohl, M. A. Pulsipher, and S. A. Grupp. 2018. Tisagenlecleucel in Children and Young Adults with B-Cell Lymphoblastic Leukemia. *New England Journal of Medicine* 378: 439-448.

23. Jacobson, C. A., J. C. Chavez, A. R. Sehgal, B. M. William, J. Munoz, G. Salles, P. N. Munshi, C. Casulo, D. G. Maloney, S. de Vos, R. Reshef, L. A. Leslie, I. Yakoub-Agha, O. O. Oluwole, H. C. H. Fung, J. Rosenblatt, J. M. Rossi, L. Goyal, V. Plaks, Y. Yang, R. Vezan, M. P. Avanzi, and S. S. Neelapu. 2022. Axicabtagene ciloleucel in relapsed or refractory indolent non-Hodgkin lymphoma (ZUMA-5): a single-arm, multicentre, phase 2 trial. *The Lancet Oncology* 23: 91-103.

24. Melenhorst, J. J., G. M. Chen, M. Wang, D. L. Porter, C. Chen, M. A. Collins, P. Gao, S. Bandyopadhyay, H. Sun, Z. Zhao, S. Lundh, I. Pruteanu-Malinici, C. L. Nobles, S. Maji, N. V. Frey, S. I. Gill, A. W. Loren, L. Tian, I. Kulikovskaya, M. Gupta, D. E. Ambrose, M. M. Davis, J. A. Fraietta, J. L. Brogdon, R. M. Young, A. Chew, B. L. Levine, D. L. Siegel, C. Alanio, E. J. Wherry, F. D. Bushman, S. F. Lacey, K. Tan, and C. H. June. 2022. Decade-long leukaemia remissions with persistence of CD4+ CAR T cells. *Nature* 602: 503-509.

25. Kaech, S. M., and W. Cui. 2012. Transcriptional control of effector and memory CD8+ T cell differentiation. *Nature Reviews Immunology* 12: 749-761.

26. Smith-Garvin, J. E., G. A. Koretzky, and M. S. Jordan. 2009. T Cell Activation. *Annual Review of Immunology* 27: 591-619.

27. Janssen, E. M., E. E. Lemmens, T. Wolfe, U. Christen, M. G. von Herrath, and S. P. Schoenberger. 2003. CD4+ T cells are required for secondary expansion and memory in CD8+ T lymphocytes. *Nature* 421: 852-856.

28. Novy, P., M. Quigley, X. Huang, and Y. Yang. 2007. CD4 T cells are required for CD8 T cell survival during both primary and memory recall responses. *J Immunol* 179: 8243-8251.

29. Sun, J. C., and M. J. Bevan. 2003. Defective CD8 T cell memory following acute infection without CD4 T cell help. *Science* 300: 339-342.

30. Prlic, M., M. A. Williams, and M. J. Bevan. 2007. Requirements for CD8 T-cell priming, memory generation and maintenance. *Current Opinion in Immunology* 19: 315-319.

31. Fowell, D. J., and M. Kim. 2021. The spatio-temporal control of effector T cell migration. *Nature Reviews Immunology* 21: 582-596.

32. Smith, N. L., R. K. Patel, A. Reynaldi, J. K. Grenier, J. Wang, N. B. Watson, K. Nzingha, K. J. Yee Mon, S. A. Peng, A. Grimson, M. P. Davenport, and B. D. Rudd. 2018. Developmental Origin Governs CD8⁺ T Cell Fate Decisions during Infection. *Cell* 174: 117-130.e114.

33. Joshi, N. S., W. Cui, A. Chandele, H. K. Lee, D. R. Urso, J. Hagman, L. Gapin, and S. M. Kaech. 2007. Inflammation directs memory precursor and short-lived effector CD8(+) T cell fates via the graded expression of T-bet transcription factor. *Immunity* 27: 281-295.

34. Jameson, S. C., and D. Masopust. 2018. Understanding Subset Diversity in T Cell Memory. *Immunity* 48: 214-226.

35. Daniels, M. A., and E. Teixeiro. 2015. TCR Signaling in T Cell Memory. *Frontiers in Immunology* 6.

36. Pearce, E. L., and H. Shen. 2007. Generation of CD8 T cell memory is regulated by IL-12. *J Immunol* 179: 2074-2081.

37. Cui, W., N. S. Joshi, A. Jiang, and S. M. Kaech. 2009. Effects of Signal 3 during CD8 T cell priming: Bystander production of IL-12 enhances effector T cell expansion but promotes terminal differentiation. *Vaccine* 27: 2177-2187.

38. Mescher, M. F., J. M. Curtsinger, P. Agarwal, K. A. Casey, M. Gerner, C. D. Hammerbeck, F. Popescu, and Z. Xiao. 2006. Signals required for programming effector and memory development by CD8+ T cells. *Immunol Rev* 211: 81-92.

39. Pipkin, M. E., J. A. Sacks, F. Cruz-Guilloty, M. G. Lichtenheld, M. J. Bevan, and A. Rao. 2010. Interleukin-2 and inflammation induce distinct transcriptional programs that promote the differentiation of effector cytolytic T cells. *Immunity* 32: 79-90.

40. Kalia, V., S. Sarkar, S. Subramaniam, W. N. Haining, K. A. Smith, and R. Ahmed. 2010. Prolonged interleukin-2Ralpha expression on virus-specific CD8+ T cells favors terminal-effector differentiation in vivo. *Immunity* 32: 91-103.

41. Pearce, E. L. 2010. Metabolism in T cell activation and differentiation. *Curr Opin Immunol* 22: 314-320.

42. Xin, A., F. Masson, Y. Liao, S. Preston, T. Guan, R. Gloury, M. Olshansky, J. X. Lin, P. Li, T. P. Speed, G. K. Smyth, M. Ernst, W. J. Leonard, M. Pellegrini, S. M. Kaech, S. L. Nutt, W. Shi, G. T. Belz, and A. Kallies. 2016. A molecular threshold for effector CD8(+) T cell differentiation controlled by transcription factors Blimp-1 and T-bet. *Nat Immunol* 17: 422-432.

43. Kallies, A., A. Xin, G. T. Belz, and S. L. Nutt. 2009. Blimp-1 transcription factor is required for the differentiation of effector CD8(+) T cells and memory responses. *Immunity* 31: 283-295.

44. Takemoto, N., A. M. Intlekofer, J. T. Northrup, E. J. Wherry, and S. L. Reiner. 2006. Cutting Edge: IL-12 inversely regulates T-bet and eomesodermin expression during pathogen-induced CD8+ T cell differentiation. *J Immunol* 177: 7515-7519.

45. Wherry, E. J., and M. Kurachi. 2015. Molecular and cellular insights into T cell exhaustion. *Nature Reviews Immunology* 15: 486-499.

46. Lucca, L. E., and M. Dominguez-Villar. 2020. Modulation of regulatory T cell function and stability by co-inhibitory receptors. *Nature Reviews Immunology* 20: 680-693.

47. Paley, M. A., D. C. Kroy, P. M. Odorizzi, J. B. Johnnidis, D. V. Dolfi, B. E. Barnett, E. K. Bikoff, E. J. Robertson, G. M. Lauer, S. L. Reiner, and E. J. Wherry. 2012. Progenitor and terminal subsets of CD8+ T cells cooperate to contain chronic viral infection. *Science* 338: 1220-1225.

48. Utzschneider, D. T., S. S. Gabriel, D. Chisanga, R. Gloury, P. M. Gubser, A. Vasanthakumar, W. Shi, and A. Kallies. 2020. Early precursor T cells establish and propagate T cell exhaustion in chronic infection. *Nature Immunology* 21: 1256-1266.

49. Dolina, J. S., N. Van Braeckel-Budimir, G. D. Thomas, and S. Salek-Ardakani. 2021. CD8+ T Cell Exhaustion in Cancer. *Frontiers in Immunology* 12.

50. Gupta, P. K., J. Godec, D. Wolski, E. Adland, K. Yates, K. E. Pauken, C. Cosgrove, C. Ledderose, W. G. Junger, S. C. Robson, E. J. Wherry, G. Alter, P. J. Goulder, P. Klenerman, A. H. Sharpe, G. M. Lauer, and W. N. Haining. 2015. CD39 Expression Identifies Terminally Exhausted CD8+ T Cells. *PLoS Pathog* 11: e1005177.

51. Chen, Y., R. A. Zander, X. Wu, D. M. Schauder, M. Y. Kasmani, J. Shen, S. Zheng, R. Burns, E. J. Taparowsky, and W. Cui. 2021. BATF regulates progenitor to cytolytic effector CD8+ T cell transition during chronic viral infection. *Nature Immunology* 22: 996-1007.

52. Hudson, W. H., J. Gensheimer, M. Hashimoto, A. Wieland, R. M. Valanparambil, P. Li, J. X. Lin, B. T. Konieczny, S. J. Im, G. J. Freeman, W. J. Leonard, H. T. Kissick, and R. Ahmed. 2019. Proliferating Transitory T Cells with an Effector-like Transcriptional Signature Emerge from PD-1(+) Stem-like CD8(+) T Cells during Chronic Infection. *Immunity* 51: 1043-1058.e1044.

53. Pauken, K. E., O. Shahid, K. A. Lagattuta, K. M. Mahuron, J. M. Luber, M. M. Lowe, L. Huang, C. Delaney, J. M. Long, M. E. Fung, K. Newcomer, K. K. Tsai, M. Chow, S. Guinn, J. R. Kuchroo, K. P. Burke, J. M. Schenkel, M. D. Rosenblum, A. I. Daud, A. H. Sharpe, and M. Singer. 2021. Single-cell analyses identify circulating anti-tumor CD8 T cells and markers for their enrichment. *J Exp Med* 218.

54. Raju, S., Y. Xia, B. Daniel, K. E. Yost, E. Bradshaw, E. Tonc, D. J. Verbaro, K. Kometani, W. M. Yokoyama, T. Kurosaki, A. T. Satpathy, and T. Egawa. 2021. Identification of a T-bet(hi) Quiescent Exhausted CD8 T Cell Subpopulation That Can Differentiate into TIM3(+)CX3CR1(+) Effectors and Memory-like Cells. *J Immunol* 206: 2924-2936.

55. Pulliam, S. R., R. V. Uzhachenko, S. E. Adunyah, and A. Shanker. 2016. Common gamma chain cytokines in combinatorial immune strategies against cancer. *Immunol Lett* 169: 61-72.

56. Giuffrida, L., K. Sek, M. A. Henderson, I. G. House, J. Lai, A. X. Y. Chen, K. L. Todd, E. V. Petley, S. Mardiana, I. Todorovski, E. Gruber, M. J. Kelly, B. J. Solomon, S. J. Vervoort,

R. W. Johnstone, I. A. Parish, P. J. Neeson, L. M. Kats, P. K. Darcy, and P. A. Beavis. 2020. IL-15 Preconditioning Augments CAR T Cell Responses to Checkpoint Blockade for Improved Treatment of Solid Tumors. *Molecular Therapy* 28: 2379-2393.

57. Codarri Deak, L., V. Nicolini, M. Hashimoto, M. Karagianni, P. C. Schwalie, L. Lauener, E. M. Varypataki, M. Richard, E. Bommer, J. Sam, S. Joller, M. Perro, F. Cremasco, L. Kunz, E. Yanguez, T. Hüsser, R. Schlenker, M. Mariani, V. Tosevski, S. Herter, M. Bacac, I. Waldhauer, S. Colombetti, X. Gueripel, S. Wullschleger, M. Tichet, D. Hanahan, H. T. Kissick, S. Leclair, A. Freimoser-Grundschober, S. Seeber, V. Teichgräber, R. Ahmed, C. Klein, and P. Umaña. 2022. PD-1-cis IL-2R agonism yields better effectors from stem-like CD8(+) T cells. *Nature* 610: 161-172.

58. Hashimoto, M., K. Araki, M. A. Cardenas, P. Li, R. R. Jadhav, H. T. Kissick, W. H. Hudson, D. J. McGuire, R. C. Obeng, A. Wieland, J. Lee, D. T. McManus, J. L. Ross, S. J. Im, J. Lee, J. X. Lin, B. Hu, E. E. West, C. D. Scharer, G. J. Freeman, A. H. Sharpe, S. S. Ramalingam, A. Pellerin, V. Teichgräber, W. J. Greenleaf, C. Klein, J. J. Goronzy, P. Umaña, W. J. Leonard, K. A. Smith, and R. Ahmed. 2022. PD-1 combination therapy with IL-2 modifies CD8(+) T cell exhaustion program. *Nature* 610: 173-181.

59. West, E. E., H. T. Jin, A. U. Rasheed, P. Penaloza-Macmaster, S. J. Ha, W. G. Tan, B. Youngblood, G. J. Freeman, K. A. Smith, and R. Ahmed. 2013. PD-L1 blockade synergizes with IL-2 therapy in reinvigorating exhausted T cells. *J Clin Invest* 123: 2604-2615.

60. Brooks, D. G., M. J. Trifilo, K. H. Edelmann, L. Teyton, D. B. McGavern, and M. B. Oldstone. 2006. Interleukin-10 determines viral clearance or persistence in vivo. *Nat Med* 12: 1301-1309.

61. Ejrnaes, M., C. M. Filippi, M. M. Martinic, E. M. Ling, L. M. Togher, S. Crotty, and M. G. von Herrath. 2006. Resolution of a chronic viral infection after interleukin-10 receptor blockade. *J Exp Med* 203: 2461-2472.

62. Tinoco, R., V. Alcalde, Y. Yang, K. Sauer, and E. I. Zuniga. 2009. Cell-intrinsic transforming growth factor-beta signaling mediates virus-specific CD8+ T cell deletion and viral persistence in vivo. *Immunity* 31: 145-157.

63. Hu, Y., W. H. Hudson, H. T. Kissick, C. B. Medina, A. P. Baptista, C. Ma, W. Liao, R. N. Germain, S. J. Turley, N. Zhang, and R. Ahmed. 2022. TGF-β regulates the stem-like state of PD-1+ TCF-1+ virus-specific CD8 T cells during chronic infection. *Journal of Experimental Medicine* 219: e20211574.

64. Ma, C., L. Wang, W. Liao, Y. Liu, S. Mishra, G. Li, X. Zhang, Y. Qiu, Q. Lu, and N. Zhang. 2022. TGF-β promotes stem-like T cells via enforcing their lymphoid tissue retention. *Journal of Experimental Medicine* 219: e20211538.

65. Hanna, B. S., L. Llaó-Cid, M. Iskar, P. M. Roessner, L. C. Klett, J. K. L. Wong, Y. Paul, N. Ioannou, S. Öztürk, N. Mack, V. Kalter, D. Colomer, E. Campo, J. Bloehdorn, S. Stilgenbauer, S. Dietrich, M. Schmidt, R. Gabriel, K. Rippe, M. Feuerer, A. G. Ramsay, P. Lichter, M. Zapatka, and M. Seiffert. 2021. Interleukin-10 receptor signaling promotes the

maintenance of a PD-1(int) TCF-1(+) CD8(+) T cell population that sustains anti-tumor immunity. *Immunity* 54: 2825-2841.e2810.

66. Snell, L. M., T. L. McGaha, and D. G. Brooks. 2017. Type I Interferon in Chronic Virus Infection and Cancer. *Trends Immunol* 38: 542-557.

67. Zander, R., M. Y. Kasmani, Y. Chen, P. Topchyan, J. Shen, S. Zheng, R. Burns, J. Ingram, C. Cui, N. Joshi, J. Craft, A. Zajac, and W. Cui. 2022. Tfh-cell-derived interleukin 21 sustains effector CD8+ T cell responses during chronic viral infection. *Immunity* 55: 475-493.e475.

68. Reina-Campos, M., N. E. Scharping, and A. W. Goldrath. 2021. CD8+ T cell metabolism in infection and cancer. *Nature Reviews Immunology* 21: 718-738.

69. Li, F., H. Liu, D. Zhang, Y. Ma, and B. Zhu. 2022. Metabolic plasticity and regulation of T cell exhaustion. *Immunology* 167: 482-494.

70. Scharping, N. E., A. V. Menk, R. S. Moreci, R. D. Whetstone, R. E. Dadey, S. C. Watkins, R. L. Ferris, and G. M. Delgoffe. 2016. The Tumor Microenvironment Represses T Cell Mitochondrial Biogenesis to Drive Intratumoral T Cell Metabolic Insufficiency and Dysfunction. *Immunity* 45: 374-388.

71. Scharping, N. E., D. B. Rivadeneira, A. V. Menk, P. D. A. Vignali, B. R. Ford, N. L. Rittenhouse, R. Peralta, Y. Wang, Y. Wang, K. DePeaux, A. C. Poholek, and G. M. Delgoffe. 2021. Mitochondrial stress induced by continuous stimulation under hypoxia rapidly drives T cell exhaustion. *Nature Immunology* 22: 205-215.

72. Vardhana, S. A., M. A. Hwee, M. Berisa, D. K. Wells, K. E. Yost, B. King, M. Smith, P. S. Herrera, H. Y. Chang, A. T. Satpathy, M. R. M. van den Brink, J. R. Cross, and C. B. Thompson. 2020. Impaired mitochondrial oxidative phosphorylation limits the self-renewal of T cells exposed to persistent antigen. *Nature Immunology* 21: 1022-1033.

73. Yu, Y.-R., H. Imrichova, H. Wang, T. Chao, Z. Xiao, M. Gao, M. Rincon-Restrepo, F. Franco, R. Genolet, W.-C. Cheng, C. Jandus, G. Coukos, Y.-F. Jiang, J. W. Locasale, A. Zippelius, P.-S. Liu, L. Tang, C. Bock, N. Vannini, and P.-C. Ho. 2020. Disturbed mitochondrial dynamics in CD8+ TILs reinforce T cell exhaustion. *Nature Immunology* 21: 1540-1551.

74. Zebley, C. C., S. Gottschalk, and B. Youngblood. 2020. Rewriting History: Epigenetic Reprogramming of CD8(+) T Cell Differentiation to Enhance Immunotherapy. *Trends in immunology* 41: 665-675.

75. Ford, B. R., P. D. A. Vignali, N. L. Rittenhouse, N. E. Scharping, R. Peralta, K. Lontos, A. T. Frisch, G. M. Delgoffe, and A. C. Poholek. 2022. Tumor microenvironmental signals reshape chromatin landscapes to limit the functional potential of exhausted T cells. *Science Immunology* 7: eabj9123.

76. Scharping, N. E., D. B. Rivadeneira, A. V. Menk, P. D. A. Vignali, B. R. Ford, N. L. Rittenhouse, R. Peralta, Y. Wang, Y. Wang, K. DePeaux, A. C. Poholek, and G. M. Delgoffe. 2021. Mitochondrial stress induced by continuous stimulation under hypoxia rapidly drives T cell exhaustion. *Nat Immunol* 22: 205-215.

77. Johnson, J. L., G. Georgakilas, J. Petrovic, M. Kurachi, S. Cai, C. Harly, W. S. Pear, A. Bhandoola, E. J. Wherry, and G. Vahedi. 2018. Lineage-Determining Transcription Factor TCF-1 Initiates the Epigenetic Identity of T Cells. *Immunity* 48: 243-257.e210.

78. Shan, Q., X. Li, X. Chen, Z. Zeng, S. Zhu, K. Gai, W. Peng, and H.-H. Xue. 2021. Tcf1 and Lef1 provide constant supervision to mature CD8+ T cell identity and function by organizing genomic architecture. *Nature Communications* 12: 5863.

79. Shan, Q., S. Zhu, X. Chen, J. Liu, S. Yuan, X. Li, W. Peng, and H.-H. Xue. 2022. Tcf1–CTCF cooperativity shapes genomic architecture to promote CD8+ T cell homeostasis. *Nature Immunology*.

80. Xing, S., F. Li, Z. Zeng, Y. Zhao, S. Yu, Q. Shan, Y. Li, F. C. Phillips, P. K. Maina, H. H. Qi, C. Liu, J. Zhu, R. M. Pope, C. A. Musselman, C. Zeng, W. Peng, and H. H. Xue. 2016. Tcf1 and Lef1 transcription factors establish CD8(+) T cell identity through intrinsic HDAC activity. *Nat Immunol* 17: 695-703.

81. Zhang, J., T. Lyu, Y. Cao, and H. Feng. 2021. Role of TCF-1 in differentiation, exhaustion, and memory of CD8(+) T cells: A review. *Faseb j* 35: e21549.

82. Wu, J., X. Xu, E.-J. Lee, A. Y. Shull, L. Pei, F. Awan, X. Wang, J.-H. Choi, L. Deng, H.-B. Xin, W. Zhong, J. Liang, Y. Miao, Y. Wu, L. Fan, J. Li, W. Xu, and H. Shi. 2016. Phenotypic alteration of CD8 + T cells in chronic lymphocytic leukemia is associated with epigenetic reprogramming. *Oncotarget* 7.

83. Roychoudhuri, R., D. Clever, P. Li, Y. Wakabayashi, K. M. Quinn, C. A. Klebanoff, Y. Ji, M. Sukumar, R. L. Eil, Z. Yu, R. Spolski, D. C. Palmer, J. H. Pan, S. J. Patel, D. C. Macallan, G. Fabozzi, H.-Y. Shih, Y. Kanno, A. Muto, J. Zhu, L. Gattinoni, J. J. O'Shea, K. Okkenhaug, K. Igarashi, W. J. Leonard, and N. P. Restifo. 2016. BACH2 regulates CD8+ T cell differentiation by controlling access of AP-1 factors to enhancers. *Nature Immunology* 17: 851-860.

84. Igarashi, K., T. Kurosaki, and R. Roychoudhuri. 2017. BACH transcription factors in innate and adaptive immunity. *Nat Rev Immunol* 17: 437-450.

85. Yao, C., G. Lou, H.-W. Sun, Z. Zhu, Y. Sun, Z. Chen, D. Chauss, E. A. Moseman, J. Cheng, M. A. D'Antonio, W. Shi, J. Shi, K. Kometani, T. Kurosaki, E. J. Wherry, B. Afzali, L. Gattinoni, Y. Zhu, D. B. McGavern, J. J. O'Shea, P. L. Schwartzberg, and T. Wu. 2021. BACH2 enforces the transcriptional and epigenetic programs of stem-like CD8+ T cells. *Nature Immunology* 22: 370-380.

86. Kurachi, M., R. A. Barnitz, N. Yosef, P. M. Odorizzi, M. A. DiIorio, M. E. Lemieux, K. Yates, J. Godec, M. G. Klatt, A. Regev, E. J. Wherry, and W. N. Haining. 2014. The

transcription factor BATF operates as an essential differentiation checkpoint in early effector CD8+ T cells. *Nature Immunology* 15: 373-383.

87. Seo, H., E. González-Avalos, W. Zhang, P. Ramchandani, C. Yang, C. J. Lio, A. Rao, and P. G. Hogan. 2021. BATF and IRF4 cooperate to counter exhaustion in tumor-infiltrating CAR T cells. *Nat Immunol* 22: 983-995.

88. Zhang, X., C. Zhang, M. Qiao, C. Cheng, N. Tang, S. Lu, W. Sun, B. Xu, Y. Cao, X. Wei, Y. Wang, W. Han, and H. Wang. 2022. Depletion of BATF in CAR-T cells enhances antitumor activity by inducing resistance against exhaustion and formation of central memory cells. *Cancer Cell* 40: 1407-1422.e1407.

89. Lynn, R. C., E. W. Weber, E. Sotillo, D. Gennert, P. Xu, Z. Good, H. Anbunathan, J. Lattin, R. Jones, V. Tieu, S. Nagaraja, J. Granja, C. F. A. de Bourcy, R. Majzner, A. T. Satpathy, S. R. Quake, M. Monje, H. Y. Chang, and C. L. Mackall. 2019. c-Jun overexpression in CAR T cells induces exhaustion resistance. *Nature* 576: 293-300.

90. Alfei, F., K. Kanev, M. Hofmann, M. Wu, H. E. Ghoneim, P. Roelli, D. T. Utzschneider, M. von Hoesslin, J. G. Cullen, Y. Fan, V. Eisenberg, D. Wohlleber, K. Steiger, D. Merkler, M. Delorenzi, P. A. Knolle, C. J. Cohen, R. Thimme, B. Youngblood, and D. Zehn. 2019. TOX reinforces the phenotype and longevity of exhausted T cells in chronic viral infection. *Nature* 571: 265-269.

91. Khan, O., J. R. Giles, S. McDonald, S. Manne, S. F. Ngiow, K. P. Patel, M. T. Werner, A. C. Huang, K. A. Alexander, J. E. Wu, J. Attanasio, P. Yan, S. M. George, B. Bengsch, R. P. Staupe, G. Donahue, W. Xu, R. K. Amaravadi, X. Xu, G. C. Karakousis, T. C. Mitchell, L. M. Schuchter, J. Kaye, S. L. Berger, and E. J. Wherry. 2019. TOX transcriptionally and epigenetically programs CD8+ T cell exhaustion. *Nature* 571: 211-218.

92. O'Flaherty, E., and J. Kaye. 2003. TOX defines a conserved subfamily of HMG-box proteins. *BMC Genomics* 4: 13.

93. Yao, C., H.-W. Sun, N. E. Lacey, Y. Ji, E. A. Moseman, H.-Y. Shih, E. F. Heuston, M. Kirby, S. Anderson, J. Cheng, O. Khan, R. Handon, J. Reilley, J. Fioravanti, J. Hu, S. Gossa, E. J. Wherry, L. Gattinoni, D. B. McGavern, J. J. O'Shea, P. L. Schwartzberg, and T. Wu. 2019. Single-cell RNA-seq reveals TOX as a key regulator of CD8+ T cell persistence in chronic infection. *Nature Immunology* 20: 890-901.

94. Seo, H., J. Chen, E. González-Avalos, D. Samaniego-Castruita, A. Das, H. Wang Yueqiang, F. López-Moyado Isaac, O. Georges Romain, W. Zhang, A. Onodera, C.-J. Wu, L.-F. Lu, G. Hogan Patrick, A. Bhandoola, and A. Rao. 2019. TOX and TOX2 transcription factors cooperate with NR4A transcription factors to impose CD8+ T cell exhaustion. *Proceedings of the National Academy of Sciences* 116: 12410-12415.

95. Scott, A. C., F. Dündar, P. Zumbo, S. S. Chandran, C. A. Klebanoff, M. Shakiba, P. Trivedi, L. Menocal, H. Appleby, S. Camara, D. Zamarin, T. Walther, A. Snyder, M. R. Femia, E. A. Comen, H. Y. Wen, M. D. Hellmann, N. Anandasabapathy, Y. Liu, N. K. Altorki, P.

Lauer, O. Levy, M. S. Glickman, J. Kaye, D. Betel, M. Philip, and A. Schietinger. 2019. TOX is a critical regulator of tumour-specific T cell differentiation. *Nature* 571: 270-274.

96. Chen, J., I. F. López-Moyado, H. Seo, C.-W. J. Lio, L. J. Hempleman, T. Sekiya, A. Yoshimura, J. P. Scott-Browne, and A. Rao. 2019. NR4A transcription factors limit CAR T cell function in solid tumours. *Nature* 567: 530-534.

97. Liu, X., Y. Wang, H. Lu, J. Li, X. Yan, M. Xiao, J. Hao, A. Alekseev, H. Khong, T. Chen, R. Huang, J. Wu, Q. Zhao, Q. Wu, S. Xu, X. Wang, W. Jin, S. Yu, Y. Wang, L. Wei, A. Wang, B. Zhong, L. Ni, X. Liu, R. Nurieva, L. Ye, Q. Tian, X.-W. Bian, and C. Dong. 2019. Genome-wide analysis identifies NR4A1 as a key mediator of T cell dysfunction. *Nature* 567: 525-529.

98. Shin, H., S. D. Blackburn, A. M. Intlekofer, C. Kao, J. M. Angelosanto, S. L. Reiner, and E. J. Wherry. 2009. A role for the transcriptional repressor Blimp-1 in CD8(+) T cell exhaustion during chronic viral infection. *Immunity* 31: 309-320.

99. Jung, I. Y., V. Narayan, S. McDonald, A. J. Rech, R. Bartoszek, G. Hong, M. M. Davis, J. Xu, A. C. Boesteanu, J. S. Barber-Rotenberg, G. Plesa, S. F. Lacey, J. K. Jadlowsky, D. L. Siegel, D. M. Hammill, P. F. Cho-Park, S. L. Berger, N. B. Haas, and J. A. Fraietta. 2022. BLIMP1 and NR4A3 transcription factors reciprocally regulate antitumor CAR T cell stemness and exhaustion. *Sci Transl Med* 14: eabn7336.

100. Mattei, A. L., N. Bailly, and A. Meissner. 2022. DNA methylation: a historical perspective. *Trends in Genetics* 38: 676-707.

101. Luo, C., P. Hajkova, and J. R. Ecker. 2018. Dynamic DNA methylation: In the right place at the right time. *Science* 361: 1336-1340.

102. Cokus, S. J., S. Feng, X. Zhang, Z. Chen, B. Merriman, C. D. Haudenschild, S. Pradhan, S. F. Nelson, M. Pellegrini, and S. E. Jacobsen. 2008. Shotgun bisulphite sequencing of the Arabidopsis genome reveals DNA methylation patterning. *Nature* 452: 215-219.

103. Harrison, A., and A. Parle-McDermott. 2011. DNA methylation: a timeline of methods and applications. *Front Genet* 2: 74.

104. Klemm, S. L., Z. Shipony, and W. J. Greenleaf. 2019. Chromatin accessibility and the regulatory epigenome. *Nature Reviews Genetics* 20: 207-220.

105. Buenrostro, J. D., P. G. Giresi, L. C. Zaba, H. Y. Chang, and W. J. Greenleaf. 2013. Transposition of native chromatin for fast and sensitive epigenomic profiling of open chromatin, DNA-binding proteins and nucleosome position. *Nature Methods* 10: 1213-1218.

106. Buenrostro, J. D., B. Wu, U. M. Litzenburger, D. Ruff, M. L. Gonzales, M. P. Snyder, H. Y. Chang, and W. J. Greenleaf. 2015. Single-cell chromatin accessibility reveals principles of regulatory variation. *Nature* 523: 486-490.

107. Strahl, B. D., and C. D. Allis. 2000. The language of covalent histone modifications. *Nature* 403: 41-45.

108. Gardner, K. E., C. D. Allis, and B. D. Strahl. 2011. OPERating ON Chromatin, a Colorful Language where Context Matters. *Journal of Molecular Biology* 409: 36-46.

109. Wang, Z., C. Zang, J. A. Rosenfeld, D. E. Schones, A. Barski, S. Cuddapah, K. Cui, T.-Y. Roh, W. Peng, M. Q. Zhang, and K. Zhao. 2008. Combinatorial patterns of histone acetylations and methylations in the human genome. *Nature Genetics* 40: 897-903.

110. Dai, Z., V. Ramesh, and J. W. Locasale. 2020. The evolving metabolic landscape of chromatin biology and epigenetics. *Nature Reviews Genetics* 21: 737-753.

111. Hyun, K., J. Jeon, K. Park, and J. Kim. 2017. Writing, erasing and reading histone lysine methylations. *Experimental & Molecular Medicine* 49: e324-e324.

112. Monaghan, L., M. E. Massett, R. P. Bunschoten, A. Hoose, P.-A. Pirvan, R. M. J. Liskamp, H. G. Jørgensen, and X. Huang. 2019. The Emerging Role of H3K9me3 as a Potential Therapeutic Target in Acute Myeloid Leukemia. *Frontiers in Oncology* 9.

113. Shvedunova, M., and A. Akhtar. 2022. Modulation of cellular processes by histone and non-histone protein acetylation. *Nature Reviews Molecular Cell Biology* 23: 329-349.

114. Ogryzko, V. V., R. L. Schiltz, V. Russanova, B. H. Howard, and Y. Nakatani. 1996. The Transcriptional Coactivators p300 and CBP Are Histone Acetyltransferases. *Cell* 87: 953-959.

115. Park, S.-Y., and J.-S. Kim. 2020. A short guide to histone deacetylases including recent progress on class II enzymes. *Experimental & Molecular Medicine* 52: 204-212.

116. Park, P. J. 2009. ChIP-seq: advantages and challenges of a maturing technology. *Nat Rev Genet* 10: 669-680.

117. Hoshino, A., and H. Fujii. 2009. Insertional chromatin immunoprecipitation: a method for isolating specific genomic regions. *J Biosci Bioeng* 108: 446-449.

118. Kaya-Okur, H. S., S. J. Wu, C. A. Codomo, E. S. Pledger, T. D. Bryson, J. G. Henikoff, K. Ahmad, and S. Henikoff. 2019. CUT&Tag for efficient epigenomic profiling of small samples and single cells. *Nat Commun* 10: 1930.

119. Skene, P. J., and S. Henikoff. 2017. An efficient targeted nuclease strategy for high-resolution mapping of DNA binding sites. *Elife* 6.

120. van Galen, P., A. D. Viny, O. Ram, R. J. Ryan, M. J. Cotton, L. Donohue, C. Sievers, Y. Drier, B. B. Liau, S. M. Gillespie, K. M. Carroll, M. B. Cross, R. L. Levine, and B. E. Bernstein. 2016. A Multiplexed System for Quantitative Comparisons of Chromatin Landscapes. *Mol Cell* 61: 170-180.

121. Zheng, H., and W. Xie. 2019. The role of 3D genome organization in development and cell differentiation. *Nature Reviews Molecular Cell Biology* 20: 535-550.

122. Mora, A., G. K. Sandve, O. S. Gabrielsen, and R. Eskeland. 2016. In the loop: promoter–enhancer interactions and bioinformatics. *Briefings in Bioinformatics* 17: 980-995.

123. Dostie, J., T. A. Richmond, R. A. Arnaout, R. R. Selzer, W. L. Lee, T. A. Honan, E. D. Rubio, A. Krumm, J. Lamb, C. Nusbaum, R. D. Green, and J. Dekker. 2006. Chromosome Conformation Capture Carbon Copy (5C): a massively parallel solution for mapping interactions between genomic elements. *Genome Res* 16: 1299-1309.

124. Lieberman-Aiden, E., N. L. van Berkum, L. Williams, M. Imakaev, T. Ragoczy, A. Telling, I. Amit, B. R. Lajoie, P. J. Sabo, M. O. Dorschner, R. Sandstrom, B. Bernstein, M. A. Bender, M. Groudine, A. Gnirke, J. Stamatoyannopoulos, L. A. Mirny, E. S. Lander, and J. Dekker. 2009. Comprehensive mapping of long-range interactions reveals folding principles of the human genome. *Science* 326: 289-293.

125. Zhao, Z., G. Tavoosidana, M. Sjölinder, A. Göndör, P. Mariano, S. Wang, C. Kanduri, M. Lezcano, K. Singh Sandhu, U. Singh, V. Pant, V. Tiwari, S. Kurukuti, and R. Ohlsson. 2006. Circular chromosome conformation capture (4C) uncovers extensive networks of epigenetically regulated intra- and interchromosomal interactions. *Nature Genetics* 38: 1341-1347.

126. Fullwood, M. J., M. H. Liu, Y. F. Pan, J. Liu, H. Xu, Y. B. Mohamed, Y. L. Orlov, S. Velkov, A. Ho, P. H. Mei, E. G. Chew, P. Y. Huang, W. J. Welboren, Y. Han, H. S. Ooi, P. N. Ariyaratne, V. B. Vega, Y. Luo, P. Y. Tan, P. Y. Choy, K. D. Wansa, B. Zhao, K. S. Lim, S. C. Leow, J. S. Yow, R. Joseph, H. Li, K. V. Desai, J. S. Thomsen, Y. K. Lee, R. K. Karuturi, T. Herve, G. Bourque, H. G. Stunnenberg, X. Ruan, V. Cacheux-Rataboul, W. K. Sung, E. T. Liu, C. L. Wei, E. Cheung, and Y. Ruan. 2009. An oestrogen-receptor-alpha-bound human chromatin interactome. *Nature* 462: 58-64.

127. Mifsud, B., F. Tavares-Cadete, A. N. Young, R. Sugar, S. Schoenfelder, L. Ferreira, S. W. Wingett, S. Andrews, W. Grey, P. A. Ewels, B. Herman, S. Happe, A. Higgs, E. LeProust, G. A. Follows, P. Fraser, N. M. Luscombe, and C. S. Osborne. 2015. Mapping long-range promoter contacts in human cells with high-resolution capture Hi-C. *Nat Genet* 47: 598-606.

128. Mumbach, M. R., A. J. Rubin, R. A. Flynn, C. Dai, P. A. Khavari, W. J. Greenleaf, and H. Y. Chang. 2016. HiChIP: efficient and sensitive analysis of protein-directed genome architecture. *Nat Methods* 13: 919-922.

129. Babichuk, C. K., B. L. Duggan, and R. C. Bleackley. 1996. In Vivo Regulation of Murine Granzyme B Gene Transcription in Activated Primary T Cells *. *Journal of Biological Chemistry* 271: 16485-16493.

130. Juelich, T., E. Sutcliffe, A. Denton, Y. He, P. C. Doherty, C. Parish, S. J. Turner, D. Tremethick, and S. Rao. 2009. Interplay between Chromatin Remodeling and Epigenetic

Changes during Lineage-Specific Commitment to Granzyme B Expression. *The Journal of Immunology* 183: 7063.

131. Araki, Y., M. Fann, R. Wersto, and N.-p. Weng. 2008. Histone Acetylation Facilitates Rapid and Robust Memory CD8 T Cell Response through Differential Expression of Effector Molecules (Eomesodermin and Its Targets: Perforin and Granzyme B). *The Journal of Immunology* 180: 8102.

132. Denton Alice, E., E. Russ Brendan, C. Doherty Peter, S. Rao, and J. Turner Stephen. 2011. Differentiation-dependent functional and epigenetic landscapes for cytokine genes in virus-specific CD8+ T cells. *Proceedings of the National Academy of Sciences* 108: 15306-15311.

133. Austin, J. W., P. Lu, P. Majumder, R. Ahmed, and J. M. Boss. 2014. STAT3, STAT4, NFATc1, and CTCF Regulate PD-1 through Multiple Novel Regulatory Regions in Murine T Cells. *The Journal of Immunology* 192: 4876.

134. Oestreich, K. J., H. Yoon, R. Ahmed, and J. M. Boss. 2008. NFATc1 Regulates PD-1 Expression upon T Cell Activation. *The Journal of Immunology* 181: 4832.

135. Agarwal, P., A. Raghavan, S. L. Nandiwada, J. M. Curtsinger, P. R. Bohjanen, D. L. Mueller, and M. F. Mescher. 2009. Gene Regulation and Chromatin Remodeling by IL-12 and Type I IFN in Programming for CD8 T Cell Effector Function and Memory. *The Journal of Immunology* 183: 1695.

136. Kuroda, S., M. Yamazaki, M. Abe, K. Sakimura, H. Takayanagi, and Y. Iwai. 2011. Basic leucine zipper transcription factor, ATF-like (BATF) regulates epigenetically and energetically effector CD8 T-cell differentiation via Sirt1 expression. *Proceedings of the National Academy of Sciences* 108: 14885-14889.

137. Tsao, H.-W., J. Kaminski, M. Kurachi, R. A. Barnitz, A. DiIorio Michael, W. LaFleur Martin, W. Ise, T. Kurosaki, E. J. Wherry, W. N. Haining, and N. Yosef. 2022. Batf-mediated epigenetic control of effector CD8+ T cell differentiation. *Science Immunology* 7: eabi4919.

138. Shan, Q., Z. Zeng, S. Xing, F. Li, S. M. Hartwig, J. A. Gullicksrud, S. P. Kurup, N. Van Braeckel-Budimir, Y. Su, M. D. Martin, S. M. Varga, I. Taniuchi, J. T. Harty, W. Peng, V. P. Badovinac, and H.-H. Xue. 2017. The transcription factor Runx3 guards cytotoxic CD8+ effector T cells against deviation towards follicular helper T cell lineage. *Nature Immunology* 18: 931-939.

139. Wang, D., H. Diao, A. J. Getzler, W. Rogal, M. A. Frederick, J. Milner, B. Yu, S. Crotty, A. W. Goldrath, and M. E. Pipkin. 2018. The Transcription Factor Runx3 Establishes Chromatin Accessibility of cis-Regulatory Landscapes that Drive Memory Cytotoxic T Lymphocyte Formation. *Immunity* 48: 659-674.e656.

140. van der Veeken, J., Y. Zhong, R. Sharma, L. Mazutis, P. Dao, D. Pe'er, C. S. Leslie, and A. Y. Rudensky. 2019. Natural Genetic Variation Reveals Key Features of Epigenetic and

Transcriptional Memory in Virus-Specific CD8 T Cells. *Immunity* 50: 1202-1217.e1207.

141. Tay, R. E., O. Olawoyin, P. Cejas, Y. Xie, C. A. Meyer, Y. Ito, Q. Y. Weng, D. E. Fisher, H. W. Long, M. Brown, H.-J. Kim, and K. W. Wucherpfennig. 2020. Hdac3 is an epigenetic inhibitor of the cytotoxicity program in CD8 T cells. *Journal of Experimental Medicine* 217: e20191453.

142. Gray, S. M., R. A. Amezquita, T. Guan, S. H. Kleinstein, and S. M. Kaech. 2017. Polycomb Repressive Complex 2-Mediated Chromatin Repression Guides Effector CD8+ T Cell Terminal Differentiation and Loss of Multipotency. *Immunity* 46: 596-608.

143. Pace, L., C. Goudot, E. Zueva, P. Gueguen, N. Burgdorf, J. Waterfall Joshua, J.-P. Quivy, G. Almouzni, and S. Amigorena. 2018. The epigenetic control of stemness in CD8+ T cell fate commitment. *Science* 359: 177-186.

144. Li, J., K. Hardy, M. Olshansky, A. Barugahare, L. J. Gearing, J. E. Prier, X. Y. X. Sng, M. L. T. Nguyen, D. Piovesan, B. E. Russ, N. L. La Gruta, P. J. Hertzog, S. Rao, and S. J. Turner. 2021. KDM6B-dependent chromatin remodeling underpins effective virus-specific CD8⁺ T cell differentiation. *Cell Reports* 34.

145. Xu, T., A. Schutte, L. Jimenez, A. N. A. Gonçalves, A. Keller, M. E. Pipkin, H. I. Nakaya, R. M. Pereira, and G. J. Martinez. 2021. Kdm6b Regulates the Generation of Effector CD8⁺ T Cells by Inducing Chromatin Accessibility in Effector-Associated Genes. *The Journal of Immunology* 206: 2170.

146. Yamada, T., S. Nabe, K. Toriyama, J. Suzuki, K. Inoue, Y. Imai, A. Shiraishi, K. Takenaka, M. Yasukawa, and M. Yamashita. 2019. Histone H3K27 Demethylase Negatively Controls the Memory Formation of Antigen-Stimulated CD8⁺ T Cells. *The Journal of Immunology* 202: 1088.

147. Fann, M., J. M. Godlove, M. Catalfamo, W. H. Wood, F. J. Chrest, N. Chun, L. Granger, R. Wersto, K. Madara, K. Becker, P. A. Henkart, and N.-p. Weng. 2006. Histone acetylation is associated with differential gene expression in the rapid and robust memory CD8+ T-cell response. *Blood* 108: 3363-3370.

148. DiSpirito, J. R., and H. Shen. 2010. Histone Acetylation at the Single-Cell Level: A Marker of Memory CD8⁺ T Cell Differentiation and Functionality. *The Journal of Immunology* 184: 4631.

149. Zediak, V. P., J. B. Johnnidis, E. J. Wherry, and S. L. Berger. 2011. Cutting Edge: Persistently Open Chromatin at Effector Gene Loci in Resting Memory CD8⁺ T Cells Independent of Transcriptional Status. *The Journal of Immunology* 186: 2705.

150. Akondy, R. S., M. Fitch, S. Edupuganti, S. Yang, H. T. Kissick, K. W. Li, B. A. Youngblood, H. A. Abdelsamed, D. J. McGuire, K. W. Cohen, G. Alexe, S. Nagar, M. M. McCausland, S. Gupta, P. Tata, W. N. Haining, M. J. McElrath, D. Zhang, B. Hu, W. J.

Greenleaf, J. J. Goronzy, M. J. Mulligan, M. Hellerstein, and R. Ahmed. 2017. Origin and differentiation of human memory CD8 T cells after vaccination. *Nature* 552: 362-367.

151. Ghoneim, H. E., Y. Fan, A. Moustaki, H. A. Abdelsamed, P. Dash, P. Dogra, R. Carter, W. Awad, G. Neale, P. G. Thomas, and B. Youngblood. 2017. De Novo Epigenetic Programs Inhibit PD-1 Blockade-Mediated T Cell Rejuvenation. *Cell* 170: 142-157.e119.

152. Pauken Kristen, E., A. Sammons Morgan, M. Odorizzi Pamela, S. Manne, J. Godec, O. Khan, M. Drake Adam, Z. Chen, R. Sen Debattama, M. Kurachi, R. A. Barnitz, C. Bartman, B. Bengsch, C. Huang Alexander, M. Schenkel Jason, G. Vahedi, W. N. Haining, L. Berger Shelley, and E. J. Wherry. 2016. Epigenetic stability of exhausted T cells limits durability of reinvigoration by PD-1 blockade. *Science* 354: 1160-1165.

153. Sen Debattama, R., J. Kaminski, R. A. Barnitz, M. Kurachi, U. Gerdemann, B. Yates Kathleen, H.-W. Tsao, J. Godec, W. LaFleur Martin, D. Brown Flavian, P. Tonnerre, T. Chung Raymond, C. Tully Damien, M. Allen Todd, N. Frahm, M. Lauer Georg, E. J. Wherry, N. Yosef, and W. N. Haining. 2016. The epigenetic landscape of T cell exhaustion. *Science* 354: 1165-1169.

154. Giles, J. R., S. Manne, E. Freilich, D. A. Oldridge, A. E. Baxter, S. George, Z. Chen, H. Huang, L. Chilukuri, M. Carberry, L. Giles, N.-P. P. Weng, R. M. Young, C. H. June, L. M. Schuchter, R. K. Amaravadi, X. Xu, G. C. Karakousis, T. C. Mitchell, A. C. Huang, J. Shi, and E. J. Wherry. 2022. Human epigenetic and transcriptional T cell differentiation atlas for identifying functional T cell-specific enhancers. *Immunity* 55: 557-574.e557.

155. Schietinger, A., M. Philip, V. E. Krisnawan, E. Y. Chiu, J. J. Delrow, R. S. Basom, P. Lauer, D. G. Brockstedt, S. E. Knoblaugh, G. J. Hämmerling, T. D. Schell, N. Garbi, and P. D. Greenberg. 2016. Tumor-Specific T Cell Dysfunction Is a Dynamic Antigen-Driven Differentiation Program Initiated Early during Tumorigenesis. *Immunity* 45: 389-401.

156. Youngblood, B., Kenneth J. Oestreich, S.-J. Ha, J. Duraiswamy, Rama S. Akondy, Erin E. West, Z. Wei, P. Lu, James W. Austin, James L. Riley, Jeremy M. Boss, and R. Ahmed. 2011. Chronic Virus Infection Enforces Demethylation of the Locus that Encodes PD-1 in Antigen-Specific CD8+ T Cells. *Immunity* 35: 400-412.

157. Beltra, J.-C., S. Manne, M. S. Abdel-Hakeem, M. Kurachi, J. R. Giles, Z. Chen, V. Casella, S. F. Ngiow, O. Khan, Y. J. Huang, P. Yan, K. Nzingha, W. Xu, R. K. Amaravadi, X. Xu, G. C. Karakousis, T. C. Mitchell, L. M. Schuchter, A. C. Huang, and E. J. Wherry. 2020. Developmental Relationships of Four Exhausted CD8+ T Cell Subsets Reveals Underlying Transcriptional and Epigenetic Landscape Control Mechanisms. *Immunity* 52: 825-841.e828.

158. Miller, B. C., D. R. Sen, R. Al Abosy, K. Bi, Y. V. Virkud, M. W. LaFleur, K. B. Yates, A. Lako, K. Felt, G. S. Naik, M. Manos, E. Gjini, J. R. Kuchroo, J. J. Ishizuka, J. L. Collier, G. K. Griffin, S. Maleri, D. E. Comstock, S. A. Weiss, F. D. Brown, A. Panda, M. D. Zimmer, R. T. Manguso, F. S. Hodi, S. J. Rodig, A. H. Sharpe, and W. N. Haining. 2019. Subsets of exhausted CD8+ T cells differentially mediate tumor control and respond to checkpoint blockade. *Nature Immunology* 20: 326-336.

159. Daniel, B., K. E. Yost, S. Hsiung, K. Sandor, Y. Xia, Y. Qi, K. J. Hiam-Galvez, M. Black, J. R. C, Q. Shi, S. L. Meier, J. A. Belk, J. R. Giles, E. J. Wherry, H. Y. Chang, T. Egawa, and A. T. Satpathy. 2022. Divergent clonal differentiation trajectories of T cell exhaustion. *Nat Immunol* 23: 1614-1627.

160. Kasmani, M. Y., R. Zander, H. K. Chung, Y. Chen, A. Khatun, M. Damo, P. Topchyan, K. E. Johnson, D. Levashova, R. Burns, U. M. Lorenz, V. L. Tarakanova, N. S. Joshi, S. M. Kaech, and W. Cui. 2023. Clonal lineage tracing reveals mechanisms skewing CD8+ T cell fate decisions in chronic infection. *J Exp Med* 220.

161. Jurkowska, R. Z., T. P. Jurkowski, and A. Jeltsch. 2011. Structure and function of mammalian DNA methyltransferases. *Chembiochem* 12: 206-222.

162. Prinzing, B., C. C. Zebley, C. T. Petersen, Y. Fan, A. A. Anido, Z. Yi, P. Nguyen, H. Houke, M. Bell, D. Haydar, C. Brown, S. K. Boi, S. Alli, J. C. Crawford, J. M. Riberdy, J. J. Park, S. Zhou, M. P. Velasquez, C. DeRenzo, C. R. Lazzarotto, S. Q. Tsai, P. Vogel, S. M. Pruett-Miller, D. M. Langfitt, S. Gottschalk, B. Youngblood, and G. Krenciute. 2021. Deleting DNMT3A in CAR T cells prevents exhaustion and enhances antitumor activity. *Science Translational Medicine* 13: eabh0272.

163. Lisiero, D. N., H. Soto, R. G. Everson, L. M. Liau, and R. M. Prins. 2014. The histone deacetylase inhibitor, LBH589, promotes the systemic cytokine and effector responses of adoptively transferred CD8+ T cells. *Journal for ImmunoTherapy of Cancer* 2: 8.

164. Vo, D. D., R. M. Prins, J. L. Begley, T. R. Donahue, L. F. Morris, K. W. Bruhn, P. de la Rocha, M.-Y. Yang, S. Mok, H. J. Garban, N. Craft, J. S. Economou, F. M. Marincola, E. Wang, and A. Ribas. 2009. Enhanced Antitumor Activity Induced by Adoptive T-Cell Transfer and Adjunctive Use of the Histone Deacetylase Inhibitor LAQ824. *Cancer Research* 69: 8693-8699.

165. Chee, J., C. Wilson, A. Buzzai, B. Wylie, C. A. Forbes, M. Booth, N. Principe, B. Foley, M. N. Cruickshank, and J. Waithman. 2020. Impaired T cell proliferation by ex vivo BET-inhibition impedes adoptive immunotherapy in a murine melanoma model. *Epigenetics* 15: 134-144.

166. Belk, J. A., W. Yao, N. Ly, K. A. Freitas, Y.-T. Chen, Q. Shi, A. M. Valencia, E. Shifrut, N. Kale, K. E. Yost, C. V. Duffy, M. A. Hwee, Z. Miao, A. Ashworth, C. L. Mackall, A. Marson, J. Carnevale, S. A. Vardhana, and A. T. Satpathy. 2022. Genome-wide CRISPR screens of T cell exhaustion identify chromatin remodeling factors that limit T cell persistence. *bioRxiv*: 2022.2004.2020.488974.

167. McDonald, B., B. Y. Chick, N. S. Ahmed, M. Burns, S. Ma, E. Casillas, D. Chen, T. H. Mann, C. O'Connor, N. Hah, D. C. Hargreaves, and S. M. Kaech. 2023. Canonical BAF complex activity shapes the enhancer landscape that licenses CD8+ T cell effector and memory fates. *Immunity* 56: 1303-1319.e1305.

168. Freitas, K. A., J. A. Belk, E. Sotillo, P. J. Quinn, M. C. Ramello, M. Malipatlolla, B. Daniel, K. Sandor, D. Klysz, J. Bjelajac, P. Xu, K. A. Burdsall, V. Tieu, V. T. Duong, M. G.

Donovan, E. W. Weber, H. Y. Chang, R. G. Majzner, J. M. Espinosa, A. T. Satpathy, and C. L. Mackall. Enhanced T cell effector activity by targeting the Mediator kinase module. *Science* 378: eabn5647.

169. Baxter, A. E., H. Huang, J. R. Giles, Z. Chen, J. E. Wu, S. Drury, K. Dalton, S. L. Park, L. Torres, B. W. Simone, M. Klapholz, S. F. Ngiow, E. Freilich, S. Manne, V. Alcalde, V. Ekshyyan, S. L. Berger, J. Shi, M. S. Jordan, and E. J. Wherry. 2023. The SWI/SNF chromatin remodeling complexes BAF and PBAF differentially regulate epigenetic transitions in exhausted CD8⁺ T cells. *Immunity* 56: 1320-1340.e1310.

170. Hargreaves, D. C., and G. R. Crabtree. 2011. ATP-dependent chromatin remodeling: genetics, genomics and mechanisms. *Cell Research* 21: 396-420.

171. Guo, A., H. Huang, Z. Zhu, M. J. Chen, H. Shi, S. Yuan, P. Sharma, J. P. Connelly, S. Liedmann, Y. Dhungana, Z. Li, D. Haydar, M. Yang, H. Beere, J. T. Yustein, C. DeRenzo, S. M. Pruett-Miller, J. C. Crawford, G. Krenciute, C. W. M. Roberts, H. Chi, and D. R. Green. 2022. cBAF complex components and MYC cooperate early in CD8(+) T cell fate. *Nature* 607: 135-141.

172. El Khattabi, L., H. Zhao, J. Kalchschmidt, N. Young, S. Jung, P. Van Blerkom, P. Kieffer-Kwon, K. R. Kieffer-Kwon, S. Park, X. Wang, J. Krebs, S. Tripathi, N. Sakabe, D. R. Sobreira, S. C. Huang, S. S. P. Rao, N. Pruett, D. Chauss, E. Sadler, A. Lopez, M. A. Nóbrega, E. L. Aiden, F. J. Asturias, and R. Casellas. 2019. A Pliable Mediator Acts as a Functional Rather Than an Architectural Bridge between Promoters and Enhancers. *Cell* 178: 1145-1158.e1120.

173. Sealfon, S. C., and T. T. Chu. 2011. RNA and DNA microarrays. *Methods Mol Biol* 671: 3-34.

174. Ye, S. Q., D. C. Usher, and L. Q. Zhang. 2002. Gene expression profiling of human diseases by serial analysis of gene expression. *J Biomed Sci* 9: 384-394.

175. Utzschneider, D. T., M. Charmoy, V. Chennupati, L. Pousse, D. P. Ferreira, S. Calderon-Copete, M. Danilo, F. Alfei, M. Hofmann, D. Wieland, S. Pradervand, R. Thimme, D. Zehn, and W. Held. 2016. T Cell Factor 1-Expressing Memory-like CD8⁺ T Cells Sustain the Immune Response to Chronic Viral Infections. *Immunity* 45: 415-427.

176. Singer, M., C. Wang, L. Cong, N. D. Marjanovic, M. S. Kowalczyk, H. Zhang, J. Nyman, K. Sakuishi, S. Kurtulus, D. Gennert, J. Xia, J. Y. H. Kwon, J. Nevin, R. H. Herbst, I. Yanai, O. Rozenblatt-Rosen, V. K. Kuchroo, A. Regev, and A. C. Anderson. 2016. A Distinct Gene Module for Dysfunction Uncoupled from Activation in Tumor-Infiltrating T Cells. *Cell* 166: 1500-1511.e1509.

177. Brummelman, J., E. M. C. Mazza, G. Alvisi, F. S. Colombo, A. Grilli, J. Mikulak, D. Mavilio, M. Alloisio, F. Ferrari, E. Lopci, P. Novellis, G. Veronesi, and E. Lugli. 2018. High-dimensional single cell analysis identifies stem-like cytotoxic CD8+ T cells infiltrating human tumors. *Journal of Experimental Medicine* 215: 2520-2535.

178. Sade-Feldman, M., K. Yizhak, S. L. Bjorgaard, J. P. Ray, C. G. de Boer, R. W. Jenkins, D. J. Lieb, J. H. Chen, D. T. Frederick, M. Barzily-Rokni, S. S. Freeman, A. Reuben, P. J. Hoover, A.-C. Villani, E. Ivanova, A. Portell, P. H. Lizotte, A. R. Aref, J.-P. Eliane, M. R. Hammond, H. Vitzthum, S. M. Blackmon, B. Li, V. Gopalakrishnan, S. M. Reddy, Z. A. Cooper, C. P. Paweletz, D. A. Barbie, A. Stemmer-Rachamimov, K. T. Flaherty, J. A. Wargo, G. M. Boland, R. J. Sullivan, G. Getz, and N. Hacohen. 2018. Defining T Cell States Associated with Response to Checkpoint Immunotherapy in Melanoma. *Cell* 175: 998-1013.e1020.

179. Thommen, D. S., V. H. Koelzer, P. Herzig, A. Roller, M. Trefny, S. Dimeloe, A. Kiialainen, J. Hanhart, C. Schill, C. Hess, S. Savic Prince, M. Wiese, D. Lardinois, P.-C. Ho, C. Klein, V. Karanikas, K. D. Mertz, T. N. Schumacher, and A. Zippelius. 2018. A transcriptionally and functionally distinct PD-1+ CD8+ T cell pool with predictive potential in non-small-cell lung cancer treated with PD-1 blockade. *Nature Medicine* 24: 994-1004.

180. Jadhav Rohit, R., J. Im Se, B. Hu, M. Hashimoto, P. Li, J.-X. Lin, J. Leonard Warren, J. Greenleaf William, R. Ahmed, and J. Goronzy Jorg. 2019. Epigenetic signature of PD-1+ TCF1+ CD8 T cells that act as resource cells during chronic viral infection and respond to PD-1 blockade. *Proceedings of the National Academy of Sciences* 116: 14113-14118.

181. Connolly, K. A., M. Kuchroo, A. Venkat, A. Khatun, J. Wang, I. William, N. I. Hornick, B. L. Fitzgerald, M. Damo, M. Y. Kasmani, C. Cui, E. Fagerberg, I. Monroy, A. Hutchins, J. F. Cheung, G. G. Foster, D. L. Mariuzza, M. Nader, H. Zhao, W. Cui, S. Krishnaswamy, and N. S. Joshi. 2021. A reservoir of stem-like CD8+ T cells in the tumor-draining lymph node preserves the ongoing antitumor immune response. *Science Immunology* 6: eabg7836.

182. Carmona, S. J., I. Siddiqui, M. Bilous, W. Held, and D. Gfeller. 2020. Deciphering the transcriptomic landscape of tumor-infiltrating CD8 lymphocytes in B16 melanoma tumors with single-cell RNA-Seq. *Oncoimmunology* 9: 1737369.

183. Andreatta, M., J. Corria-Osorio, S. Müller, R. Cubas, G. Coukos, and S. J. Carmona. 2021. Interpretation of T cell states from single-cell transcriptomics data using reference atlases. *Nature Communications* 12: 2965.

184. Zhou, Y., B. Zhou, L. Pache, M. Chang, A. H. Khodabakhshi, O. Tanaseichuk, C. Benner, and S. K. Chanda. 2019. Metascape provides a biologist-oriented resource for the analysis of systems-level datasets. *Nat Commun* 10: 1523.

185. Yu, B., K. Zhang, J. J. Milner, C. Toma, R. Chen, J. P. Scott-Browne, R. M. Pereira, S. Crotty, J. T. Chang, M. E. Pipkin, W. Wang, and A. W. Goldrath. 2017. Epigenetic landscapes reveal transcription factors that regulate CD8+ T cell differentiation. *Nature Immunology* 18: 573-582.

186. Sjoerd, T. T. S., R. Ernesto, J. W. K. Laura, H. W. C. Matheus, B. Louis, B. Jan Van den, M. M. D. H. Joke, and K. Yvette Van. 2020. Monocyte-derived APCs are central to the response of PD1 checkpoint blockade and provide a therapeutic target for combination therapy. *Journal for ImmunoTherapy of Cancer* 8: e000588.

187. Im, S. J., M. Hashimoto, M. Y. Gerner, J. Lee, H. T. Kissick, M. C. Burger, Q. Shan, J. S. Hale, J. Lee, T. H. Nasti, A. H. Sharpe, G. J. Freeman, R. N. Germain, H. I. Nakaya, H. H. Xue, and R. Ahmed. 2016. Defining CD8+ T cells that provide the proliferative burst after PD-1 therapy. *Nature* 537: 417-421.

188. Siddiqui, I., K. Schaeuble, V. Chennupati, S. A. Fuertes Marraco, S. Calderon-Copete, D. Pais Ferreira, S. J. Carmona, L. Scarpellino, D. Gfeller, S. Pradervand, S. A. Luther, D. E. Speiser, and W. Held. 2019. Intratumoral Tcf1(+)PD-1(+)CD8(+) T Cells with Stem-like Properties Promote Tumor Control in Response to Vaccination and Checkpoint Blockade Immunotherapy. *Immunity* 50: 195-211.e110.

189. Kurtulus, S., A. Madi, G. Escobar, M. Klapholz, J. Nyman, E. Christian, M. Pawlak, D. Dionne, J. Xia, O. Rozenblatt-Rosen, V. K. Kuchroo, A. Regev, and A. C. Anderson. 2019. Checkpoint Blockade Immunotherapy Induces Dynamic Changes in PD-1(-)CD8(+) Tumor-Infiltrating T Cells. *Immunity* 50: 181-194.e186.

190. Chen, Z., Z. Ji, S. F. Ngiow, S. Manne, Z. Cai, A. C. Huang, J. Johnson, R. P. Staupe, B. Bengsch, C. Xu, S. Yu, M. Kurachi, R. S. Herati, L. A. Vella, A. E. Baxter, J. E. Wu, O. Khan, J. C. Beltra, J. R. Giles, E. Stelekati, L. M. McLane, C. W. Lau, X. Yang, S. L. Berger, G. Vahedi, H. Ji, and E. J. Wherry. 2019. TCF-1-Centered Transcriptional Network Drives an Effector versus Exhausted CD8 T Cell-Fate Decision. *Immunity* 51: 840-855.e845.

191. Giles, J. R., S. F. Ngiow, S. Manne, A. E. Baxter, O. Khan, P. Wang, R. Staupe, M. S. Abdel-Hakeem, H. Huang, D. Mathew, M. M. Painter, J. E. Wu, Y. J. Huang, R. R. Goel, P. K. Yan, G. C. Karakousis, X. Xu, T. C. Mitchell, A. C. Huang, and E. J. Wherry. 2022. Shared and distinct biological circuits in effector, memory and exhausted CD8(+) T cells revealed by temporal single-cell transcriptomics and epigenetics. *Nat Immunol* 23: 1600-1613.

192. Panigrahi, A., and B. W. O'Malley. 2021. Mechanisms of enhancer action: the known and the unknown. *Genome Biology* 22: 108.

193. Larke, M. S. C., R. Schwessinger, T. Nojima, J. Telenius, R. A. Beagrie, D. J. Downes, A. M. Oudelaar, J. Truch, B. Graham, M. A. Bender, N. J. Proudfoot, D. R. Higgs, and J. R. Hughes. 2021. Enhancers predominantly regulate gene expression during differentiation via transcription initiation. *Mol Cell* 81: 983-997.e987.

194. Wang, H., Z. Fan, P. V. Shliaha, M. Miele, R. C. Hendrickson, X. Jiang, and K. Helin. 2023. H3K4me3 regulates RNA polymerase II promoter-proximal pause-release. *Nature* 615: 339-348.

195. Gates, L. A., J. Shi, A. D. Rohira, Q. Feng, B. Zhu, M. T. Bedford, C. A. Sagum, S. Y. Jung, J. Qin, M. J. Tsai, S. Y. Tsai, W. Li, C. E. Foulds, and B. W. O'Malley. 2017. Acetylation on histone H3 lysine 9 mediates a switch from transcription initiation to elongation. *J Biol Chem* 292: 14456-14472.

196. Henning, A. N., R. Roychoudhuri, and N. P. Restifo. 2018. Epigenetic control of CD8+ T cell differentiation. *Nature Reviews Immunology* 18: 340-356.

197. Belk, J. A., B. Daniel, and A. T. Satpathy. 2022. Epigenetic regulation of T cell exhaustion. *Nature Immunology* 23: 848-860.

198. Simoni, Y., E. Becht, M. Fehlings, C. Y. Loh, S. L. Koo, K. W. W. Teng, J. P. S. Yeong, R. Nahar, T. Zhang, H. Kared, K. Duan, N. Ang, M. Poidinger, Y. Y. Lee, A. Larbi, A. J. Khng, E. Tan, C. Fu, R. Mathew, M. Teo, W. T. Lim, C. K. Toh, B. H. Ong, T. Koh, A. M. Hillmer, A. Takano, T. K. H. Lim, E. H. Tan, W. Zhai, D. S. W. Tan, I. B. Tan, and E. W. Newell. 2018. Bystander CD8(+) T cells are abundant and phenotypically distinct in human tumour infiltrates. *Nature* 557: 575-579.

199. Natoli, G. 2010. Maintaining cell identity through global control of genomic organization. *Immunity* 33: 12-24.

200. Mognol Giuliana, P., R. Spreafico, V. Wong, P. Scott-Browne James, S. Togher, A. Hoffmann, G. Hogan Patrick, A. Rao, and S. Trifari. 2017. Exhaustion-associated regulatory regions in CD8+ tumor-infiltrating T cells. *Proceedings of the National Academy of Sciences* 114: E2776-E2785.

201. Martinez, G. J., R. M. Pereira, T. Äijö, E. Y. Kim, F. Marangoni, M. E. Pipkin, S. Togher, V. Heissmeyer, Y. C. Zhang, S. Crotty, E. D. Lamperti, K. M. Ansel, T. R. Mempel, H. Lähdesmäki, P. G. Hogan, and A. Rao. 2015. The Transcription Factor NFAT Promotes Exhaustion of Activated CD8⁺ T Cells. *Immunity* 42: 265-278.

202. Williams, J. B., B. L. Horton, Y. Zheng, Y. Duan, J. D. Powell, and T. F. Gajewski. 2017. The EGR2 targets LAG-3 and 4-1BB describe and regulate dysfunctional antigen-specific CD8+ T cells in the tumor microenvironment. *J Exp Med* 214: 381-400.

203. Menk, A. V., N. E. Scharping, D. B. Rivadeneira, M. J. Calderon, M. J. Watson, D. Dunstane, S. C. Watkins, and G. M. Delgoffe. 2018. 4-1BB costimulation induces T cell mitochondrial function and biogenesis enabling cancer immunotherapeutic responses. *J Exp Med* 215: 1091-1100.

204. Sharpe, A. H., and K. E. Pauken. 2018. The diverse functions of the PD1 inhibitory pathway. *Nature Reviews Immunology* 18: 153-167.

205. Phanstiel, D. H., K. Van Bortle, D. Spacek, G. T. Hess, M. S. Shamim, I. Machol, M. I. Love, E. L. Aiden, M. C. Bassik, and M. P. Snyder. 2017. Static and Dynamic DNA Loops form AP-1-Bound Activation Hubs during Macrophage Development. *Mol Cell* 67: 1037-1048.e1036.

206. Vierbuchen, T., E. Ling, C. J. Cowley, C. H. Couch, X. Wang, D. A. Harmin, C. W. M. Roberts, and M. E. Greenberg. 2017. AP-1 Transcription Factors and the BAF Complex Mediate Signal-Dependent Enhancer Selection. *Mol Cell* 68: 1067-1082.e1012.

207. Yukawa, M., S. Jagannathan, S. Vallabh, A. V. Kartashov, X. Chen, M. T. Weirauch, and A. Barski. 2020. AP-1 activity induced by co-stimulation is required for chromatin opening during T cell activation. *J Exp Med* 217.

208. Kim, A. M. J., M. R. Nemeth, and S.-O. Lim. 2022. 4-1BB: A promising target for cancer immunotherapy. *Frontiers in Oncology* 12.

209. McLane, L. M., S. F. Ngiow, Z. Chen, J. Attanasio, S. Manne, G. Ruthel, J. E. Wu, R. P. Staupe, W. Xu, R. K. Amaravadi, X. Xu, G. C. Karakousis, T. C. Mitchell, L. M. Schuchter, A. C. Huang, B. D. Freedman, M. R. Betts, and E. J. Wherry. 2021. Role of nuclear localization in the regulation and function of T-bet and Eomes in exhausted CD8 T cells. *Cell Reports* 35.

210. Chen, Z., Z. Ji, S. F. Ngiow, S. Manne, Z. Cai, A. C. Huang, J. Johnson, R. P. Staupe, B. Bengsch, C. Xu, S. Yu, M. Kurachi, R. S. Herati, L. A. Vella, A. E. Baxter, J. E. Wu, O. Khan, J.-C. Beltra, J. R. Giles, E. Stelekati, L. M. McLane, C. W. Lau, X. Yang, S. L. Berger, G. Vahedi, H. Ji, and E. J. Wherry. 2019. TCF-1-Centered Transcriptional Network Drives an Effector versus Exhausted CD8 T Cell-Fate Decision. *Immunity* 51: 840-855.e845.

211. Pritykin, Y., J. van der Veeken, A. R. Pine, Y. Zhong, M. Sahin, L. Mazutis, D. Pe'er, A. Y. Rudensky, and C. S. Leslie. 2021. A unified atlas of CD8 T cell dysfunctional states in cancer and infection. *Molecular Cell* 81: 2477-2493.e2410.

212. Maurice, N. J., J. Berner, A. K. Taber, D. Zehn, and M. Prlic. 2021. Inflammatory signals are sufficient to elicit TOX expression in mouse and human CD8+ T cells. *JCI Insight* 6.

213. Glasmacher, E., S. Agrawal, A. B. Chang, T. L. Murphy, W. Zeng, B. Vander Lugt, A. A. Khan, M. Ciofani, C. J. Spooner, S. Rutz, J. Hackney, R. Nurieva, C. R. Escalante, W. Ouyang, D. R. Littman, K. M. Murphy, and H. Singh. 2012. A genomic regulatory element that directs assembly and function of immune-specific AP-1-IRF complexes. *Science* 338: 975-980.

214. Man, K., S. S. Gabriel, Y. Liao, R. Gloury, S. Preston, D. C. Henstridge, M. Pellegrini, D. Zehn, F. Berberich-Siebelt, M. A. Febbraio, W. Shi, and A. Kallies. 2017. Transcription Factor IRF4 Promotes CD8(+) T Cell Exhaustion and Limits the Development of Memory-like T Cells during Chronic Infection. *Immunity* 47: 1129-1141.e1125.

215. Quigley, M., F. Pereyra, B. Nilsson, F. Porichis, C. Fonseca, Q. Eichbaum, B. Julg, J. L. Jesneck, K. Brosnahan, S. Imam, K. Russell, I. Toth, A. Piechocka-Trocha, D. Dolfi, J. Angelosanto, A. Crawford, H. Shin, D. S. Kwon, J. Zupkosky, L. Francisco, G. J. Freeman, E. J. Wherry, D. E. Kaufmann, B. D. Walker, B. Ebert, and W. N. Haining. 2010. Transcriptional analysis of HIV-specific CD8+ T cells shows that PD-1 inhibits T cell function by upregulating BATF. *Nat Med* 16: 1147-1151.

216. Le, N. Q. K., E. K. Y. Yapp, N. Nagasundaram, and H.-Y. Yeh. 2019. Classifying Promoters by Interpreting the Hidden Information of DNA Sequences via Deep Learning

and Combination of Continuous FastText N-Grams. *Frontiers in Bioengineering and Biotechnology* 7.

217. Blanco, E., M. González-Ramírez, A. Alcaine-Colet, S. Aranda, and L. Di Croce. 2020. The Bivalent Genome: Characterization, Structure, and Regulation. *Trends Genet* 36: 118-131.

218. Bernstein, B. E., T. S. Mikkelsen, X. Xie, M. Kamal, D. J. Huebert, J. Cuff, B. Fry, A. Meissner, M. Wernig, K. Plath, R. Jaenisch, A. Wagschal, R. Feil, S. L. Schreiber, and E. S. Lander. 2006. A bivalent chromatin structure marks key developmental genes in embryonic stem cells. *Cell* 125: 315-326.

219. Azuara, V., P. Perry, S. Sauer, M. Spivakov, H. F. Jørgensen, R. M. John, M. Gouti, M. Casanova, G. Warnes, M. Merkenschlager, and A. G. Fisher. 2006. Chromatin signatures of pluripotent cell lines. *Nat Cell Biol* 8: 532-538.

220. Mikkelsen, T. S., M. Ku, D. B. Jaffe, B. Issac, E. Lieberman, G. Giannoukos, P. Alvarez, W. Brockman, T. K. Kim, R. P. Koche, W. Lee, E. Mendenhall, A. O'Donovan, A. Presser, C. Russ, X. Xie, A. Meissner, M. Wernig, R. Jaenisch, C. Nusbaum, E. S. Lander, and B. E. Bernstein. 2007. Genome-wide maps of chromatin state in pluripotent and lineage-committed cells. *Nature* 448: 553-560.

221. Brookes, E., I. de Santiago, D. Hebenstreit, K. J. Morris, T. Carroll, S. Q. Xie, J. K. Stock, M. Heidemann, D. Eick, N. Nozaki, H. Kimura, J. Ragoussis, S. A. Teichmann, and A. Pombo. 2012. Polycomb associates genome-wide with a specific RNA polymerase II variant, and regulates metabolic genes in ESCs. *Cell Stem Cell* 10: 157-170.

222. Kumar, D., S. Cinghu, A. J. Oldfield, P. Yang, and R. Jothi. 2021. Decoding the function of bivalent chromatin in development and cancer. *Genome Res* 31: 2170-2184.

223. Harker, N., A. Garefalaki, U. Menzel, E. Ktistaki, T. Naito, K. Georgopoulos, and D. Kioussis. 2011. Pre-TCR signaling and CD8 gene bivalent chromatin resolution during thymocyte development. *Journal of immunology (Baltimore, Md. : 1950)* 186: 6368-6377.

224. Kinkley, S., J. Helmuth, J. K. Polansky, I. Dunkel, G. Gasparoni, S. Fröhler, W. Chen, J. Walter, A. Hamann, and H. R. Chung. 2016. reChIP-seq reveals widespread bivalency of H3K4me3 and H3K27me3 in CD4(+) memory T cells. *Nature communications* 7: 12514.

225. Araki, Y., Z. Wang, C. Zang, W. H. Wood, 3rd, D. Schones, K. Cui, T. Y. Roh, B. Lhotsky, R. P. Wersto, W. Peng, K. G. Becker, K. Zhao, and N. P. Weng. 2009. Genome-wide analysis of histone methylation reveals chromatin state-based regulation of gene transcription and function of memory CD8+ T cells. *Immunity* 30: 912-925.

226. Abraham, B. J., K. Cui, Q. Tang, and K. Zhao. 2013. Dynamic regulation of epigenomic landscapes during hematopoiesis. *BMC genomics* 14: 193.

227. Rohan, N. S., T. G. Adrian, E. Jimmy, C. Zhonglei, H. Takamitsu, C. L. Carolin, W. L. Peter, K. Shohei, F. Beat, and J. R. Alexander. 2021. Re-evaluating the role of nucleosomal bivalency in early development. *bioRxiv*: 2021.2009.2009.458948.

228. Meissner, A., T. S. Mikkelsen, H. Gu, M. Wernig, J. Hanna, A. Sivachenko, X. Zhang, B. E. Bernstein, C. Nusbaum, D. B. Jaffe, A. Gnirke, R. Jaenisch, and E. S. Lander. 2008. Genome-scale DNA methylation maps of pluripotent and differentiated cells. *Nature* 454: 766-770.

229. Russ, Brendan E., M. Olshanksy, Heather S. Smallwood, J. Li, Alice E. Denton, Julia E. Prier, Angus T. Stock, Hayley A. Croom, Jolie G. Cullen, Michelle L. T. Nguyen, S. Rowe, Matthew R. Olson, David B. Finkelstein, A. Kelso, Paul G. Thomas, Terry P. Speed, S. Rao, and Stephen J. Turner. 2014. Distinct Epigenetic Signatures Delineate Transcriptional Programs during Virus-Specific CD8+ T Cell Differentiation. *Immunity* 41: 853-865.

230. Araki, Y., Z. Wang, C. Zang, W. H. Wood, D. Schones, K. Cui, T.-Y. Roh, B. Lhotsky, R. P. Wersto, W. Peng, K. G. Becker, K. Zhao, and N.-p. Weng. 2009. Genome-wide Analysis of Histone Methylation Reveals Chromatin State-Based Regulation of Gene Transcription and Function of Memory CD8+ T Cells. *Immunity* 30: 912-925.

231. Ernst, J., and M. Kellis. 2012. ChromHMM: automating chromatin-state discovery and characterization. *Nature Methods* 9: 215-216.

232. Ernst, J., and M. Kellis. 2017. Chromatin-state discovery and genome annotation with ChromHMM. *Nat Protoc* 12: 2478-2492.

233. Hattori, N., T. Niwa, K. Kimura, K. Helin, and T. Ushijima. 2013. Visualization of multivalent histone modification in a single cell reveals highly concerted epigenetic changes on differentiation of embryonic stem cells. *Nucleic Acids Res* 41: 7231-7239.

234. Gomez, D., L. S. Shankman, A. T. Nguyen, and G. K. Owens. 2013. Detection of histone modifications at specific gene loci in single cells in histological sections. *Nat Methods* 10: 171-177.

235. Chakraborty, A. A., T. Laukka, M. Myllykoski, A. E. Ringel, M. A. Booker, M. Y. Tolstorukov, Y. J. Meng, S. R. Meier, R. B. Jennings, A. L. Creech, Z. T. Herbert, S. K. McBrayer, B. A. Olenchock, J. D. Jaffe, M. C. Haigis, R. Beroukhim, S. Signoretti, P. Koivunen, and W. G. Kaelin, Jr. 2019. Histone demethylase KDM6A directly senses oxygen to control chromatin and cell fate. *Science* 363: 1217-1222.

236. Batie, M., J. Frost, M. Frost, J. W. Wilson, P. Schofield, and S. Rocha. 2019. Hypoxia induces rapid changes to histone methylation and reprograms chromatin. *Science* 363: 1222-1226.

237. Manna, S., J. K. Kim, C. Baugé, M. Cam, Y. Zhao, J. Shetty, M. S. Vacchio, E. Castro, B. Tran, L. Tessarollo, and R. Bosselut. 2015. Histone H3 Lysine 27 demethylases Jmjd3 and Utx are required for T-cell differentiation. *Nat Commun* 6: 8152.

238. Li, J., K. Hardy, M. Olshansky, A. Barugahare, L. J. Gearing, J. E. Prier, X. Y. X. Sng, M. L. T. Nguyen, D. Piovesan, B. E. Russ, N. L. La Gruta, P. J. Hertzog, S. Rao, and S. J. Turner. 2021. KDM6B-dependent chromatin remodeling underpins effective virus-specific CD8(+) T cell differentiation. *Cell Rep* 34: 108839.

239. Nutt, S. L., C. Keenan, M. Chopin, and R. S. Allan. 2020. EZH2 function in immune cell development. *Biol Chem* 401: 933-943.

240. Shema, E., D. Jones, N. Shoresh, L. Donohue, O. Ram, and B. E. Bernstein. 2016. Single-molecule decoding of combinatorially modified nucleosomes. *Science* 352: 717-721.

241. Prickaerts, P., M. E. Adriaens, T. V. D. Beucken, E. Koch, L. Dubois, V. E. H. Dahlmans, C. Gits, C. T. A. Evelo, M. Chan-Seng-Yue, B. G. Wouters, and J. W. Voncken. 2016. Hypoxia increases genome-wide bivalent epigenetic marking by specific gain of H3K27me3. *Epigenetics Chromatin* 9: 46.

242. Kim, K. H., and C. W. Roberts. 2016. Targeting EZH2 in cancer. *Nat Med* 22: 128-134.

243. Cao, R., L. Wang, H. Wang, L. Xia, H. Erdjument-Bromage, P. Tempst, R. S. Jones, and Y. Zhang. 2002. Role of histone H3 lysine 27 methylation in Polycomb-group silencing. *Science* 298: 1039-1043.

244. Jadhav, U., K. Nalapareddy, M. Saxena, N. K. O'Neill, L. Pinello, G. C. Yuan, S. H. Orkin, and R. A. Shivdasani. 2016. Acquired Tissue-Specific Promoter Bivalency Is a Basis for PRC2 Necessity in Adult Cells. *Cell* 165: 1389-1400.

245. Qin, A., T. Zhong, H. Zou, X. Wan, B. Yao, X. Zheng, and D. Yin. 2019. Critical role of Tim-3 mediated autophagy in chronic stress induced immunosuppression. *Cell & Bioscience* 9: 13.

246. Dan, P. Z., V. M. Ashley, V. Maria, N. Daniel, D. Kristin, L. Angen, L. F. Robert, and M. D. Greg. 2021. Tumor hypoxia is associated with resistance to PD-1 blockade in squamous cell carcinoma of the head and neck. *Journal for ImmunoTherapy of Cancer* 9: e002088.

247. Jayaprakash, P., P. D. A. Vignali, G. M. Delgoffe, and M. A. Curran. 2022. Hypoxia Reduction Sensitizes Refractory Cancers to Immunotherapy. *Annual Review of Medicine* 73: 251-265.

248. Jones, P. A., H. Ohtani, A. Chakravarthy, and D. D. De Carvalho. 2019. Epigenetic therapy in immune-oncology. *Nat Rev Cancer* 19: 151-161.

249. Chen, X., X. Pan, W. Zhang, H. Guo, S. Cheng, Q. He, B. Yang, and L. Ding. 2020. Epigenetic strategies synergize with PD-L1/PD-1 targeted cancer immunotherapies to enhance antitumor responses. *Acta Pharmaceutica Sinica B* 10: 723-733.

250. Niborski, L. L., P. Gueguen, M. Ye, A. Thiolat, R. N. Ramos, P. Caudana, J. Denizeau, L. Colombeau, R. Rodriguez, C. Goudot, J. M. Luccarini, A. Soudé, B. Bournique, P. Broqua, L. Pace, S. Baulande, C. Sedlik, J. P. Quivy, G. Almouzni, J. L. Cohen, E. Zueva, J. J.

Waterfall, S. Amigorena, and E. Piaggio. 2022. CD8+T cell responsiveness to anti-PD-1 is epigenetically regulated by Suv39h1 in melanomas. *Nat Commun* 13: 3739.

251. Woods, D. M., A. L. Sodré, A. Villagra, A. Sarnaik, E. M. Sotomayor, and J. Weber. 2015. HDAC Inhibition Upregulates PD-1 Ligands in Melanoma and Augments Immunotherapy with PD-1 Blockade. *Cancer Immunology Research* 3: 1375-1385.

252. Li, X., X. Su, R. Liu, Y. Pan, J. Fang, L. Cao, C. Feng, Q. Shang, Y. Chen, C. Shao, and Y. Shi. 2021. HDAC inhibition potentiates anti-tumor activity of macrophages and enhances anti-PD-L1-mediated tumor suppression. *Oncogene* 40: 1836-1850.

253. Burke, B., C. Eden, C. Perez, A. Belshoff, S. Hart, L. Plaza-Rojas, M. Delos Reyes, K. Prajapati, C. Voelkel-Johnson, E. Henry, G. Gupta, and J. Guevara-Patiño. 2020. Inhibition of Histone Deacetylase (HDAC) Enhances Checkpoint Blockade Efficacy by Rendering Bladder Cancer Cells Visible for T Cell-Mediated Destruction. *Frontiers in Oncology* 10.

254. Zheng, H., W. Zhao, C. Yan, C. C. Watson, M. Massengill, M. Xie, C. Massengill, D. R. Noyes, G. V. Martinez, R. Afzal, Z. Chen, X. Ren, S. J. Antonia, E. B. Haura, B. Ruffell, and A. A. Beg. 2016. HDAC Inhibitors Enhance T-Cell Chemokine Expression and Augment Response to PD-1 Immunotherapy in Lung Adenocarcinoma. *Clin Cancer Res* 22: 4119-4132.

255. Sheng, W., M. W. LaFleur, T. H. Nguyen, S. Chen, A. Chakravarthy, J. R. Conway, Y. Li, H. Chen, H. Yang, P. H. Hsu, E. M. Van Allen, G. J. Freeman, D. D. De Carvalho, H. H. He, A. H. Sharpe, and Y. Shi. 2018. LSD1 Ablation Stimulates Anti-tumor Immunity and Enables Checkpoint Blockade. *Cell* 174: 549-563.e519.

256. Morschhauser, F., H. Tilly, A. Chaidos, P. McKay, T. Phillips, S. Assouline, C. L. Batlevi, P. Campbell, V. Ribrag, G. L. Damaj, M. Dickinson, W. Jurczak, M. Kazmierczak, S. Opat, J. Radford, A. Schmitt, J. Yang, J. Whalen, S. Agarwal, D. Adib, and G. Salles. 2020. Tazemetostat for patients with relapsed or refractory follicular lymphoma: an open-label, single-arm, multicentre, phase 2 trial. *The Lancet Oncology* 21: 1433-1442.

257. Straining, R., and W. Eighmy. 2022. Tazemetostat: EZH2 Inhibitor. *J Adv Pract Oncol* 13: 158-163.

258. Fraietta, J. A., C. L. Nobles, M. A. Sammons, S. Lundh, S. A. Carty, T. J. Reich, A. P. Cogdill, J. J. D. Morrissette, J. E. DeNizio, S. Reddy, Y. Hwang, M. Gohil, I. Kulikovskaya, F. Nazimuddin, M. Gupta, F. Chen, J. K. Everett, K. A. Alexander, E. Lin-Shiao, M. H. Gee, X. Liu, R. M. Young, D. Ambrose, Y. Wang, J. Xu, M. S. Jordan, K. T. Marcucci, B. L. Levine, K. C. Garcia, Y. Zhao, M. Kalos, D. L. Porter, R. M. Kohli, S. F. Lacey, S. L. Berger, F. D. Bushman, C. H. June, and J. J. Melenhorst. 2018. Disruption of TET2 promotes the therapeutic efficacy of CD19-targeted T cells. *Nature* 558: 307-312.

259. Yingqin, H., Z. Jaroslav, S. Yujie, P. Isaraphorn, D. Brandon, W. Wenjian, Q. Ke, W. Evan, R. T. John, and W. Peng. 2023. Transient EZH2 suppression by Tazemetostat during in vitro expansion maintains T cell stemness and improves adoptive T cell therapy. *bioRxiv*: 2023.2002.2007.527459.

260. Pellakuru, L. G., T. Iwata, B. Gurel, D. Schultz, J. Hicks, C. Bethel, S. Yegnasubramanian, and A. M. De Marzo. 2012. Global levels of H3K27me3 track with differentiation in vivo and are deregulated by MYC in prostate cancer. *Am J Pathol* 181: 560-569.

261. Levy, S., L. Somasundaram, I. X. Raj, D. Ic-Mex, A. Phal, S. Schmidt, W. I. Ng, D. Mar, J. Decarreau, N. Moss, A. Alghadeer, H. Honkanen, J. Sarthy, N. A. Vitanza, R. D. Hawkins, J. Mathieu, Y. Wang, D. Baker, K. Bomsztyk, and H. Ruohola-Baker. 2022. dCas9 fusion to computer-designed PRC2 inhibitor reveals functional TATA box in distal promoter region. *Cell Reports* 38: 110457.

262. Buttitta, L. A., and B. A. Edgar. 2007. Mechanisms controlling cell cycle exit upon terminal differentiation. *Curr Opin Cell Biol* 19: 697-704.

263. Wherry, E. J., D. L. Barber, S. M. Kaech, J. N. Blattman, and R. Ahmed. 2004. Antigen-independent memory CD8 T cells do not develop during chronic viral infection. *Proc Natl Acad Sci U S A* 101: 16004-16009.

264. Shin, H., S. D. Blackburn, J. N. Blattman, and E. J. Wherry. 2007. Viral antigen and extensive division maintain virus-specific CD8 T cells during chronic infection. *J Exp Med* 204: 941-949.

265. Xiong, H., Y. Luo, Q. Wang, X. Yu, and A. He. 2021. Single-cell joint detection of chromatin occupancy and transcriptome enables higher-dimensional epigenomic reconstructions. *Nat Methods* 18: 652-660.

266. Zhu, C., Y. Zhang, Y. E. Li, J. Lucero, M. M. Behrens, and B. Ren. 2021. Joint profiling of histone modifications and transcriptome in single cells from mouse brain. *Nat Methods* 18: 283-292.

267. Rang, F. J., K. L. de Luca, S. S. de Vries, C. Valdes-Quezada, E. Boele, P. D. Nguyen, I. Guerreiro, Y. Sato, H. Kimura, J. Bakkers, and J. Kind. 2022. Single-cell profiling of transcriptome and histone modifications with EpiDamID. *Mol Cell* 82: 1956-1970.e1914.

268. Gopalan, S., Y. Wang, N. W. Harper, M. Garber, and T. G. Fazzio. 2021. Simultaneous profiling of multiple chromatin proteins in the same cells. *Mol Cell* 81: 4736-4746.e4735.

269. Meers, M. P., G. Llagas, D. H. Janssens, C. A. Codomo, and S. Henikoff. 2022. Multifactorial chromatin regulatory landscapes at single cell resolution. *bioRxiv*: 2021.2007.2008.451691.